UNIVERSITÀ DEGLI STUDI DI PALERMO
Dottorato in Scienze della Terra - Geochimica
Dipartimento di Scienze della Terra e del Mare (Di.S.Te.M.)
GEO/08

ZIRCONIUM, HAFNIUM AND RARE EARTHS BEHAVIOUR DURING THE TRANSPORT IN VOLCANIC FLUIDS. GEOCHEMICAL EFFECTS THROUGHOUT THE SUBLIMATION AND AFTER INTERACTIONS WITH AQUEOUS MEDIA

IL DOTTORE
Edda Elisa Falcone

IL COORDINATORE
Prof. Francesco Parello

IL TUTOR
Prof. Paolo Censi

CO TUTOR
Dr. Francesco Sortino

CICLO XXV
ANNO CONSEGUIMENTO TITOLO 2015

UNIVERSITÀ DEGLI STUDI DI PALERMO
Dottorato in Scienze della Terra - Geochimica
Dipartimento di Scienze della Terra e del Mare (Di.S.Te.M.)
GEO/08

ZIRCONIUM, HAFNIUM AND RARE EARTHS BEHAVIOUR DURING THE TRANSPORT IN VOLCANIC FLUIDS. GEOCHEMICAL EFFECTS THROUGHOUT THE SUBLIMATION AND AFTER INTERACTIONS WITH AQUEOUS MEDIA

IL DOTTORE
Edda Elisa Falcone

IL COORDINATORE
Prof. Francesco Parello

IL TUTOR
Prof. Paolo Censi

CO TUTOR
Dr. Francesco Sortino

CICLO XXV
ANNO CONSEGUIMENTO TITOLO 2015

Abstract

This research indicates the fate of Zr, Hf and Rare Earths during their sublimation from the high-temperature gas phase (100° - 420 °C), in volcanic systems associated with different geodynamic regimes, and processes associated with volcanic sublimation representing the last natural "inorganic" interface where a detailed investigation into the behaviour of Rare Earths had never been conducted. The research was carried out in active volcanic systems at Vulcano (Aeolian Islands, Italy), Santorini (Cyclades Islands, Greece), Phlegrean Fields (Italy), Tenerife (Canary Islands, Spain) and Fogo Island (Cape Verde) where both fumaroles and thermal waters from submarine springs and inland wells were collected and investigated. Both solid newly forming sublimates and the coexisting volcanic gas phase were studied in fumaroles in order to evaluate partitioning of the elements studied during the sublimation.

Volatile geochemistry of Zr, Hf and Rare Earths (hereafter reported REE, being the sum of lanthanides and yttrium) data suggested a scenario where REE are transported in the volcanic gas phase as chloride complexes. This indication is apparently also confirmed for Zr and Hf by the Zr partitioning in the volcanic gas phase during sublimation relative to Hf. This evidence is attributed to the formation of $[(Zr,Hf)Cl_4(H_2O)_4]$ and other Cl-complexes that are more stable in the volatile phase when Zr is the coordinating metal relative to Hf. Features of shale-normalised REE patterns show positive Gd anomalies in volcanic gas during the sublimation whose amplitude progressively grows with increasing HCl contents in volcanic gas. These features are consistent with reference values of stability constants for chloride-REE complexes rather than for fluorine- and other REE complexes. This data may explain several instances of medium REE enrichments in natural waters during and immediately after large volcanic eruptions and suggests a particular Gd fate relative to other REE during the emission of volcanic soluble substances.

Geochemical evidence coming from hydrothermal waters from Vulcano and Santorini Islands confirm the above-mentioned suggestion about the particular Gd behaviour in volcanic fluids since positive Gd anomalies are recognised in waters from submarine vents. Here Gd/Gd*

up to 1.6 are associated with clear signs of W-type tetrad effects that allow us to identify these fluids as those leaching the authigenic solids that are immediately formed during the mixing between the hot reducing and acidic hydrothermal fluids with cold, oxidizing and basic seawater close to the vent. This and other geochemical evidence along with model calculations allow us to identify two different water groups in terms of physical-chemical characters, calculated saturation/oversaturation with respect to carbonates (group 1 waters) and Fe-oxyhydroxides (group 2 waters) and reciprocal Zr-Hf behaviour dissolved in natural pools. In both waters, the dissolved speciation of these elements is dominated by $[Zr(OH)_4]^0$ e $[Hf(OH)_5]^-$ complexes. These species being differently charged, they fractionate during interactions with occurring solid surfaces. Our data confirms that Zr and Hf undergo a competition process between dissolved speciation and surface adsorption, but also suggests that the larger Hf surface reactivity, especially onto Fe-oxyhydroxides, can be related to the Hf surface complexation rather than to a simple interaction attributed to electrostatic attractions.

Our findings prove that passive volcanic degassing can represent a suitable Gd source in a soluble and bioavailable form. Model calculations based of CO_2 fluxes from the studied active volcanic areas indicate that about 1 kg Gd per year is released as a whole into the atmosphere. Comparing this value with reference data, this indication suggests that the volcanic Gd-flux is of the same order of magnitude as the yearly anthropogenic Gd delivered to the hydrosphere from hospital wastewaters in Germany. Therefore, Gd from volcanic source could represent a potential environmental risk under particular conditions.

Table of contents

List of tables

List of figures

CHAPTER 1

INTRODUCTION

GENERAL ASPECTS AND PURPOSE OF THE STUDY

It is widely accepted that metal transport by volcanic fluids occurs via volatile complexes (Williams-Jones and Heinrich, 2005 and references therein). This process explained why the concentration of some metals in volatiles can sometimes exceed those measured in coexisting fluids (Heinrich et al., 1999) and needs to be completed by investigating the geochemical behaviour of the most interesting elements during sublimation where fractionations relative to volcanic fluids can occur.

Sublimation requires the deposition of a wide spectrum of S, N and halogen-bearing minerals with other geochemically coherent metals. Sublimate surfaces are a good context where trace element adsorption can occur from volcanic fluids by means of simple Coulomb interactions or through surface complexation. The best geochemical tool to study these processes is the fractionation of lanthanides and Y (hereafter defined as REE). Recent studies allow us to couple the REE to Zr and Hf investigations in "extreme" aqueous environments (Raso et al., 2013) and the "simplified electrostatic model" by Koschinsky and Hein (2003) forwarded by Bau and Koschinsky (2009) suggested that the decoupling of Zr and Hf can give further information about processes involving solid-liquid Coulomb interactions.

REE are a strategic resource and their exploitation has been increasing greatly as a result of their wide use in technological devices. As a consequence, several research studies focused on the capability of volcanic gas in transporting and concentrating REE until metal deposits were formed (Chao et al., 1992; Williams-Jones and Wood, 1992; Williams-Jones et al., 2000; Gultekin et al., 2003; Wood and Samson, 2006; Salvi and Williams-Jones, 2006). In these research studies, the effective REE transport as gaseous volcanic complexes was only verified in the water-saturated gas

phase where these elements occurred as water vapour complexes (Moller et al., 2003) and in CO_2-dominated fluids where REE occurred as carbonate complexes (Gilbert and Williams-Jones, 2008). For this reason, these studies left a lack of knowledge regarding volcanic systems where the REE transport through aqueous or carbonate gaseous species cannot be invoked. Furthermore, sharp temperature and compositional changes in the volcanic gas phase cause the deposition of volcanic sublimates in fumaroles (Richards, 2011 and references therein) and also during this process, the effects on the REE partitioning are poorly understood. Only Zelenski et al. (2013) demonstrated that a wide spectrum of metals is partitioned between newly formed solids and the coexisting residual gas phase during high temperature sublimation ($T \approx 1000°C$) by studying the Erta Ale volcanic system. In that system, REE showed only a weak partitioning as basaltic microspheres and the behaviour observed for these elements was probably due to the high sublimation temperature in the Erta Ale system. At the same time the Zr and Hf behaviour during transport in volcanic fluids was never studied and only Zelensky et al. (2013) measured their concentrations in high temperature ($T > 1000$ °C) fumaroles where these are higher than in lower temperature vents and can be determined without any particular manipulations.

Therefore, there is a lack of knowledge regarding the Zr, Hf and REE fate at the sublimate-volcanic gas interface, which could provide information about the transport of these elements in the volcanic gas phase. Hence, the stated aim of the research carried out within the framework of this PhD is precisely to establish the mutual behaviour of Zr, Hf and REE during the sublimation of volcanic fluids.

GEOCHEMISTRY OF ZIRCONIUM AND HAFNIUM - CHEMICAL FEATURES

Zirconium and Hafnium are transition metals of IV B group, tetravalent (+4) and having very close ionic radii, 0.84 Å e 0.83 Å in octahedral coordination, respectively (Shannon, 1976). The similarity of the ionic radii is a result of the lanthanide contraction and bestow on two elements similar chemical-physical properties (Tab. 1.1).

Tab. 1.1 Zirconium and Hafnium chemical properties

	Zr	Hf
Electronic configuration	$[Kr]4d^2\ 5s^2$	$[Xe]4f^{14}\ 5d^2\ 6s^2$
Valence state	+4	+4
Atomic radius	1.45 Å	1.45 Å
Ionic radius (octahedral coordination)	0.84 Å	0.83 Å

For this reason, Zr and Hf are always found together in nature, although in different proportions. According to Goldschmidt (1937), a pair of isovalent elements during primary magmatic processes, such as crystallization and melting, do not fractionate with each other. Behaving like "twin pair" (Taylor and McLennan, 1995), it can be expected that Zr and Hf are tightly coupled during these processes (Bau, 1996; Linnen and Keppler, 2002). Bau (1996), called this geochemical behaviour CHARAC (CHarge and Radius- Controlled). Differences in charge and size between these two elements and other elements are more abundant (Si, Al, K, Na, Fe, Mg etc…), making them hardly interchangeable in the lattices of the common silicate that make up the rocks (Linnen et al., 2014). Erlank et al. (1978) have analysed the abundances of Zr and Hf in silicate minerals, detecting trace concentrations in the feldspar/feldspathoids up to about 100 ppm in the pyroxene minerals and in the most advanced stage of crystallization. The Zr/Hf ratio in silicate rocks tends to decrease as the degree of differentiation (silica-rich magma) in a co-magmatic sequence (Irber, 1999). During solid/liquid interaction, the charge/radius ratio is not the only factor controlling the fate of these elements. The electron configuration plays an important role in their geochemical behaviour in these systems. It follows a progressive loss of geochemistry coherency in a Zr-Hf pair that results in non-CHARAC geochemical behaviour (Bau, 1996). In these systems, the transport of metals is strongly affected by the solubility of minerals containing metals coexisting with aqueous fluids. Hoskim and Schaltegger (2003) suggest that the Zr and Hf mobility is controlled by the dissolution and recrystallization processes of the zircon. During

weathering processes, Zr and Hf have always been considered as immobile elements in relation to the low solubility of the zircon mineral and the reduced residence time that they have in the aqueous phase, due to the tendency to hydrolyse and react with the surfaces. Therefore, it is important to consider the nature of Zr and Hf behaviour during the aqueous phase processes.

GEOCHEMISTRY OF ZIRCONIUM AND HAFNIUM - AQUEOUS SPECIATION

The remarkable chemical similarity between this pair of elements may be the key to being able to trace the geochemical processes that influence the distribution of trace metals in natural waters. Zr and Hf are considered "hard metals" (high charge/radius ratio) according to the classification of Ahrland (1958) and Pearson (1963) and tend to form very stable complexes with strong anions (Norén, 1967), in the following order:

$$O^{2-}, F^{-} > SO_4^{2-} >> Cl^{-}, Br^{-}, I^{-} \text{ and } NO_3^{-}$$

Several studies (Baesand Mesmer, 1976; Turner et.al., 1981; Cabaniss, 1987) have shown that the Zr and Hf speciation in solution, in the pH conditions of natural waters (pH> 6), is dominated by the formation of hydroxide complexes, $Zr(OH)_4^{-}$ e $Hf(OH)_5^{-}$ respectively. However, with decreasing of pH (<3.5), the hydroxo-species of Zr and Hf are present as a cationic type in solution (Fig. 1.1), although very little or nothing is known of the actual behaviour of Zr and Hf in the aqueous phase in natural systems at pH <3 (Byrne, 2002).

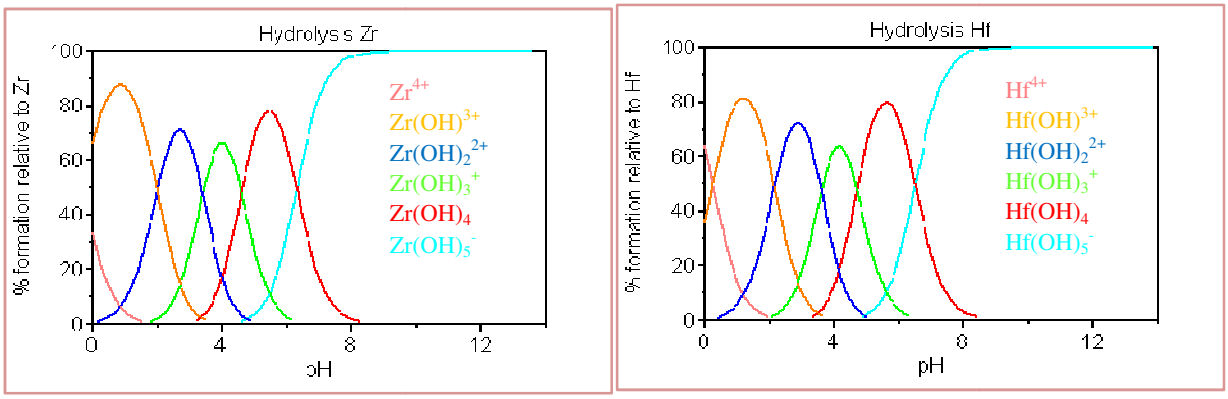

Fig. 1.1- Distribution diagram of hydroxide species for Zirconium and Hafnium

Knowledge concerning the solubility of Zr and Hf in high pressure and temperature fluids is very limited, as is knowledge of the mechanisms with which they are transported in these systems. In this regard, recent studies (Wilke et al., 2012; 2013) have focused on the possible relationship between the chemistry of the fluids (NaOH, HCl e Na, Al- silica solution) and changes in the complexation of Zr and Hf in these conditions. X-Ray adsorption/fluorescence spectroscopy analyses highlighted a direct dependency between the degree of coordination of these elements and the composition of the fluid concerned. The spectra showed that under alkaline conditions the Zr is 6-fold coordinated by oxygen atoms; under acidic conditions, the complexes are a mixing of oxo-chlorides. Molecular dynamics simulations (MDS) ab-initio have been used to study the complexation of these two elements (Fig. 1.2).

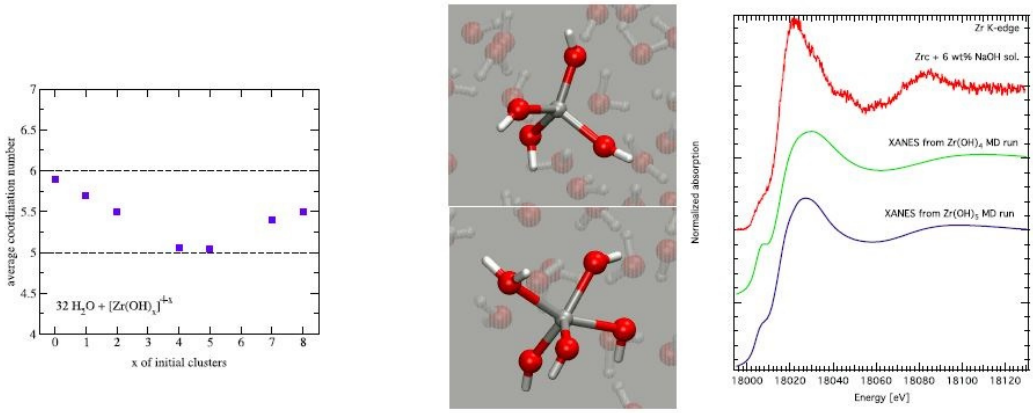

Fig. 1.2- (left) Zr coordination in fluids with [Zr(OH)n]4-n with n=1 to 8. (middle) snapshot of MD runs for 4-fold and 5-fold coordinated Zr monomers. (right) XANES spectra calculated with Feff based on indicated MD simulations in comparison to Zr measured in NaOH solution.
From Wilke et al., 2013.

GEOCHEMISTRY OF RARE EARTH ELEMENTS - CHEMICAL FEATURES

Rare earths (REE) are a coherent group of elements consisting of the lanthanides (La-Ce-Pr-Nd- (Pm) -SM-Eu-Gd-Tb-Dy-Ho-Er-Tm-Yb-Lu) which is added yttrium, by virtue of the similar charge and ionic radius. The Lanthanides are elements of the *f*-block, commonly called inner transition elements, and are found in nature as trivalent cations, except Ce (III, IV) and Eu (II, III), which have two oxidation states. Conventionally, the rare earths are split into light (La-Ce-

Pr-Nd), middle (Eu-Gd-Tb-Dy) and heavy (Er-Tm-Yb-Lu) (Byrne et al. 1996). The external electronic configuration $[Xe](4f)^n5d^16s^2$ is the same for all the elements of the series and this allows them to have quite similar chemical properties and similar ionization energies. The progressive filling of the 4*f* orbitals, along the lanthanide series, ($Nd^{3+}[Xe](4f)^3 \rightarrow Gd^{3+}[Xe](4f)^7 \rightarrow Er^{3+}[Xe](4f)^{11} \rightarrow Lu^{3+}$ $[Xe](4f)^{14}$) is responsible for a phenomenon known as ***Lanthanide contraction*** (Shannon, 1976). As the atomic number increases (from La to Lu = 57 = 71), the atomic radii decrease from 1.02 (La) to 0.86 Å (Lu) due to the poor shielding of the 4*f* orbitals, which results in a greater attraction to the nucleus outer 5d orbitals. From Lanthanum onwards, electrons are added to the 4*f* orbitals (low energy levels) rather than occupying the 5*d* orbitals. The gradual change of the ionic radius induces subtle, but significant, differences in the chemical nature of these elements, resulting in possible splits during the geochemical processes in which they are involved. The ability of lanthanides to describe different processes in different geochemical environments is linked to the presence of the 4*f*orbital. One of the effects of the lanthanide contraction is *CHARAC* behaviour of these metals. The distribution of isovalenti metals between the newly formed solid phase and the parental liquid depends on the ionic radius and the charge (Bau, 1996; 1999). This fractionation, induced by major or minor compatibility of rare earth for either one or the other phase, will be "registered" in both the concentrations of newly formed solids and the parental liquid. During these processes, the yttrium behaves as a heavy REE due to having an ionic radius very similar to the Ho. On the other hand, in highly evolved magmatic systems (e.g. hydrothermal systems) and in aqueous media, the behaviour of the rare earths does not depend exclusively on the charge and radius, as previously discussed. In natural systems, in which a dissolved phase coexists with solid surfaces of a different nature, the geochemical behaviour of the rare earths is driven by the processes that take place at the solid-liquid interface. The formation of REE-complex is controlled by electronic configuration and the ligands species in solution, which determine the nature of the chemical bond (covalent vs electrostatic) forming complexes of non-CHARAC. During these processes, the yttrium will become decoupled with

respect to Ho and other rare earths, because there are no 4*f* orbitals. The geochemical distribution of rare earth in natural substances is usually studied by normalising the concentrations to chondrite or the shale (Masuda, 1962; Coryell et al., 1963). This necessity stems from the need to minimize the "Oddo-Harkins" effect, "odd-even", associated with the increased abundance of even elements in the atomic number range than odd elements, in order to make data processing less difficult. During the heterogeneous solid/liquid reactions, rare earths can be divided into 4 segments called "tetrads" (Masuda et al., 1987; Monecke et. al, 2002). This splitting, called the ***tetrad-effect*** can be induced by adsorption, co-precipitation, dissolution and complexation. The magnitude of these processes can be calculated according to the equation of Irber (1999):

$$t_i = \sqrt{\frac{[REE]_2 \times [REE]_3}{[REE]_1 \times [REE]_4}}$$

where $[REE]_{1,2,3,4}$ shows the normalised concentrations of rare earth elements of the tetrad under consideration. Considering the pattern's shape, which provides guidance on the processes that generated them, there are two types of *tetrad effect*: W-type, for values less than 0.95, in which the covalent character of rare earth and ligand is weak; M-type, for values greater than 1.05, in which the increase in the formation of covalently REE-O bonds on solid surfaces is invoked. Jørgensen and Nugent (1970) have developed a theory, the *RSPET (Refined Spin-pairing Energy Theory),* which suggests the existence of a direct relationship between the electronic configuration of the rare earths and chemical equilibria in solution. The bonds formation implies energy variations which depend on the different nature of the ligands and are not realized only through electrostatic interactions. According to the *Field of the Ligands Theory,* the variation in the electron-electron repulsion in the bonds formation, measurable through electrostatic parameters (Racah parameters), determines the possibility or otherwise of forming covalent bonds (Jørgensen, 1979). The higher values of the Racah parameters result in an increase in the inter-electronic repulsion (e.g. aquo-complexes), while lower values indicate an increase in covalently (e.g. surface

adsorption and/or coprecipitation). This phenomenon, known as the *nefelauxetico effect* is revealed through the *tetrad effect* (Kawabe, 1992).

GEOCHEMISTRY OF RARE EARTH ELEMENTS - AQUEOUS SPECIATION

The rare earths are considered strong acids and tend to form complexes with strong bases (Pearson's rules), as F^- and OH^-, via electrostatic interactions (Wood, 1990). The complex formation is closely linked to the aqueous systems in which the REE move and is controlled by the physical-chemical parameters (pH value, T and Eh) of the interest system. The REE may occur in solution mostly as complexes with halides and hydroxides (strong ligands), sulphates, carbonates and phosphates (moderately strong ligands) and as free ions (Wood, 1990a; Haas et al. 1995; Byrne and Sholkovitz, 1996; Lewis et al, 1998) and their speciation is controlled by the availability (ion activity) of the ligands in solution (Morton-Bermea et al. 2010 and references therein). In aqueous solution, the only reduction potentials that must be taken into account are those of Ce and Eu (redox-sensitive elements):

Acid Solution	$Ce^{4+}(aq) \rightarrow Ce^{3+}(aq)$	($E° = 1.72$ V)
Alkaline solution	$CeO_2(s) \rightarrow Ce(OH)_3(s)$	($E° = -0.7$ V)
and	$Eu^{3+}(aq) \rightarrow Eu^{2+}(aq)$	($E° = 1.72$ V)

The lanthanides speciation (Fig. 1.3) was calculated in seawater on the basis of the association constants of Turner et al. (1981) for the chloride, fluoride and hydroxide- Ln^{3+}, and those of the carbonate-complexes proposed by Cantrell and Byrne (1987).

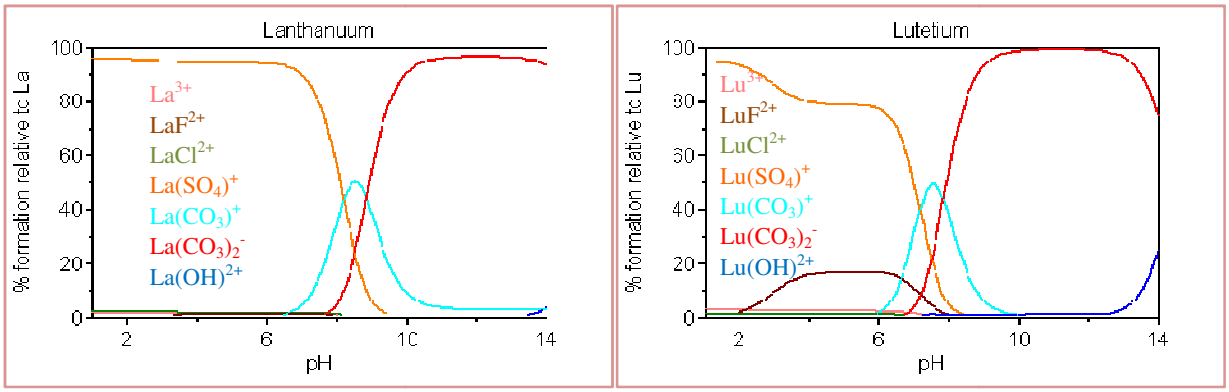

Fig. 1.3- Speciation of La^{3+} and Lu^{3+}varying pH.

The rare earths can be found in solution as free ions (REE^{3+}), mainly at more acidic pH values, such as complexes with F^-, OH^-, SO_4^{2-}, CO_3^{2-} and PO_4^{3-} (Lee and Byrne, 1992; Wood, 1990a) or with organic ligands (Byrne and Li, 1995). The hydrolysis of rare earths is achieved with the hydrate complexes formation, from 8- to 9-fold coordinated, according to the variation along the series of the size of the metal that affects the stability of complexes (Fig. 1.4). The constants of hydrolysis tend to increase with the temperature increase (Byrne and Sholkovitz, 1996).

Metal (M)	$\log^* \beta_1$(M)	Metal (M)	$\log^* \beta_1$(M)
La	−9.20	Tb	−8.40
Ce	−8.95	Dy	−8.35
Pr	−8.81	Ho	−8.32
Nd	−8.70	Er	−8.27
Sm	−8.50	Tm	−8.22
Eu	−8.44	Yb	−8.14
Gd	−8.47	Lu	−8.13

Fig. 1.4- Lanthanide hydrolysis constants at 25°C and 0.7 mol kg-1 ionic strength. Estimates expressed in terms of free-ion concentrations. From Byrne and Sholkovitz, 1996.

The different nature and stability of complexes along the rare earth series can induce fractionations (Byrne and Li, 1995; Lee and Byrne, 1992), which reflect competitive equilibria between surface adsorption on particulate matter and/or co-precipitation processes of newly-formed phases and complexation in solution (Fig. 1.5).

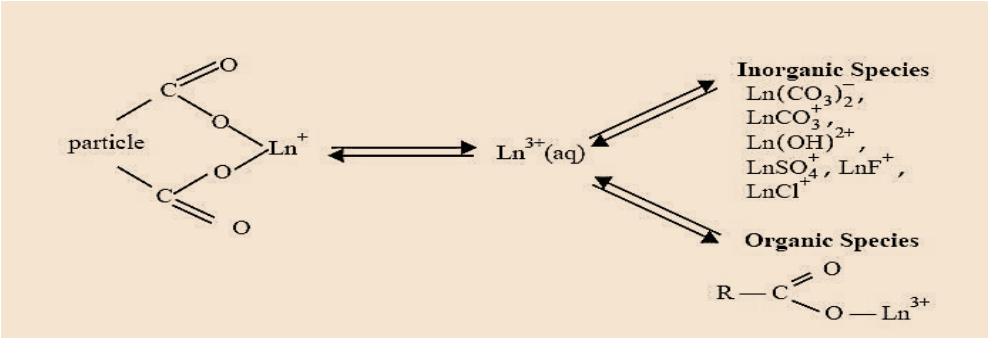

Fig. 1.5- Adsorption vs complexing reactions for Lanthanides in aqueous solution.

Some authors (Wood, 1990b; Haas et al., 1995) have estimated the stability constants of REE-complexes under hydrothermal conditions and have observed that the temperature and the pressure play a antithetical role on the stability of most of the complexes. A temperature increase enhances stability of the complexes in solution, while increasing pressure make it less stable. In addition, the calculations of Haas et al. (1995) show that with temperature increasing the REE-chloride complexes become more stable than REE-fluoride complexes. The magnitude of these effects depends on the nature of the ligand, as well as by the stoichiometry of the complex.

SUBLIMATION PROCESSES

The sublimation process is associated with active volcanism and takes place through the rapid cooling to below the liquid/solid temperature, of a gas exhaled from a fumarolic vent (Fig. 1.6). This process involves state changes from the gaseous phase to the solid phase without involving the liquid phase (Hawley, 1971). During sublimation, supercooling occurs in response to sharp temperature gradients to which volcanic gas is subjected when it comes into contact with the atmosphere.

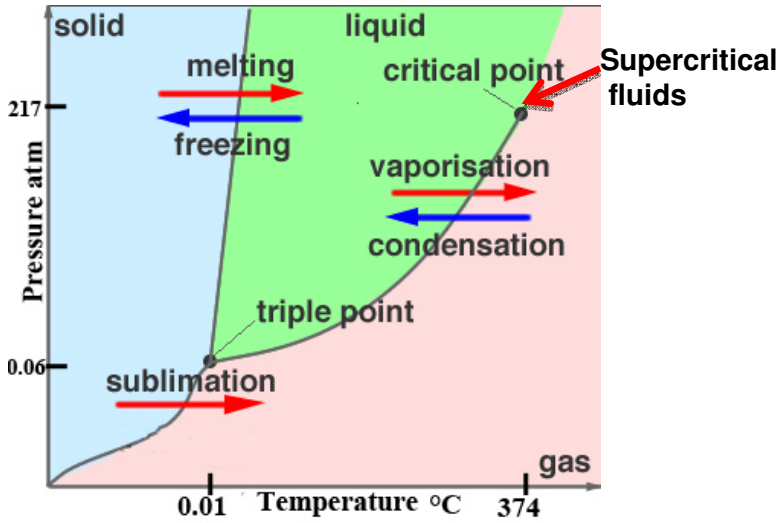

Fig. 1.6 – Phase diagram: at the interfaces between solid/liquid, liquid/gas and solid/gas it is possible for more than one phase to exist in equilibrium. Triple point, represents the temperature and pressure for which all three states of matter can exist; Critical point, the liquid and gaseous phases of a pure stable substance become identical.

This process is well described by the following exothermic reaction, where (g) and (s) indicate gaseous and solid phase, respectively:

$$X_{gas} \xrightarrow[\text{supercooling}]{\text{sublimates}} X_{solid}$$

Although the sublimation process does not require the formation of a solid through the liquid phase, since the enthalpy is a state function, it is possible to build a "thermodynamic cycle" according to the variations of required energy in this process (Fig. 1.7). The sum of the enthalpy changes, for each step involved in the sublimation, can be expressed according to the following equation:

$$\Delta H_{\text{sub}} = \Delta E_{\text{thermal (solid)}} + \Delta E_{\text{bond (solid}\rightarrow\text{liquid)}} + \Delta E_{\text{bond (solid)}} + \Delta E_{\text{bond (liquid-gas)}}$$

where $\mathbf{\Delta E therm_s}$ indicates the variation of thermal energy (expressed as a temperature change) of a substance; $\mathbf{\Delta E bond}$ is the amount of energy that a substance needs to absorb to switch to a higher energystate, from a lower energystate.

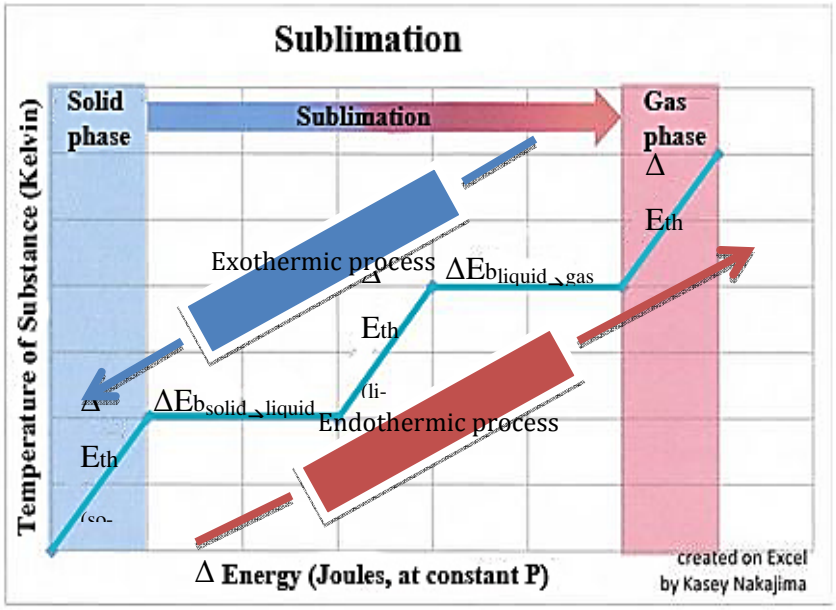

Fig. 1.7- The graph represents how much energy is needed to sublimate a solid substance.

The abundance, size and morphology of the crystals constituting the sublimate depend on the nucleation and growth rates (Fig. 1.8). The nucleation process takes place through a series of collisions between atoms/molecules, which becomes faster with increases in the thermal agitation of the fluid and the supersaturation. The formation of crystals nucleus (or germs) represents an unstable stage in the crystal growth, since the "primordial germ" is destined to dissolve once again if it cannot grow beyond a critical size (r*). The growth of the crystal is favoured in the absence of thermal agitation, as temperature decreases. The surface energy of a crystal germ grows proportionally to its size, but at the same time its intrinsic energy decreases. Switching from supersaturated solution in the crystalline solid is a process that decreases the energy of the whole. As long as the growth of surface energy prevails over the decrease of the free energy, the germ's format will be unstable. Once a critical value (ΔG*, critical energy of nucleation or nucleation barrier) is exceeded, the germ will tend to grow beyond the critical size (r*).

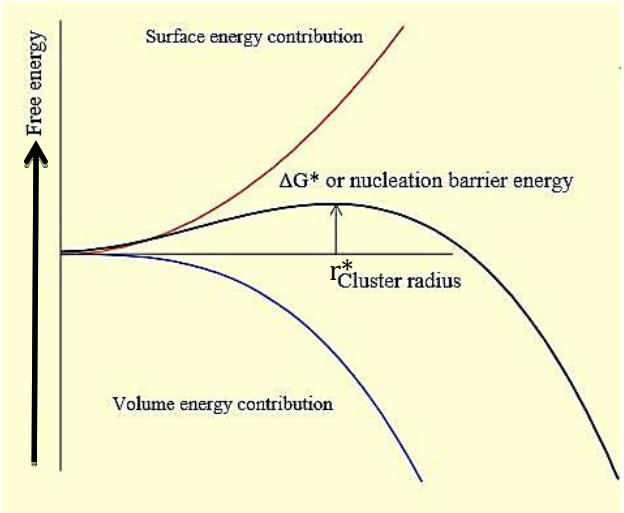

Fig. 1.8- Illustration of the most simple nucleation theory.

TRANSPORT AND DEPOSITION OF TRACE ELEMENTS

Since the early studies of Mizutani (1962) and Egoroff (1965), several research studies have been carried out on metals transport mechanisms in volcanic gases, through the comparative study of the emission flows and products associated with fumarolic sublimation (Le Guern and Bernard, 1982; Bernard, 1985; Toutain, 1987; Toutain et al., 1990; Cheynet et al., 2000; Africano et al., 2002; Gilbert and Williams-Jones, 2008; Pokrovski et al., 2013; Zelenski et al., 2013). The systematic study of the mineralogical associations which form deposits around and within the fumarolic vents, enables evaluations to be made on the volatility of the metal species as a function of their distribution, mainly controlled by the temperature. However, the sublimation of the volatile phase is not exclusively controlled by the temperature, but also by the redox conditions of the fumaroles. Stroiber and Rose (1974) and Naughton et al. (1976) have given an interesting contribution to the study of the relationship between the gas phase composition and the solid phases, comparing natural observations with theoretical studies. Experimental calculations on the equilibrium compositions for volcanic gases of Kilauea, indicate that sulphates and halides are the main phases present in oxidizing and reducing conditions, respectively (Naughton et al., 1976). Le Guern and Bernard (1982), analysing the collected sublimates in silica tubes, have indicated the main mineralogical phases in a temperature range between 900 °C and 400 °C. Cristobalite mineral

(SiO_2) and Fe and Al oxides (Magnetite and Hercynite) sublimate at higher temperatures, while alkali chlorides and sulphide of Zn, Fe and Pb with the gradual temperature decrease. Toutain et al. (1990) have observed that low-temperature deposits (200 °C <T <100 °C) are formed by the most volatile elements (Rb, Cs, Se, Au, Cu, Pb and Tl). In contrast, high- temperature (850 °C -550 °C) sublimates are characterized by alkali chlorides (Halite and Sylvite). The bromine and chromium in these deposits has been interpreted as an isovalency effect between these two metals and chlorine, which is replaced in the lattice of chlorides. The sublimation range for ammonium chloride (NH_4Cl) ranging between 300 °C, at which sublimation begins, and 100°C (Caradossi, 1980). Zhu et al.(2007) have developed a scheme that describes the mechanism of sublimation/dissociation of the ammonium salt (NH_4Cl), based on calculations using the plane-wave (plane-wave) DFT (density function theory). The process of sublimation/dissociation of NH_4Cl is achieved in three steps, illustrated in Fig. 1.9.

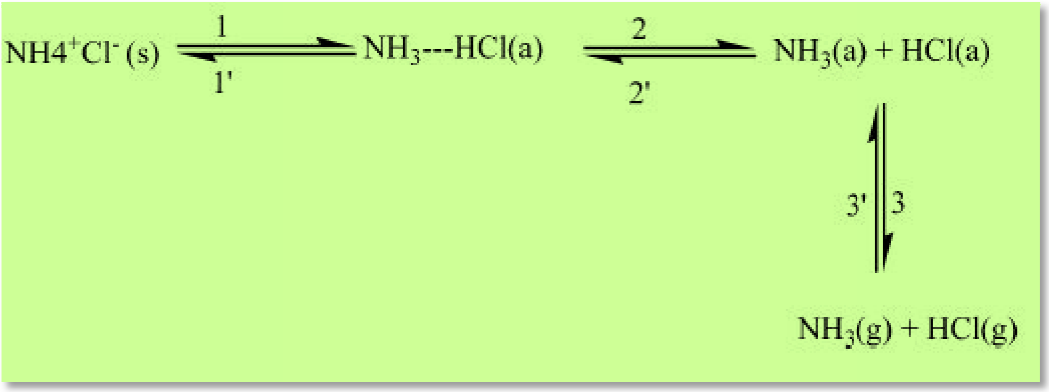

Fig. 1.9- Sublimation/dissociation mechanism for NH4Cl. (s) denotes solid, (a) denotes adsorbed species and (g) denotes gas-phase species. From Zhu et al., 2007.

At the initial stage, the molecules of $NH_4^+Cl^-$ (solid) begin to "relax" from their crystalline system (1). Subsequently, one of the molecules on the surface undergoes the transfer of a proton to form a NH_3--HCl complex that is released from the surface (2). Finally, the molecular complex HN_3--HCl(g) rapidly dissociates into NH_3(g) e HCl(g).

The transport of trace metals in fumarolic gases, associated with the study of the sublimates as a function of temperature, has been investigated by several authors through the thermochemical

approach (Toutain, 1987; Quisefit et al., 1989; Symonds and Reed, 1993). Comparative analysis of the chemical composition of volcanic gases, in terms of metal species present as major and trace components, and mineral phases encrusting the fumarolic vents allowed to model these processes.Cheynet et al. (2000) have carried out a semi-quantitative study on the emission rates of some trace metals (As, Bi, Cd, Pb, Tl and Zn) from several fumaroles of Vulcano (Aeolian Islands, Italy) and solid phases of the fumarolic deposits collected by the Le Guern and Bernard method (1982). In a temperature range between 100 °C and 400 °C, sulfur (S_8), sulphides, chlorides and chlorine-sulphides of As, Pb, Bi and K phases are mainly observed (Fig. 1.10). One of the key features of this study is the role played by the chlorine in the trace metals transport. The presence of chlorine-sulphides in environments characterized by high fCl_2 and fS_2, suggests that chlorine influence the sublimation of sulphur and sulphur-salts, because the latter could be the result of the reaction between chlorine-sulphur (already formed) and hydrogen sulphide gas. Recent studies (Gilbert and Williams-Jones, 2008; Migdisov and Williams-Jones, 2008; Migdisov et al; 2009) focus on the REE transport in high-temperature condition, have emphasized the role of halides, in particular chloride, in the formation of stable complexes at temperatures above 150 °C.

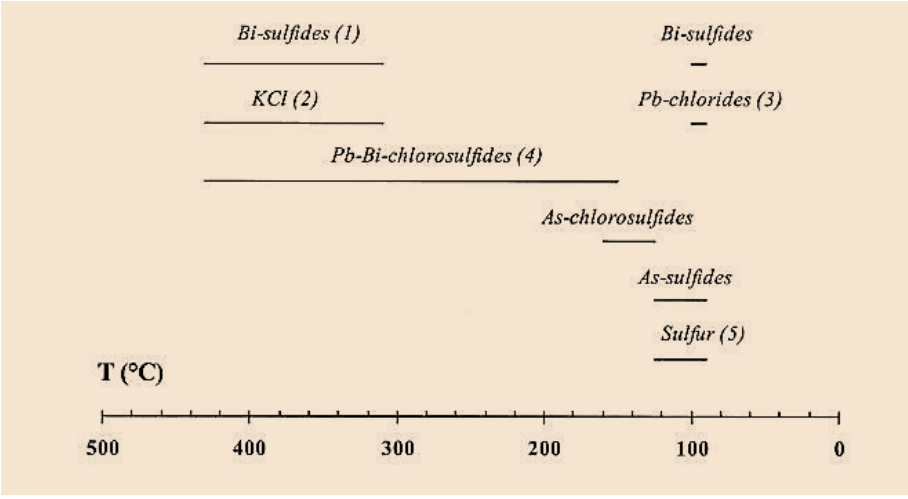

Fig. 1.10- Sublimates assemblages in silica tube as a function of the decrease in temperature and solid phase identified by XRD. From Cheynet et al., 2000.

CHAPTER 2

INVESTIGATED AREAS

COMPRESSIVE ENVIRONMENT: VULCANO AND SANTORINI ISLANDS

Vulcano island (Aeolian archipelago, Italy)

Vulcano island belongs to the Aeolian archipelago, consisting of seven islands and several seamounts that form a large magmatic arc, which extends for about 200 km in the southern margin of the Tyrrhenian Sea. Aeolian islands are part of a trench-arc system, which is the result of the complex collision between the converging African and Eurasian plates (Fig. 2.1).

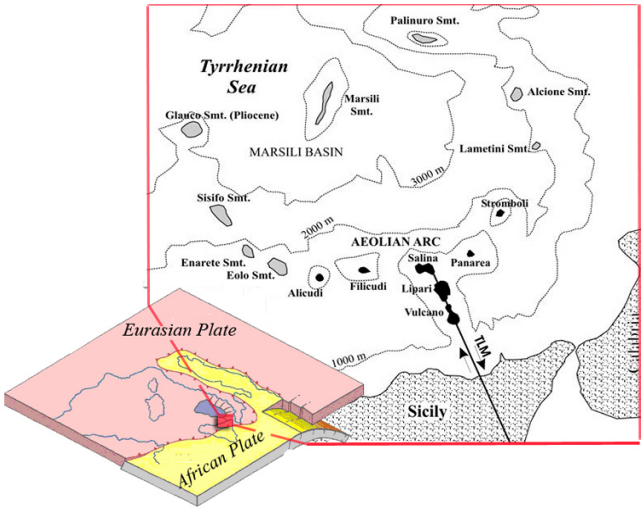

Fig. 2.1- Geodynamic setting of the Aeolian Islands.

It is located in a graben structure (Barberi et al., 1994) linked to a strike-slip fault in NNW-SSE direction, referred to as Tindari-Letojanni-Malta (TLM), which dissects the arc in two parts (Beccaluva, 1985). The subducting slab can be located along the edge of the Ionian margin of Calabria, having W-NW direction and inclination of about 50-60 degrees below the Tyrrhenian sea. The Aeolian magmatic activity started about 1 Ma years ago, with the resumption of subduction (Scandone, 1982). The rocks of Vulcano island belong to the shoshonitic series and range from basalts to rhyolites (Keller, 1980). Since the last eruption at La Fossa crater (1888-

1890), the magmatic activity was limited to fumarolic emissions of variable intensity located on the northern edge of the La Fossa crater, which is a high-temperature fumarolic field (100° C < T < 500 °C), and along the Levante Bay (Isthmus), with low temperature emissions (T < 100°C). Moreover, in the area called Vulcano Porto, there are also several shallow thermal wells (Carapezza et al.,1981; Cioni and D'Amore, 1984; Capasso et al.,1992; Bolognesi and D'Amore, 1993; Chiodini et al., 1995; Nuccio et al., 1999; Aiuppa et al., 2000).

Recent geophysical surveys (Ferrucci et al., 1991) have suggested the existence of a magmatic body, basaltic and volatile-rich (Fulignati el al., 1998), beneath Vulcano island approximately 2-3 km in depth. Several authors have long debated the dynamics of hydrothermal circulation that takes place below the La Fossa volcanic cone (Fig. 2.2).

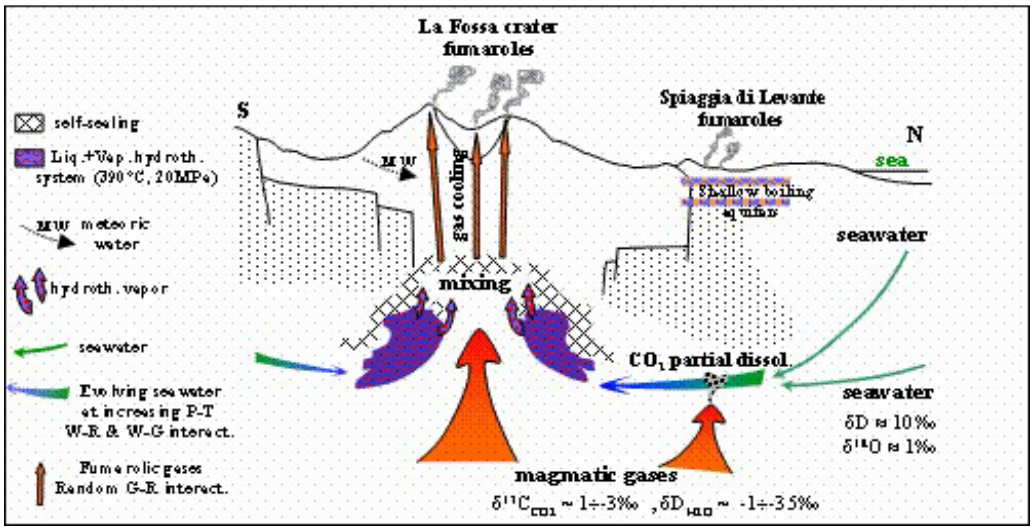

Fig. 2.2- Hydrothermal system Sketch for Vulcano Island
http://www.pa.ingv.it/sorveglianza/vulcano_fumarole_crateriche/vul_fum_cra.html

Carapezza et al. (1981) have proposed a deep biphasic hydrothermal model (1-2 km), suggesting the existence of a brine (5-15 wt% NaCl) boiling at about 340°C and 16 MPa. The analysis of fluid inclusions in hydrothermally altered rocks, coming from geothermal drilling carried out by AGIP in the '80s, have supported this hypothesis, revealing contents up to 25 wt% NaCl (Garavetta et al., 1988). In the second half of the '80s, following an increase in the magma input, the hydrothermal reservoir has evolved into a monophasic system, in response to the total vaporization of the central portion of the brine (Nuccio et al., 1999). Chiodini et al. (1995) have

proposed a three-phase hydrothermal model, in which in addition to the magmatic and hydrothermal end-members, the meteoric component that infiltrates the system is added. Fumarolic emissions at La Fossa crater consist mainly of water steam (86-95% vol) and carbon dioxide (4-12% vol), followed by 0.1-1 vol% of the total sulfur, 0.1% vol of HCl, 0.001% vol of HF and other gas (H_2, CO, CH_4ed He) in the range of ppm (Chiodini et al., 1996).The chemical composition reflects mixing between magmatic and hydrothermal end-members as evidenced by the linear correlation between He vs CO_2 and N_2 vs CO_2, (Nuccio et al., 1999; Paonita et al., 2001). Bolognesi and D'Amore (1993) have suggested that the hydrothermal system of Levante Bay is associated with the presence of three aquifers located in three different levels (≈10 m depth; ≈96m depth e 226m depth). This hypothesis is supported by the drilling AGIP carried out in 1956. The chemical composition of emissions indicates the emission of low-temperature hydrothermal fluids, with high levels in CH_4 and H_2S, low concentrations in CO and absence of SO_2.

Several studies on fumarolic emissions (Stoiber and Rose, 1970; Gemmel, 1987; Symonds, et al., 1987; Symonds and Reed, 1993; Cheynet et al., 2000) e solid products (encrustations and sublimates) their associated (La Guern and Bernard, 1982; Quisefit et al., 1989; Garavelli et al., 1994; 1997; Ferrara et al., 1995; Fulignati et al., 1999; Cheynet et al, 2000), have demonstrated the important role played by the volcanic gases (carrier) on the chemistry of trace elements. Early studies on emissions fumarole at La Fossa crater (Piccardi et al., 1979) indicated the presence of trace metals (Cu, Zn, Cd, Sb, Bi and Pb), which probably result from interactions between the rising acid fluids and the wall rock. Cheynet et al. (2000) have reported semi-quantitative estimates on the rates of transport of some trace metals, which are considered highly toxic, (Tl, Pb, Bi, As, Cd, and Zn) from the crater fumaroles La Fossa. The estimated flows showed that the highest emissions are measured for As, Pb and Bi. However, the absence of Arsenic in encrustations and sublimates to the ground, which are instead enriched in Pb and Bi, suggests that this is released as a volatile compound in the environment. Sortino and Bichler (1997) have pointed on the particular enrichment in As and Sb in these fumaroles, highlighted by studies on atmospheric particulate

matter (Dongarrà and Varrica, 1998) which have also revealed the concomitant presence of metals such as Pb, Cu, Zn, and Au. Few studies exist on the geochemical behavior of REE in current magmatic-hydrothermal system of Vulcano. Fulignati et al. (1998) carried out a research on the geochemical behavior of REE in alteration facies (high-sulphidation-type superficial and phyllic and propylitic ain the subsurface) at La Fossa crater. The results of this study are consistent with the hypothesis that the hydrothermal fluids play a key role in the mobilization of rare earth (REE), under acidic and extremely acidic conditions, and that the variability of the concentrations of REE in these systems is controlled by the fluid-rock interactions (water or rock dominant), as suggested by several authors (Michard, 1989; Bau, 1991; Wood et al., 2006; Morton-Bermea et al., 2010). The geochemistry of the major and trace elements in the waters of Vulcano island is widely documented (Cellini Legittimo et al., 1980; Martini, 1980; Carapezza et al., 1983; Dongarrà et al., 1988; Brondi e Dell'Aglio, 1991; Capasso et al., 1991; 1992; 1999; Bolognesi and D'Amore, 1993; Aiuppa et al., 2000). These studies agree with the fact that the dissolution of the acid gases of volcanic origin is responsible for reducing conditions, which characterize most of these waters, and for increased capacity of the leaching solution to extract metals from the rocks. On the basis of the main constituents (HCO_3-SO_4-Cl), Bolognesi e D'amore (1993) identify at least four groups of waters (waters bicarbonate, chloride-sulphate groundwaters, chloride-rich waters and sulphate-rich waters), according to different feeding areas (ie aquifers at three different depths, above) (i.e. aquifers at three different depths, above). Aiuppa et al. (2000) suggest that the variable content in trace metals in hydrothermal waters of Vulcano (Na-Cl-rich and acid-reduced Fe-S-rich) is controlled by the magmatic gases input, the duration of the leaching processes, the formation of aqueous stable complexes (enrichments in volatile metals such as As, Mo, W, Tl, in, Au and Hg) and secondary hydrothermal minerals (removal of metals such as Al and Fe).

Santorini island (Cyclades islands, Greece)

Santorini island, also known as Thera, is the most active and well-known volcanic centre of the Hellenic Arc, in the southern Aegean Sea. The Hellenic Volcanic Arc (HVA) originates from the still active subduction of the African plate beneath the Aegean microplate that moves in NE-SW direction in the eastern Mediterranean Sea.(Fig. 2.3).

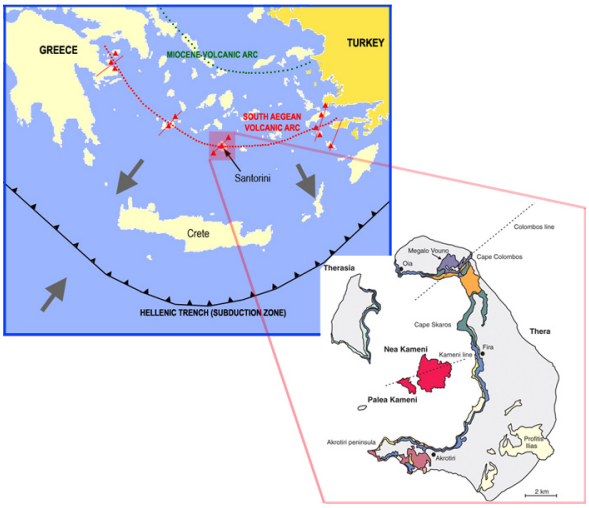

Fig. 2.3- Geodynamic setting of Santorini Island.

The subduction occurs at a low angle (about 30 deg.), according to an intermediate depth seismicity. The Hellenic Arc separates the southern Mediterranean Sea, about 3 km deep and undeformed, from the Aegean Sea, which has a remarkably complex structure. The two main tectonic systems affecting the Santorini island, called Kameni-Kolumbo lines, are generated by a distensive stress system with NNW-SSE direction and interpreted as an active strike-slip fault zone that extends for about 40 km (Vougioukalakis and Fytikas, 2005; Sakellariou et al., 2010). The eruptive activity of Santorini island started about 2-3 million years ago, with the extrusion of dacitic lava, and continued alternating lava and pyroclastic material emissions to violent eruptive phases that led to the collapse of the volcano. Santorini is a composite caldera; caldera is a composite resulting from the succession of at least four collapses. The last eruption, the most catastrophic, occurred about 1400 years ago and is known as the Minoan eruption. The archipelago of Santorini is located in the southern part of the Cyclades islands and consists of five islands:

Thera, Thirasia and Aspronisi, which form the outer ring, and the two central islands of Palea and Nea Kameni, linked to the intra-caldera activity subsequent to Minoan eruption.

The hydrothermal activity at Santorini island is located along the main tectonic discontinuities, Kolumbo-Kameni lines (Vougioukalakis and Fytikas, 2005), indicating that thermal anomalies are closely associated with fault zones. Submarine hydrothermal emissions are mainly found in the Kameni islands, in the areas known as Agios Nikolaos (north of the Palea Kameni islet) and Agios Giorgios (east of the Nea Kameni islet) and associated to active ore deposition (Smith and Cronan, 1983). The thermal springs of Palea Kameni emit steam-heated seawater, while those distributed on Thera are fed by a mixture of steam-heated seawater and diluted deep water (Chiodini et al., 1998). Several authors (Butuzova, 1966, 1969; Bonatti et al., 1972; Smith and Cronan, 1983; Minissale et al., 1997; Cronan et al., 2000; Dando et al., 2000; Varnavas and Cronan, 2005; Dotsika et al., 2009; Tassi et al., 2013 studied the hydrothermal activity of Santorini. Böstrom and Widenfalk (1984) measured temperatures released of 40 ° and 34 °C close to the two vents of Palea and Nea Kameni islets, respectively. Some studies on the geochemistry of sediments from these areas have revealed the presence of biogenic phases, terrigenous and volcaniclastic (Hodkinson et al., 1994; Cronan et al., 1995). These sediments can contain up to 30 - 40 wt% Fe_2O_3 and considerable amounts of silica opal. Other minerals are found in smaller amounts (Mn, Ba, Zn) or in low concentrations as Cu (Butuzova, 1966, 1969; Bonatti et al., 1972; Puchelt, 1973; Schroll, 1978; Smith and Cronan, 1983; Böstrom and Widenfalk, 1984). In particular, Böstrom and Widenfalk (1984) suggest that the sulfuric acid, produced by the oxidation of H_2S due to deep oxygen, alters the rocks (i.e. Dacite) poor in M, Zn, Cu and Ba producing fluids equally impoverished and enriched, instead, in Fe. The venting activity of the thermal springs along the coasts of both islands has caused changes in the chemical composition of these waters, producing iron and manganese-supersaturated solutions (Varnavas and Cronan, 2005) and precipitating ferrihydrite [$(Fe^{3+})_2O_3 \bullet 0.5H_2O$)]. Kilias et al. (2013) demonstrated the influence of bacterial activity (Archaebacteria) on the ferrihydrite origin in acidic shallow-submarine

hydrothermal vents, suggesting that there is a strong relationship between the anaerobic oxidation of Fe^{2+} and the formation of this mineralogical phase. Tassi et al. (2013) detected the presence of bacterial colonies both at great depths (from 200 to 350 m) in low-temperature fluids (17°C), NE of the North Basin of Santorini, in the surface waters of the Kameni islands. The numerous hot springs and fumaroles active on the Nea Kameni summit craters, testify to the presence of a magma chamber beneath the island. The magmatic-hydrothermal system of Santorini (Fig. 2.4) is the result of mixing between deep fluids and gas provided by a hydrothermal aquifer interposed between the surface and the magma chamber. The magmatic contribution to the fumarole emissions of Nea Kameni has been highlighted by significant contents of mantle Helium, resulting in higher ratios R/R_{air} (Shimizu et al., 2005). Anomalous high concentrations in H_2 and absence of H_2S in fumarolic gases are due to the vapour condensation, in response to low and high solubility of these two gases, respectively (Tassi et al., 2013).

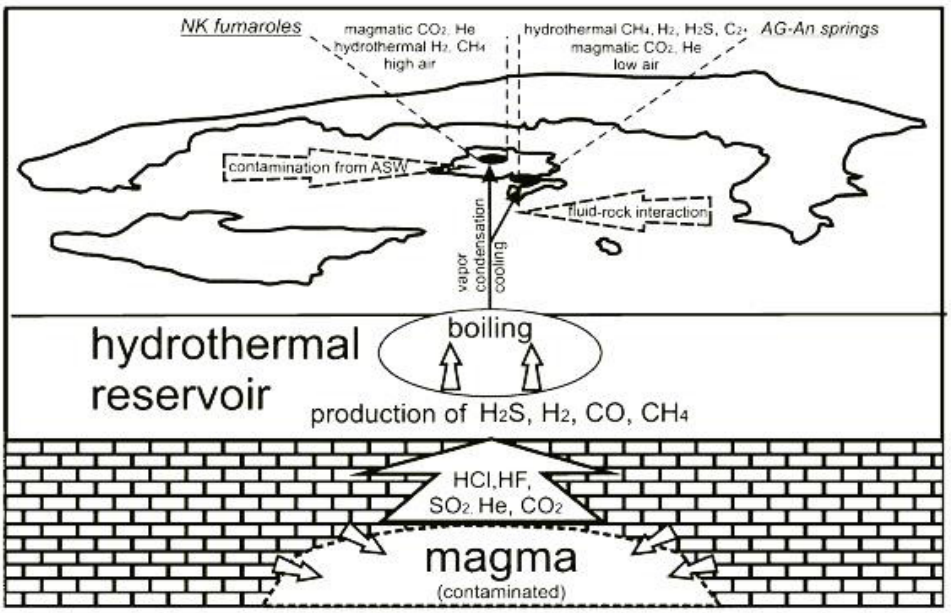

Fig. 2.4- Geochemical conceptual model of the hydrothermal–magmatic system of Santorini. From Tassi et al., 2013.

Low temperatures, which characterize these vents, are probably controlled by a shallow aquifer that is partly fed by hydrothermal uprising fluids. The latter could explain the low contamination from atmospheric gas in the springs of the Kameni islands. In contrast, the

fumaroles at the crater show signs of atmospheric contamination with high content in N_2, O_2 e Ar, probably obtained during ascent through the fractured rock (Vougioukalakis and Fytikas, 2005).

About the origin of these hydrothermal waters were indicated more potential sources. At least three main processes that control the origin of these hydrothermal fluids were recognized:1) water/rock exchange of oxygen-18 isotope similarly to that observed at Vulcano (Aeolian islands) as a result by seawater contamination (Panichi and Noto, 1992); 2) mixing of waters of different origin; 3) boiling and vapour phase separation (Panichi et al., 2000). Chemical analysis classify these waters as chloride- alkaline type, indicating the mixing of deep warm waters, rainwater and seawater. Minissale et al. (1997) suggest that the waters of Santorini are distributed along a mixing line between two hypothetical end-menbers of sodium -chloride composition (seawater) and the bicarbonate-calcium deep waters (Dotsika et al.,2009). Geothermometers of SiO_2, Na-K, Na-K-Ca have estimated a probable temperature of the deep fluids origin between 120 ° and 180 °C at a depth of 800-1000 m (Mendrinos et al. 2010).

DISTENSIVE ENVIRONMENT: PHLEGREAN FIELDS (ITALY)

Phlegrean Fields, from the greek (phlegraios = burning), are located in the centre of the Campania Plain graben in the north-west of the city of Naples (Fig. 2.5). Their origin is connected to extensional tectonic events, linked to the opening of the Tyrrhenian basin, which led to the formation of the Campanian Plain. During the Quaternary, a very intense volcanism occurred that produced potassic alkaline magmas associated by Washington (1906) with a magmatic province, called the Roman Magmatic Province (PMR).

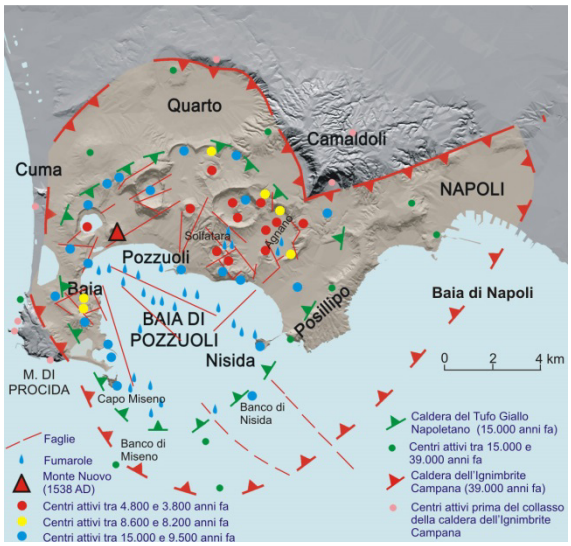

Fig. 2.5- Schematic structural map of the Phlegrean Fields. Modified by Santacroce et al. 2003.

Phlegrean Fields are a large volcanic field in which more than 70 eruptive centres were active in the last 39,000 years. This area has the typical form of volcanic structures called calderas and consists of a nearly circular depression characterized by numerous volcanic cones. The precise origins of the volcanic activity in the Phlegrean Fields is not known. The oldest products are dated between 47,000 and 37,000 years ago and consist of the lava domes of Cumaand Punta della Marmolite. The morphology of the area and the development of its eruptive activity were affected by two major eruptions occurring around 34,000 and 12,000 years ago, which produced extensive deposits called Campanian Ignimbrite and Neapolitan Yellow Tuff, respectively. The origin of the emission centre of the Campanian Ignimbrite has been long debated. Several studies (Di Girolamo, 1970; Barberi et al, 1978; Di Girolamo et al., 1984) hypothesize that the emission area of the flux is located in the north of the Phlegrean Fields and the Gulf of Naples. Rosi and Sbrana (1987), suggest that the genesis of the Phlegrean caldera is posthumous to the eruption and the fracture has an annular geometry that includes only the Phlegrean Fields. Other authors (Lirer et al., 1987; Scandone et al., 1991), believe that the eruptive centres of Campanian Ignimbrite are located along a NE-SW fracture and that the caldera's collapse followed the eruption of the Neapolitan Yellow Tuff.

The Solfatara, about 3 km from Pozzuoli, is one of the most recent eruptions of the last period of activity of the Phlegrean Fields. In the last 14 ka, volcanic activity was mainly concentrated inside the caldera and along the edge, according to the main regional faults (De Astis et al., 2004; Bruno, 2004; Bruno et al., 2003; D'Antonio et al., 1999). The erupted products show a compositional range varying from potassic-basalts to trachyte and phonolite (De Vivo et al., 2001). La Solfatara is characterized by intense fumarolic activity, which is an outlet for magma beneath the Phlegrean Fields, focused mainly in the vents called Bocca Grande (164 °C) and Bocca Nuova (145 °C). In the center, there is also a mud pool (pH 1-2, T 50°C), called "La Fangaia", produced by the interaction between meteoric water, vapor condensation and clay material that constitutes the bottom. The elemental compositions of the mud indicate the presence of traces of Ba, Na, Mg, Va, As, Zn, Sb, I, and Rb. These muds are made up also by bacterial colonies (Sulfolobus solfataricus), able to withstand in extreme conditions of acidity and temperature (Pol et al., 2008). The Bocca Grande vent, insted, is surrounded by deposits of sulfur compounds such as Realgar (AsS), Cinnabar (HgS) and Orpiment (As2S3) (Brand, 2008), products as a result of the sublimation process in response to the abrupt decrease of T and P to which the vapors emitted are subjected.Valentino et al. (1999) indicated that the formation of sulfur minerals and elemental sulfur is the result of supergenic oxidation of volcanic H_2S(g) which, with NH3(g), are found in high concentrations in hydrothermal vapor condensing (Chiodini et al., 2001; 2003). The high concentrations in As (tra 1.6 e 6900 $\mu g \cdot l^{-1}$), measured in groundwaters at Phlegrean Foelds (Aiuppa et al., 2006), increases by means of temperature and chlorine content increasing in the water, as a result of intensive leaching due to the hydrothermal fluids on the rocks.

The hydrogeochemistry of the hydrothermal system of Phlegrean Fields is well documented (Dall'Aglio et al., 1972; Celico et al., 1992a; Rolandi and Stanzione, 1993; Tedesco et al., 1996), as well as the influence of water-rock interactions on the chemistry and mineralogy of the fluid phases (Ghiara and Stanzione, 1988). Baldi et al. (1975) e Guglielmetti (1996), during drilling conducted up to depths less than 2000 m, identified two main types of water: Na-chloride and, less

widely, sulfate-Ca. Other authors (Caprarelli, 1991; Caprarelli et al., 1997) have studied hypersaline brine (T≈400°C), recovered at depths exceeding 2000 m, which were interpreted as the surface emission of deep fluids (Aiuppa et al., 2006). High-temperature brine (250–337°C) exhibit high concentrations of Li (13–28 $mg \cdot l^{-1}$), B (110–140 $mg \cdot l^{-1}$) and NH_4 (20–37 $mg \cdot l^{-1}$) in deep-geothermal system at Phlegrean Fields (Panichi et al., 1992). The hypothesis that these waters, both cold and hot, are the result of the mixing processes between seawater and meteoric component is supported by the linear and positive correlation between Na^+ and Cl^- (Valentino et al., 1999 and references therein; Valentino and Stanzione, 2004). Based on studies on isotopic sulfur ($\delta\ ^{34}S$), Cortecci et al. (1978) suggested that the dissolved sulfate in these thermal waters are derived not only from seawater, but also from the oxidation and dissolution of minerals such as pyrite and secondary anhydrite (Baldi et al., 1975). However, Allard et al. (1991) identified a sulfur-magmatic component in H_2S from fumaroles at La Solfatara.

The gas geothermometry (H_2O-CO_2-H_2-CO-CH_4 system) indicates that the power supply system (Fig. 2.6) of the Bocca Grande and Bocca Nuova fumaroles consists of superheated vapours, with temperatures from 200 to240 °C and P_{H2O} from 1 to 20 bars, coming from a deeper hydrothermal system at temperatures exceeding 360 ° C (Caliro et al., 2007; Vaselli et al., 2011).

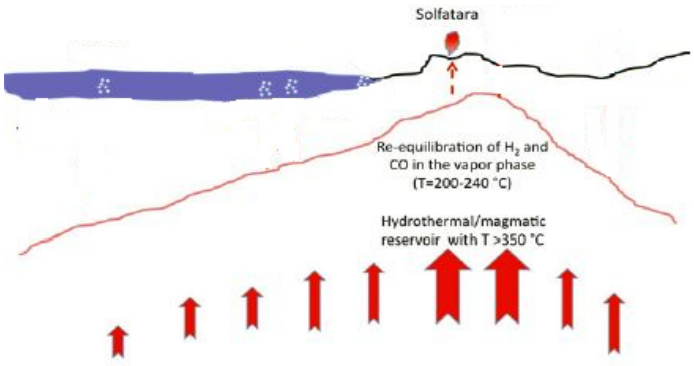

Fig. 2.6- Geochemical conceptual model of the Phlegrean Fields (Vaselli et al., 2011).

The fumaroles emit at varying temperature (from 95 °C to 165 °C) are a mixture of H_2O and CO_2 with minor amounts of H_2S, N_2, H_2 and CH_4 (Chiodini et al., 2011). Geochemical studies for this geothermal system began in the early 80s. A conceptual geochemical model was first proposed by Cioni et al. (1984) and later modified by Cioni et al. (1989), Chiodini et al. (1992, 1996), Chiodini and Marini (1998) and Chiodini et al. (2000a, 2001a). This model suggests the existence of a magma localized in depththat provides heat to the overlying aquifer, causing the separation of gaseous phase under thermo-baric conditions of 236 °C and 31 bar (Cioni et al, 1984). Several studies based on stable isotopes (Cortecci et al., 1978; Allard et al., 1991; Panichi and Volpi, 1999; Tedesco and Scarsi, 1999) indicated that this geothermal system is influenced by the movement of magmatic fluids, varying degrees contaminated by metamorphic and meteoric components. Caliro et al. (2007) proposed a geochemical model according to which the system is fed by a mixture of degassed fluids from the magmatic body and the steam generated at temperatures at about 360 °C, due to the vaporization of hydrothermal fluids of meteoric origin. This process seems to occur at the base of the hydrothermal system, where a plume it forms, mainly composed of a gas phase which migrates towards the surface.

HOT SPOTS: CANARY (SPAIN) AND CAPE VERDE (CAPE VERDE) ISLANDS

Canary Islands

Several authors have long debated the controversial origin of hot spots, interpreted as intra-oceanic plate volcanism associated with mantle plumes, most notably Morgan (1971). His idea, concerned the possibility that the hot spots originated in the upper mantle by ascending plumes. However, Courtillot et al. (2003) have suggested the existence of three different possible types of hot spots, assuming deep source (primary or Morganian), transition or shallow (Andersonian). The conflicting interpretations are related to the variability and quality of seismic data. The Canary and Cape Verde islands are the surface expression of two distinct hot spots located along the African

coast, in the Central Atlantic Ocean (Fig. 2.7). Recent seismic data (Patriat and Labails, 2006) has suggested a possible link between both groups of islands, resulting in a *continuum* morphology of the seabed. Stratigraphic studies support the hypothesis of a similar geological evolution and a synchronous origin.

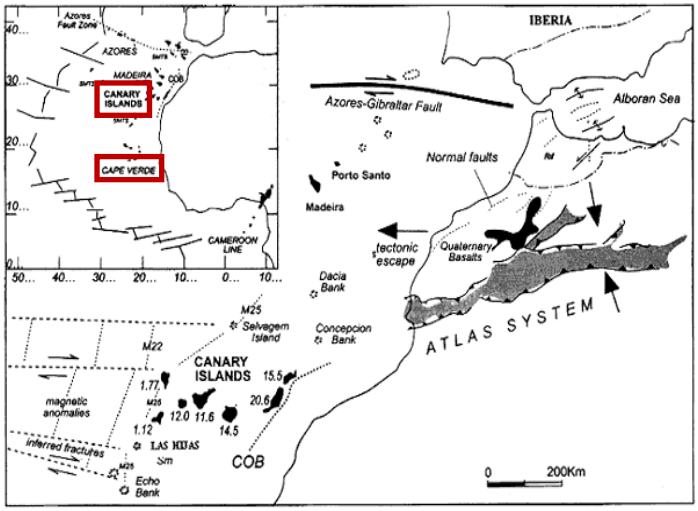

Fig. 2.7- Geographic and geodynamic setting of the NW African continental margin with the Canary Islands and other archipelagos (Carracedo et al., 2002).

The Canary islands lie on oceanic crust from the Jurassic age that was formed during the first opening phase of the Atlantic Ocean (180-150 Ma). The formation process dates back to the Miocene period, 23 million years ago. The Canary islands, along with the islands Selvagen and a group of seamounts, form the Canary volcanic provinces and have approximately a ENE-WSW trend (Gill et al., 1994). This volcanic belt is characterized by a decrease in the age of volcanism, from north-eastern islands (> 20 M) to the south-western (Araña, 1995). Tenerife belongs to the group of the youngest Canary Islands and is the largest in the archipelago. The volcanic structure is represented by the main central building of the Teide, which reaches a height of 3718 m, located within the caldera of the Las Cañadas volcano. The rocks of the Canary Islands can be attributed to a sodic alkaline magmatism that is slightly under-saturated in silica.

Cape Verde islands

The Cape Verde islands are arranged in a horseshoe shape, open to the west, and show an increase in age from east to west. The volcanic activity started in the early Miocene (24-22 Ma). The magmatism has an alkaline composition, from basanite to tephrite, with the presence of phonolites and carbonatites on some islands. Located to the southwest of the Cape Verde archipelago, Fogo Island is an active strato-volcano, which reaches a height of 2829 m above sea level, culminating in the Pico do Fogo. The volcano is located in a caldera, 9 km wide, of which we have only the western side, the Bordeira, more than 1,000 meters high. The caldera is divided into two main entities, the Cha das Caldeiras plain and the Pico do Fogo (Fig. 2.8).

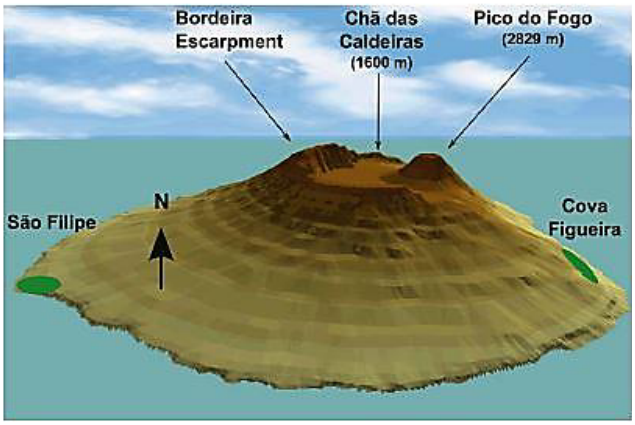

Fig. 2.8- Main geomorphological and structural features of Fogo.
Perspective view from the south. Adapted from Day et al. (1999) and Fonseca et al. (2003).

CHAPTER 3

MATERIALS AND METHOD

LABORATORY EQUIPMENT

For sampling and chemical treatment of hydrothermal waters, condensates and sublimates containers in polyethylene (PE), polypropylene (PP), Teflon (PTFE), high-density polyethylene (HDPE) and quartz (fused quartz 200 ml flasks and silica glass tubes) have been used. Calibration of pipettes and volumetric labware was verifed. Prior to use, the materials were washed with ultra clean acids.

All the chemical reagents (HNO_3, HCl, NH_3 and H_2O_2, 70%, 32-35%, 20% and 30% respectively) had a high-degree of purity and products were from BAKER ULTRA II™ (Netherlands). The deionised water, 18.2 MΩ cm, used for the preparation of STDs and the dilutions of the samples, was obtained by a Milli-Q® Gradient Quantum purification system equipped with UV lamp. A calibrated CP224S Sartorius (Germany) balance was used to weigh all samples and standards.

SAMPLETREATMENTS

Waters

During the sampling campaign carried out between July 2012 and October 2013, 30 hydrothermal waters, including submarine springs, shallow wells and small natural boiling pools, were collected from 21 sites located in Vulcano (Aeolian Islands, Italy) and Santorini (Cyclades Islands, Greece) (Fig.3.1-3.2).

Fig. 3.1- Sampling points at Vulcano Island (Aeolian Islands, Italy).

Fig. 3.2- Sampling points at Santorini Island (Cyclades islands, Greece)

Submarine hydrothermal springs were collected using a cylinder in polypropylene (PP) positioned directly at the vent in order to limit, as far as possible, the effects of mixing with seawater (Fig. 3.3). A Teflon tube equipped with a three-way cock was connected to the cylinder for transferring the samples into 1L bottles in polyethylene (PE). All bottles used for sampling were previously washed with 30% ultrapure HNO_3. The measures of T, pH and conductivity of the investigated waters were carried out *in situ*.

Fig. 3.3- Sample collection system for submarine hydrothermal springs.

The content of the major constituents (Na, K, Mg, Ca, F, Cl and SO42-) was determined in Ion Chromatography (Dionex ICS-1100) and that of bicarbonates by titration with HCl. The concentrations of metals present as minor constituents were measured by ICP-OES (Horiba JobinYvon Ultima-2). To determine the content of rare earths (REE), Zr and Hf, the collected hydrothermal waters were subjected to selective enrichment processes of the relevant analytes, using the co-precipitation of Fe $(OH)_3$ technique perfected by Raso et al. (2013). The enriched fractions were analyzed by ICP-MS (Agilent 7500 CE).

The treatment was performed for a volume of 1.000 ± 0.005 mL. The waters were filtered (Millipore™ membranes with 0.45 µm porosity), transferred into bottles in popypropylene (PP) and subsequently acidified with 70% HNO_3, to pH≈2. Each sample was added to a Fe standard solution (1000 ± 5 mg mL^{-1}), 1% $FeCl_3$ ultrapure solution (Plasma HIQU, CHEM LAB solution 1,000 µg/ml Fe^{3+}) and 25% NH_4OH solution to obtain a pH ranging between 8.0 and 8.5 and to co-precipitate lanthanides onto solid $Fe(OH)_3$. The treated solutions were capped and agitated for two hours to allow the homogenization and the precipitation of Fe-hydroxide. After 48 hours, the iron gelatinous flake precipitates were matured, then filtered and dissolved in 5 ml 6M HCl (Fig. 3.4). The obtained solution was diluted 1:5 with ultrapure water, obtaining an enrichment factor (EF) of $33.\overline{3}$ times for each sample, and analysed by ICP-MS.

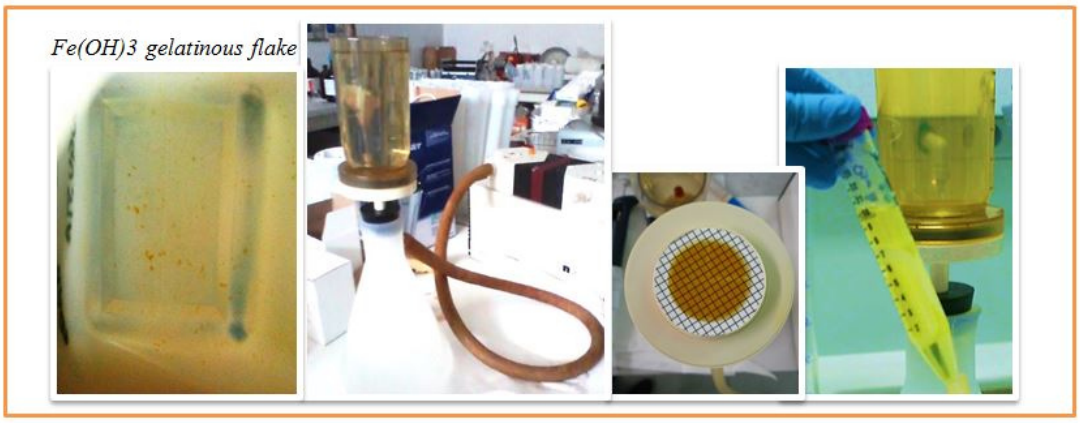

Fig. 3.4- Steps in the co-precipitation process.

Condensates and sublimates

Fumarolic condensates and sublimates were collected from volcanic systems of intermediate temperature (spanning between 82° and 420°C) at Vulcano (Aeolian Islands, Italy), Phlegrean Fields (Naples, Italy), Santorini (Cyclades Islands, Greece), Fogo (Cape Verde Islands, Africa) and Tenerife (Canary Islands, Spain). The sampling sites are shown in Fig.3.5.

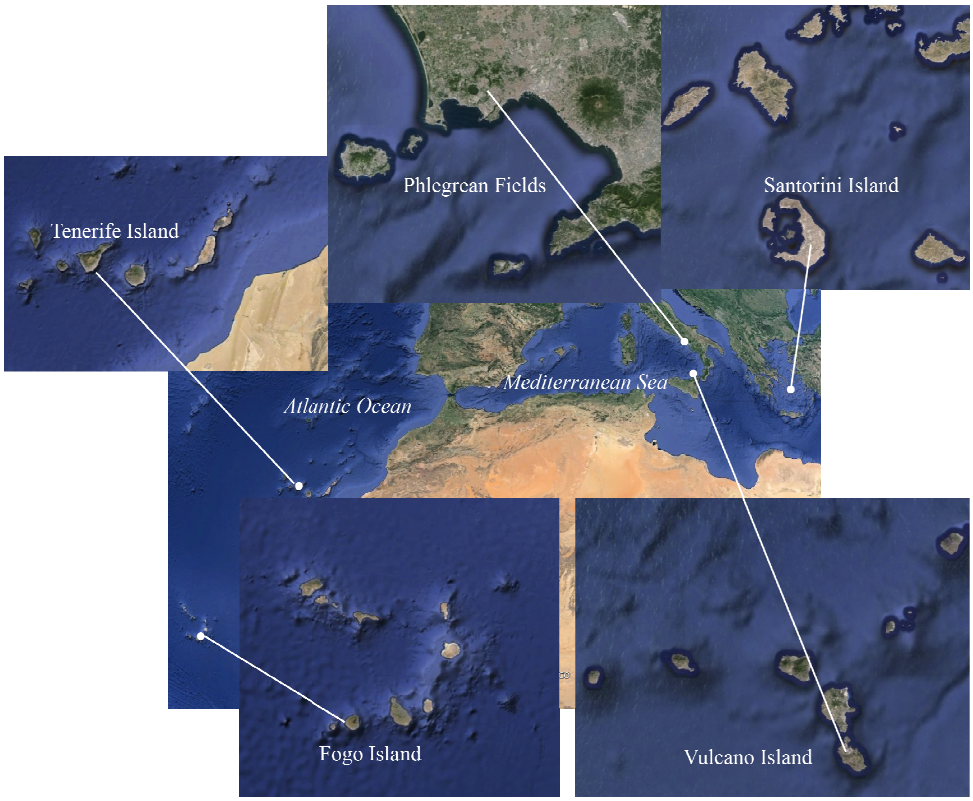

Fig. 3.5- Sampling sites at Vulcano (Aeolian islands), Phlegrean Fields (Naples), Santorini (Cyclades islands), Fogo (Cape Verde islands) and Tenerife (Canary islands).

Due to the flows being too low it was not possible to sample the alkali condensates at Santorini island. A K-TYPE, OMEGA-HH506R thermocouple was used to measure the temperatures of all the fumaroles studied *in situ*. The flasks were weighed before and after sampling with a calibrate Europe 1700 (Gibertini, Italy) balance.

Volcanic condensates were sampled using previously washed (30% HNO_3 and 4N NH_4OH solutions overnight) fused quartz 200 ml flasks as detailed in Sortino et al.(2006). The sampling system is organized in such a way as to avoid any atmospheric contamination. The gas flows into the flask bubbling into the solution so that the acid gases (HCl, HF, H_2S, SO_2, CO_2) are trapped in the alkaline solution as a result of salification reactions. On the other hand, the non-condensable gases (He, H_2, O_2, N_2, CO, CH_4) pass through the solution accumulating in the vacuum head-space of the flask. This technique enables the study of the chemistry of fumaroles, directly analysing a large amount of metal species (Fig. 3.6). To determine the anionic species (F^-, Cl^- and SO_4^{2-} as total S), samples were transferred to PE bottles and an aliquot was oxidized in 50 ml flasks by adding 30% H_2O_2 and 4N NaOH. Prior to ion chromatographic analysis, 2.5 ml of the sample were filtered with ion exchange resins (Dionex OnGuard® II H Cartridge) to neutralize the solution (Sortino et al., 1991). The analysis of the non-condensable gases were performed in Gas Chromatography (PerkinElmer Clarus 500).

Fig. 3.6 - Sample collection system for fumarolic condensates

For the REE, Zr e Hf analyses in alkaline condensates, an aliquot of NH_4OH condensing solution was filtered (Millipore™ membranes with 0.22 µm porosity), transferred into a PTFE vessel and placed on a hot plate CB 300 Stuart (about 150°C) to remove any NH_4OH traces and enrich solutes. The resulting solution was treated with the addition of 1% HNO3 and analysed (Q-ICP-MS AGILENT 7500 CE) without further preparation (Fig. 3.7).

Fig. 3.7- Fumarolic condensates treatment for ICP analyses.

Sublimates were collected from the inner walls of silica tubes (1.5 m long) positioned within the fumarolic vent, as described by the Le Guern and Bernard method, (1982) shown in Fig. 3.8. The inclination of the tube has been taken into account in order to avoid condensation of water vapour. The sublimation along the inner walls of the sampling tube is induced by cooling of the fluid in response to thermal shock, to the different volatility of the species present in the gas phase and their concentration. The temperature was measured before and after the tube installation in the fumarolic vent.

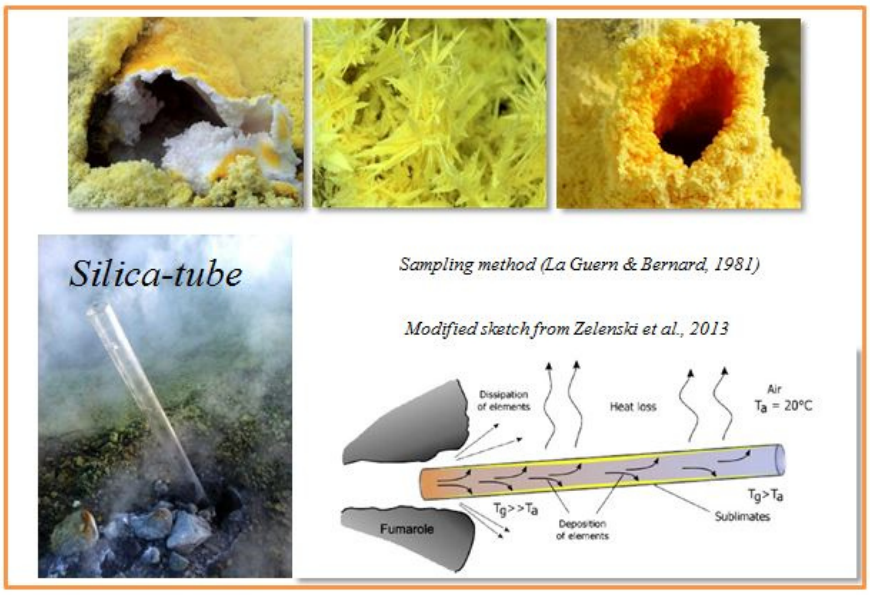

.

Fig. 3.8- Sample collection system for fumarolic sublimates.

A weighed (± 0.0001 g) sublimate aliquot was put into a silica glass vessel with a mixture of 2 ml 70% HNO_3 and 4 ml 30% HCl, which was boiled for 10 min and then cooled. The solution obtained was transferred to a PFA flask, diluted to 50 ml with ultrapure water and then treated by the co-precipitation method onto $Fe(OH)_3$ (Fig.3.9). The resulting solution was appropriately diluted for the measures in Q-ICP-MS.

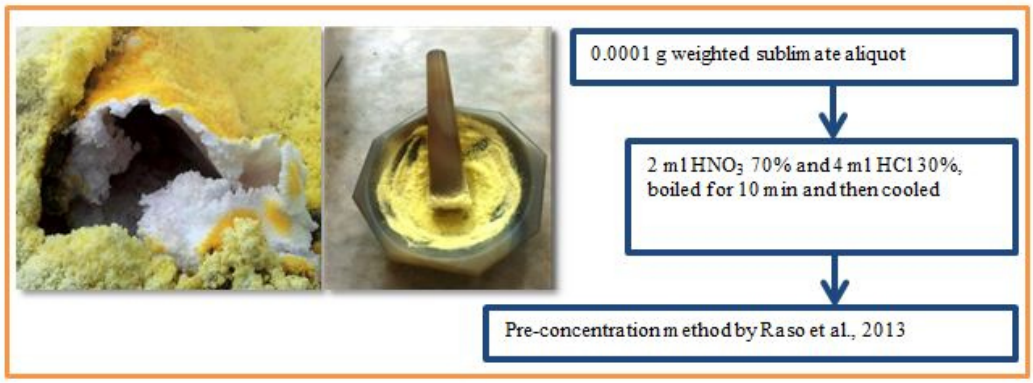

Fig. 3.9- Sublimates treatment for ICP analyses.

High Arsenic content: problem solving

High concentrations of As (up to 82 g/kg) were measured in the products of sublimation (Fig. 3.10) at the Solfatara (Phlegrean Fields, Italy). The treatment of these samples by the co-precipitation method was not effective. The high Arsenic contents inhibit the ferric hydroxide formation as the effect of the Fe^{3+} removal for the formation of iron arsenate. Increasing the pH, by addition of NH_3, also increases the concentrations of $[AsO_4]^{3-}$ in the solution.

Fig. 3.10- Fumaroles at Phlegrean Fields with the sampling tube for sublimates and arsenic-rich red encrustations surrounding the vents.

The arsenate ion, combining with the Fe^{3+} added to co-precipitate, produces iron-arsenate [$FeAsO_4$] blocking the $Fe(OH)_3$ formation. To determine the REE, Zr and Hf concentrations, while avoiding the occlusion of the cones during ICP-MS analysis, it was necessary to treat the samples according to the methods described by Hogness et al. (1972). The samples underwent two different treatments for comparison purposes.

- A weighed (± 500 mg) sample aliquot was dissolved in 3 ml 20% NH_3 to bring only into solution Realgar (As_2S_3). Subsequently, the solution was filtered to remove Arsenic in solution from the undissolved residue (Millipore™ membranes with 0.45 µm porosity). Hence, as recovered on the filter is dissolved in 2 ml 70% HNO_3.
- Another aliquot of the same sample (± 500 mg) was treated 3 m 35%HCl 8M to dissolve the sulphide of all the metals with the exception of Realgar. The solution was filtered (Millipore™ membranes with 0.45 µm porosity). Both of the resulting solutions were diluted with ultrapure water and analyzed by Q-ICP-MS.

ANALYTICAL METHODS AND OPERATIONAL PARAMETERS

ICP-AES and ICP-MS analyses

The metals present as minor constituents were determined using ICP-AES (JobinYvon Ultima2 at INGV National Institute of Geophysics and Volcanology of Palermo). The measurements were carried out with the spectrometer parameters listed in Table 3.1. The contents of the elements in aqueous solutions were determined with quantitative methods using the calibration solutions in a range 0.5 - 100 mg/L of each element and calculating the weighted regression curve constructed with 10 calibration points. The concentrations of the elements in the analyzed samples were calculated with the spectrometer software (ICP Analyst, version 5.4). The

detection limits (DL) for the ICP-AES measurements were calculated using the following equation:

$$DL\boldsymbol{i} = C\boldsymbol{i} + 3 \bullet \sigma$$

where C***i*** is the average content of an element of interest to the measures in the control samples, and σ is the standard deviation of its determination. The accuracy of the analysis was greater than 5% for elements with C> 5•DL and has not exceeded 10% for elements with C <5•DL. For most of the elements, concentrations were higher than 5•DL.

Tab. 3.1 ICP-AES operating conditions and measurement parameters

PARAMETERS	CONDITIONS
RF generator power	1200 W
Plasma gas flowrate (Ar)	12 l min-1
Auxilary gas flowrate	0 l min-1
Sheat gas flowrate (Ar)	0.4 l min-1
Nebulizer flowrate	1.2 bars
Torch	Fully demountable torch, 3 mm i.d. injector
Nebuliser	concentric nebulizer Meinhard
Spray chamber	Cyclonic
Number of repetitions	3
Integration time for each elements	3 sec
Peaks position, Peaks profiles and Auto-attenuate of signal	adjusted daily to obtain max signal intensity
Washing time	1 min (2% HCl+5%HNO3)
Measured wavelengths (nm)	B 249,773, Si 251,611, Ca422,673, Fe 259,940, K 766,490, Mg 279,079, Na 589,592

Determinations of rare earth (REE), Zr, Hf and other metals present as traces in the samples were carried out using ICP-MS (Agilent 7500ce at INGV National Institute of Geophysics and Volcanology of Palermo) interfaced to spectrometer software (ICP Analyst, version 5.4). The operational parameters are listed in Table 3.2.

For elements having different isotopes, the DL was used for the most abundant isotopes. The accuracy of the analysis was greater than 10% for the elements with C> 5•DL and has not exceeded 20% for the elements with C <5•DL. Even in this case, the concentrations were higher than 5•DL for most of the samples. The concentrations of the analytes in aqueous solutions were determined

by the quantitative method using the calibration solutions in a range from 0.1 to 100 µg/L or most of the elements, from0.05 to 25 µg/L for Zr and from 2 to 2000 ng/L for REE e Hf. The weighted regression line was calculated on 10 calibration points. All data was processed for calibration and quantitative measurements in the samples were made using ICP software (ICP Mass Hunter, version B.01.01).The standard solutions used for routine calibration of both instruments were prepared daily with CertiPUR ICP Standards Merck (Germany) and deionized water to 18.2MOhm produced with double system (Elix + Milli-Q, Millipore).

Tab. 3.2 ICP-MS operating conditions and measurement parameters

PARAMETERS	CONDITIONS
RF generator power	1550 W
Plasma gas flowrate (Ar)	15 l min^{-1}
Sample uptake rate	0.400 ml min^{-1}
Carrier argon flow rate	0.75 l min^{-1}
Make-up argon flow rate	0.22 l min^{-1}
Torch	Quartz
Nebuliser	MicroMist 200 µl
Sampler and Skimmer Cones	Nickel
Number of repetitions	5
Ion lens settings, Electron Multiplier, Resolution/Axis mass and Torch position	adjusted daily to obtain the best. signal/background ratio with 10 ppb solution of Li, Co, Y, Ce, Tl
Washing time	1 min (2% HCl+5%HNO_3)+1 min (5% HNO_3)
Oxide $^{156}CeO^+/^{140}Ce^+$ ratio	< 1.5%
Double charged $^{70}Ce^{++}/^{140}Ce^+$ ratio	< 2%
Measured Isotope:	^{89}Y, ^{90}Zr, ^{139}La, ^{140}Ce, ^{141}Pr, ^{143}Nd, ^{147}Sm, ^{151}Eu, ^{158}Gd, ^{159}Tb, ^{161}Dy, ^{165}Ho, ^{167}Er, ^{171}Yb, ^{175}Lu, ^{178}Hf.
On-line Internal Standards	^{103}Rh, ^{115}In and ^{185}Re 8µg L^{-1}

The assessment of the analytical precision of REE, Zr and Hf measurements was hard to carry out since, to the author's knowledge, aqueous standard reference materials with REE, Zr and Hf concentrations referenced or simply indicated are not known. Hence, as previously carried out by Raso et al. (2013), three aliquots (one litre each) of NASS-6 (distributed by National Research Council of Canada) were treated as water samples according to the above mentioned procedure and the concentrations obtained compared with those previously reported in literature (Raso et al., 2013 for Zr, Hf and REE, Willie and Sturgeon, 2001; Shaw et al., 2003; Sohrin et al., 2008; Zhu et al. 2009 only for REE) and values reported in Table 3.3.

Tab. 3.3 Concentrations inNASS-6standard

	NASS-6				NASS-5			
	Raso et al. (2013)	±σ	this study	±σ	REF*	±σ	Zhu et al. (2009)	±σ
	pmol l^{-1}							
^{89}Y	188.55	16.33	167.72	15.48	nd	nd	nd	nd
^{90}Zr	255.65	37.34	235.18	36.64	nd	nd	nd	nd
^{139}La	91.22	3.17	101.08	3.22	87.83	5.76	86.39	2.16
^{140}Ce	44.04	1.93	39.04	1.76	32.69	3.78	37.54	1.14
^{141}Pr	10.86	14.48	12.49	9.03	12.63	1.21	13.91	0.14
^{146}Nd	44.45	18.72	38.97	17.68	61.03	7.63	60.33	4.85
^{147}Sm	5.39	0.47	6.91	0.47	28.79	2.06	29.92	0.93
^{151}Eu	1.58	0.26	1.91	0.24	1.78	0.26	1.78	0.13
^{156}Gd	9.15	9.66	8.33	9.77	9.98	1.08	11.25	0.57
^{159}Tb	1.45	1.51	1.13	1.41	1.57	0.25	2.33	0.25
^{163}Dy	10.03	1.42	9.17	1.40	10.65	0.98	11.45	0.31
^{165}Ho	1.87	0.12	1.69	0.11	2.35	0.24	2.65	0.24
^{166}Er	10.40	1.61	9.21	1.46	8.07	0.78	8.91	0.48
^{169}Tm	1.42	0.53	0.95	0.51	0.95	0.18	1.12	0.12
^{172}Yb	7.28	0.92	6.53	0.87	6.59	0.87	8.09	0.98
^{175}Lu	1.49	0.23	1.26	0.23	1.09	0.17	1.20	0.11
^{178}Hf	4.99	0.67	6.28	0.62	nd	nd	nd	nd

"nd" stands for non-detected

Scanninig Electron Microscopy

Scanning Electron Microscopic (SEM) observations and EDS spectra were carried out on selected sublimate samples. These solids were gently dried under vacuum, mounted on aluminium stubs and gold coated. SEM observations were carried out using a LEO 440 SEM equipped with an EDS system OXFORD ISIS Link and Si (Li) PENTAFET detector that was used to perform EDS spectra in the SIDERCEM S.R.L. x-ray lab (Caltanissetta, Italy).

Speciation Calculations

Dissolved speciation of investigated elements and saturation indexes of minerals have been calculated with the PHREEQC software package (version 3.0.6; Parkhurst and Appelo, 2010). This choice was carried out in order to get only qualitative information about suitable REE, Zr and Hf dissolved speciation is such extreme environments. These calculations were performed using compilations of stability constants of REE, Zr and Hf complexes occurring in the LLNL database, integrated with compilations reported in Millero (1992), Luo and Byrne (2004) and Migdisov et al. (2009).

CHAPTER 4

FUMAROLIC CONDENSATES ANDSUBLIMATES

RESULTS

Alkaline condensates

REE concentrations in the alkaline condensates studied are reported in Table 4.1. These range from 0.02 and 16.17 nmol l^{-1}. The largest values were found in samples collected in the Vulcano fumaroles, Tenerife and Volcano de Fogo Island whereas those collected from the Bocca Grande and Bocca Nuova vents (Phlegrean Fields) show lower REE contents. On Santorini island where lower emission temperatures were found, condensates were not collected since the fluid flux was very low. Since fumaroles at Vulcano and Volcano de Fogo are those with the highest emission temperatures, their larger REE contents in sublimates relative to samples from Tenerife, Phlegrean Fields and Santorini suggest that temperature can play an important part in the REE concentration in volcanic fluids. Y/Ho molar ratio in these materials spans between 40.65 and 84.64, even if a large number of condensates show Y/Ho values close to the chondritic signature (51.2±5; n = 75, Jochum et al. 1986). Fig. 4.1(a) shows that chondritic Y/Ho values prevail in condensates from higher temperature vents samples whereas the few super-chondritic terms are found in samples coming from some vents with lower emission temperature. This evidence suggests that in general Y and Ho behave as a geochemical twin whereas their decoupling is sometimes observed at temperatures close to 200°-250 °C.

Features of REE-normalised to Post Archean Australian Shale (PAAS, Taylor and McLennan, 1995) in alkaline condensates are reported in Fig. 4.2a. Shale-normalised patterns of condensates show Eu anomaly values ranging from 0.21 and 1.88 with prevailing values Eu/Eu*≤1 in samples coming from Vulcano and Phlegrean Fields whereas positive Eu anomaly values are found in condensates collected in Canary and Capo Verde Islands. This finding suggests that

changes of Eu/Eu* values are not related to the temperature of emission vents since those occurring at Vulcano and Phlegrean Fields show the largest temperature range from 145 and 421 °C whereas vent emissions in Canary and Capo Verde Islands have a narrower temperature range from 82 to 285 °C.

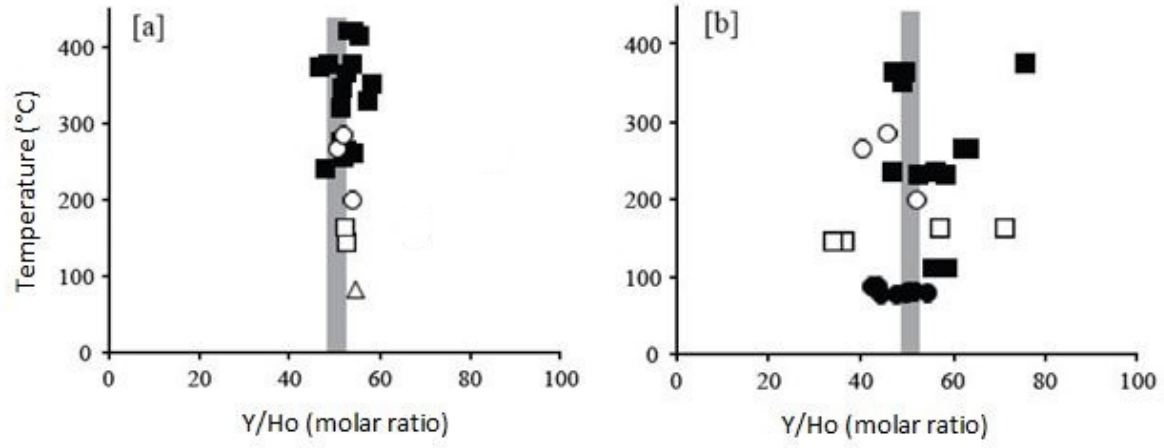

Fig. 4.1- Distribution of Y/Ho values in condensates (a) and sublimates (b) collected in Vulcano Island (full squares), Santorini Islands (full circles), Cape Verde (open circles), Canary Islands (triangle) and Phlegrean fields (open squares).

The occurrence of positive Gd anomalies is another characteristic feature of shale-normalised REE patterns found in condensates, especially from fumaroles with temperature between 400° and 260°C ($1.3 \leq Gd/Gd^* \leq 8.9$). On the contrary, Gd/Gd^* values are lower in those collected in emission vents with temperature between 82° and 250°C ($2.1 \leq Gd/Gd^* \leq 8.9$).

The amplitude of Gd anomaly is calculated according to the equation:

$$\frac{Gd_n}{Gd^*} = \frac{2 * Gd}{Eu_n + Tb_n} \quad (1)$$

(Alibo and Nozaki, 1999) depends on the HCl/HF ratio of fluids in the highest temperature condensates (Fig. 4.3). This evidence suggests that Gd and other REE are preferentially transported as chloride complexes in high temperature fluids (Haas et al., 1995; Gilbert and Williams-Jones, 2008; Pokrovski et al., 2013). In condensates from lower temperature fumaroles this covariance is not observed, resulting hence related to the emission temperature.

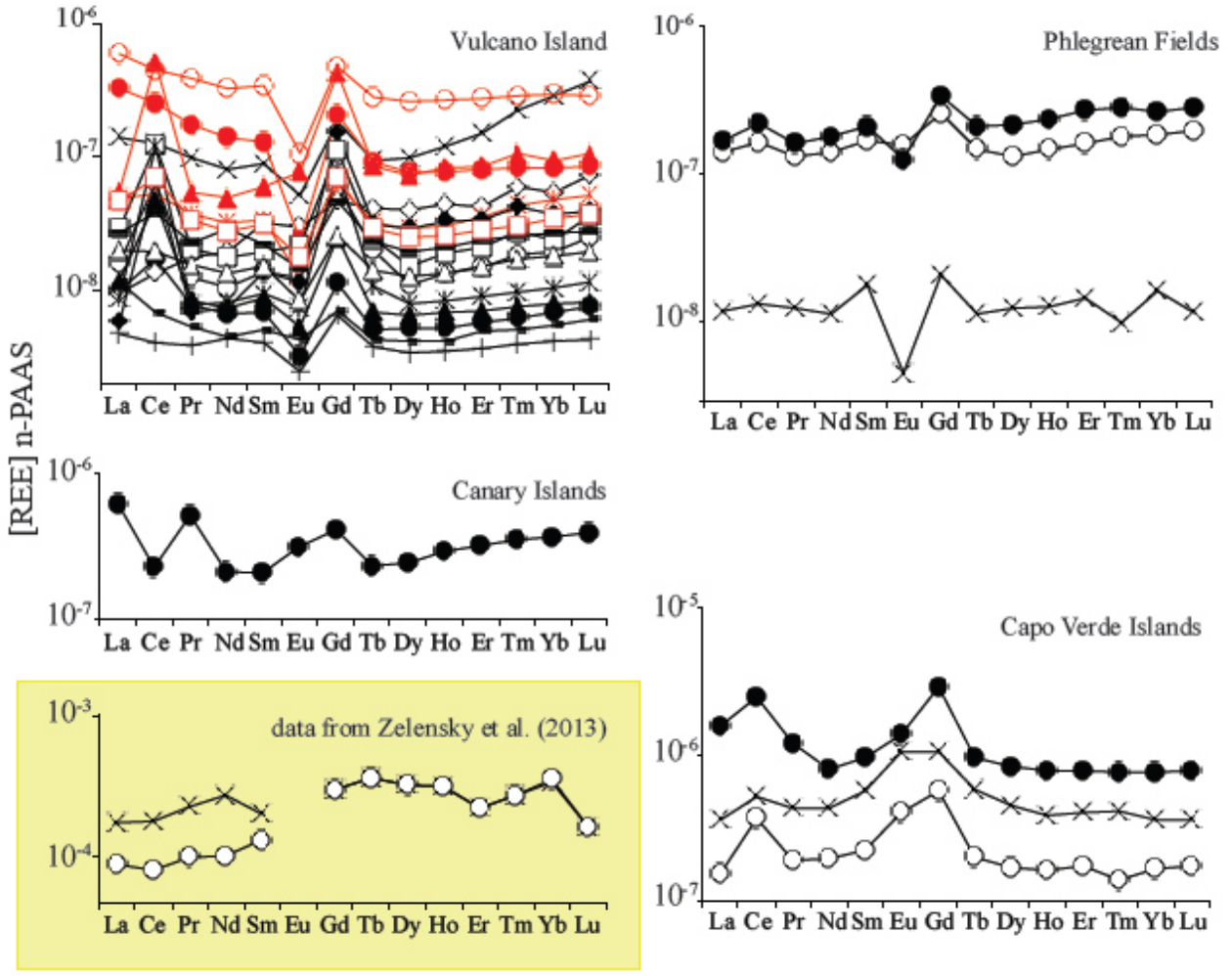

Fig. 4.2a - Shale normalised REE concentrations (vs. PAAS) measured in alkaline condensates from investigated areas. REE distributions in condensates from Erta Ale volcano (Zelensky et al., 2013) are reported for comparison.

Positive Gd anomalies are also coupled with significant Ce anomalies ($0.4 \leq Ce/Ce^* \leq 10$) whose amplitude is calculated according to the equation:

$$\frac{Ce_n}{Ce^*} = \frac{2 * Ce_n}{La_n + \Pr_n} \quad (2)$$

((Alibo and Nozaki, 1999). Both in equation 1 and 2 the suffix n indicates that normalised REE concentrations are used for calculation. Gd* and Ce* are the expected normalised Gd and Ce concentrations compared to its neighbours Tb-Ho and La-Pr, respectively. Figure 4.4 shows that there is a positive relationship between Gd/Gd* and Ce/Ce* and the observed covariance is more

evident in vents with temperatures ranging between 400° and 260°C. At lower temperatures, Ce/Ce* and Gd/Gd* values in condensates are clustered around 2.

The relationship observed in Fig. 4.4 represents further confirmation that chloride-complexes are responsible for the REE transport in volcanic fluids. In fact, Ce and Gd usually have a different geochemical behaviour in the REE series. Ce is coherent with other light REE (LREE) in low oxygen fugacity condition occurring as Ce(III). Ce (III) and other LREE as well, have larger particle reactivity compared to heavier REE (HREE). Moreover, Ce occurs as Ce(IV) precipitating as CeO_2 under oxidizing conditions (Byrne and Sholkovitz, 1996). On the contrary HREE, mainly Gd, preferentially remain in the dissolved phase during solid-liquid processes (Erel and Stolper, 1993; Byrne and Li, 1995). As a consequence, the coupled Ce and Gd behaviour is expected only during the formation of chloride-complexes at temperatures ranging between 400° and 250°C when the stability of $[(Gd,Ce)Cl_3]^0$ and $[(Gd,Ce)Cl_4]^-$ species is larger relative to those formed with their neighbours (Flynn and Burnham, 1978; Haas et al., 1995). Therefore, findings of Fig. 4.4 represent further evidence that the REE transport in the investigated fumarolic fluids occurs as Cl-complexes and lead to the growth of Ce and Gd in a narrow temperature range, probably between 250° and 400 °C.

Another indication regarding the role played by Cl-complexes in the REE transport in the fluids studied is the relationship between the slight growth of the shale-normalised REE patterns from Tb to Lu ($0.25 < Tb/Lu < 1.61$) and the HCl/HF molar ratio in fluids (Fig. 4.5). Therefore, our data indicates that the chloride complexation is the main factor influencing REE transport in the volcanic fluids studied. Since REE^{3+} are considered hard acids forming strong aqueous complexes preferentially with hard bases as F^-, SO_4^{2-}, CO_3^{2-} OH^-, PO_4^{3-} (Pearson, 1963), their REE complexation via chloride complexes provide the further suggestion that REE transport in volcanic fluids occurs as gaseous species rather than in aqueous droplets nebulised in gaseous flux.

Zr concentrations in the condensates representative of the gaseous fraction of the residual volcanic fluids range from about 480 to 21000 pmol l^{-1} in the Vulcano island samples, from about 200 to about 4000 pmol l^{-1} for the Phlegrean Fields and from about 3500 to 6000 pmol l^{-1} at Cape Verde and the Canary Islands (see APPENDIX Tab. 4.1).

In the same samples, Hf concentrations span between 2-210 pmol l^{-1}, 2-42 pmol $l^{-1}$and 60-82 pmol l^{-1}, respectively. It follows that the Zr/Hf molar ratios in the condensate are distributed on chondritic terms up to significantly super-chondritic values. These findings show a significant linear relationship that connects the concentrations of Zr and Hf in the condensate samples (Fig. 4.6). In Fig. 4.6, the angular coefficient of the calculated alignment for the samples from Vulcano island is somewhat higher than that calculated for the samples from other volcanic systems, ranging from about 100 to about 75. Considering that the fumaroles from Vulcano island are those highest in temperature, this evidence suggests that, similarly to what is observed for the REE, the efficiency of the Zr and Hf transport in volcanic fluids increases with temperature and this increase leads to a greater enrichment in Zr of residual fraction of the fluids after sublimation occurred.

Sublimates

REE concentrations in the sublimates studied are reported in Table 4.2 and show larger REE concentrations relative to condensates. In sublimates, REE values range from 0.18 to 213.68 μmol kg^{-1} being about three orders of magnitude higher relative to the whole REE contents in alkaline condensates. The largest REE concentrations were found in sublimates collected in the Phlegrean Fields and Santorini fumaroles whereas lower concentrations occurred in samples coming from the Vulcano and Fogo Island vents. This evidence is opposite to findings in alkaline condensates where the largest REE contents were found in higher temperature emissions at Vulcano and Fogo Island. Therefore it represents further confirmation that the REE distribution between alkaline condensates and associated sublimates in volcanic fumaroles is a cause-and-effect related process.

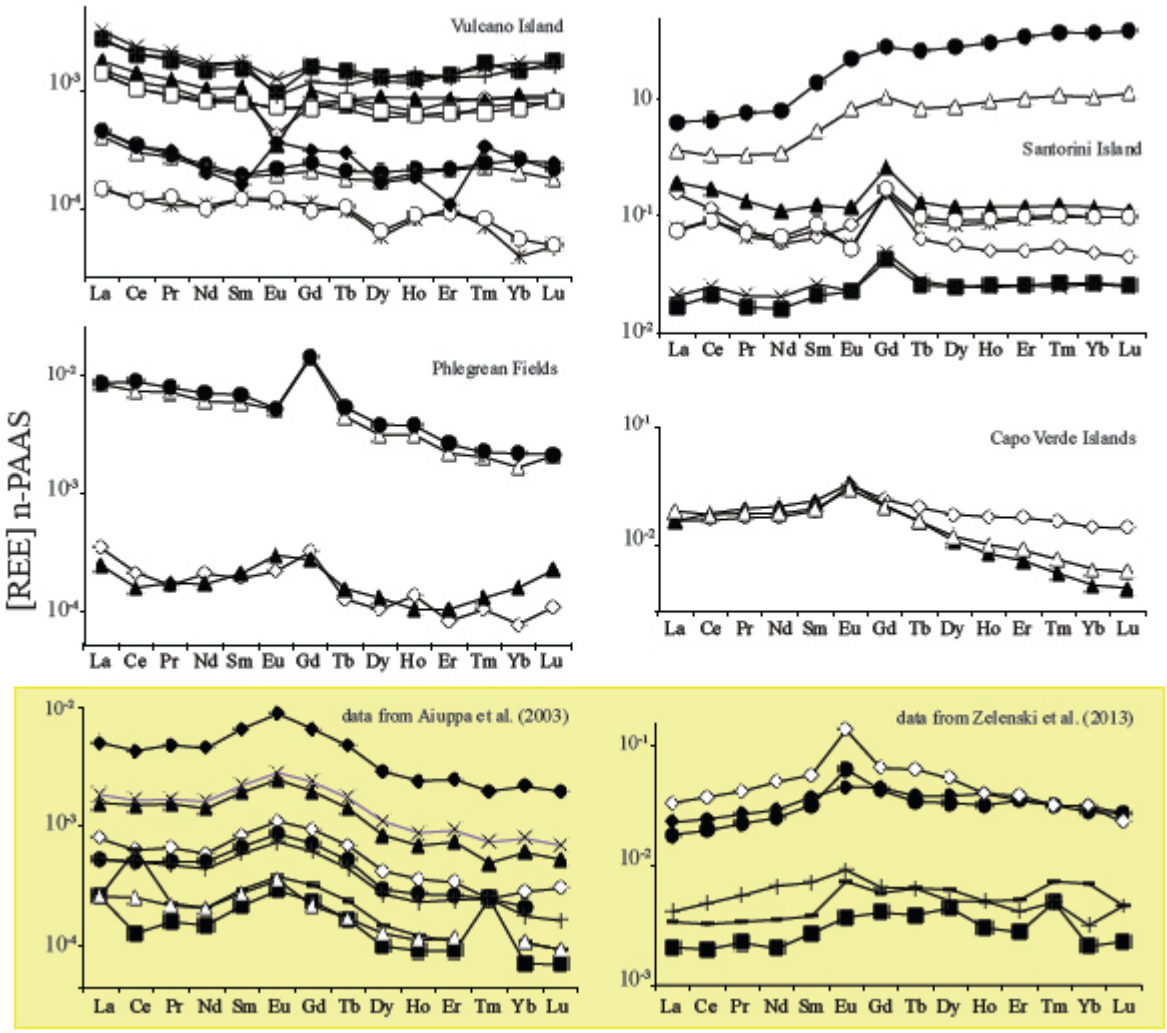

Fig. 4.2b - Shale normalised REE concentrations (vs. PAAS) measured in sublimates from investigated areas. REE distributions in sublimates from Erta Ale volcano (Zelensky et al., 2013) and in plume particles from Mt. Etna (Aiuppa et al., 2003) are reported for comparison.

Y/Ho molar ratio in sublimates span between 34.1 and 103.1 and several sublimates show chondritic values around 50-54. According to evidence reported for alkaline condensates, Fig. 4.1(b) shows that super-chondritic values are prevailing in sublimates especially for temperatures ranging from 130 to 250 °C.

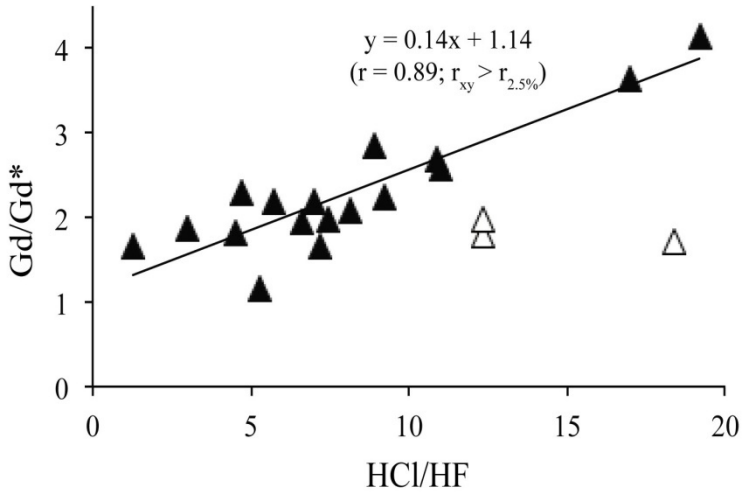

Fig. 4.3- Relationship occurring be-tween Gd anomaly and HCl/HF molar ratio values in condensates from higher temperature fumaroles (full triangles) and lower temperature vents (open triangles).

These findings are consistent with Y/Ho behaviour in alkaline condensates showing preferential Ho scavenging relative to Y at lower temperature. Figure 4.2b shows that shale normalised REE patterns show different features. Sublimates from Vulcano fumaroles show light REE, from La to Nd (LREE), enrichments relative to intermediate (MREE) and heavy REE (HREE) according to the sequence LREE>HREE>MREE. Sublimates from Phlegrean Fields have progressively decreasing patterns according to the sequence LREE>MREE>HREE.

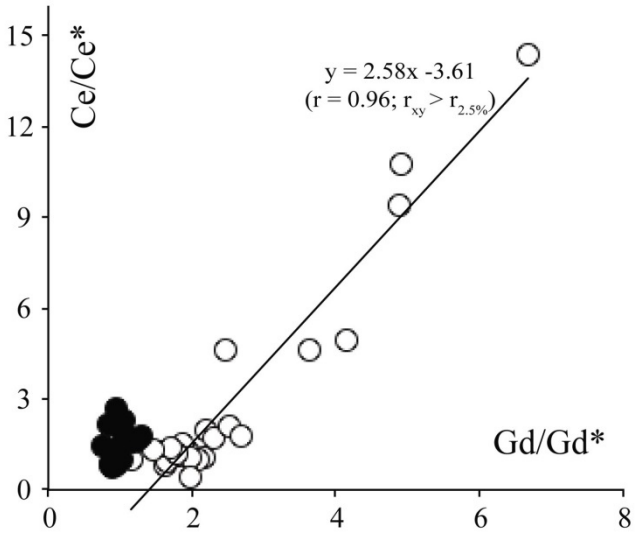

Fig. 4.4- Amplitude of Ce and Gd anomaly values in condensates (open circles) and sublimates (full circles). The occurring linear relationship observed in condensates is reported.

Shale normalised patterns of sublimates from Santorini show progressively increasing patterns with opposite feature relative to those found in Phlegrean Fields whereas patterns of sublimates from Fogo Island are enriched in MREE according to the sequence MREE>LREE≈HREE. These shale-normalised REE findings are summarized in Fig. 4.7 in terms of $(La/Sm)_n$ and $(Tb/Lu)_n$ ratios.

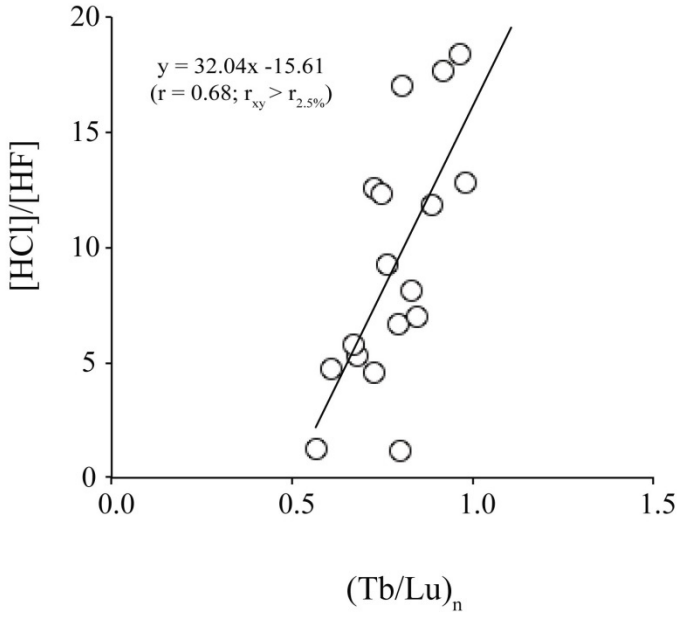

Fig. 4.5- Relationship occurring between Tb/Lu and HCl/HF molar ratio values in condensates. The significant linear relationship testifies the key role played by chloride species into the REE transport in vapour phase.

As shown in Fig. 4.4, the amplitude of Ce anomaly in sublimates is not related to Gd/Gd* differently from in condensates. This lack of correlation further corroborates the indication that the Gd/Gd*-Ce/Ce* relationship in condensates occurs as a consequence of the REE transport in the vapour phase being unrelated to the sublimation. Hence, in sublimates usually Ce anomalies of low significance are found ($0.9 \leq Ce/Ce^* \leq 1$) and positive Ce anomaly values are found only in sublimates from Santorini island, probably due to the large Fe concentration characterising the hydrothermal system in Santorini (Varnavas and Cronan, 2005). This suggestion supports the oxidative Ce scavenging as CeO_2 during the precipitation of Fe-oxyhydroxides occurring in these sublimates (Bau and Koschinsky, 2009 and references therein).

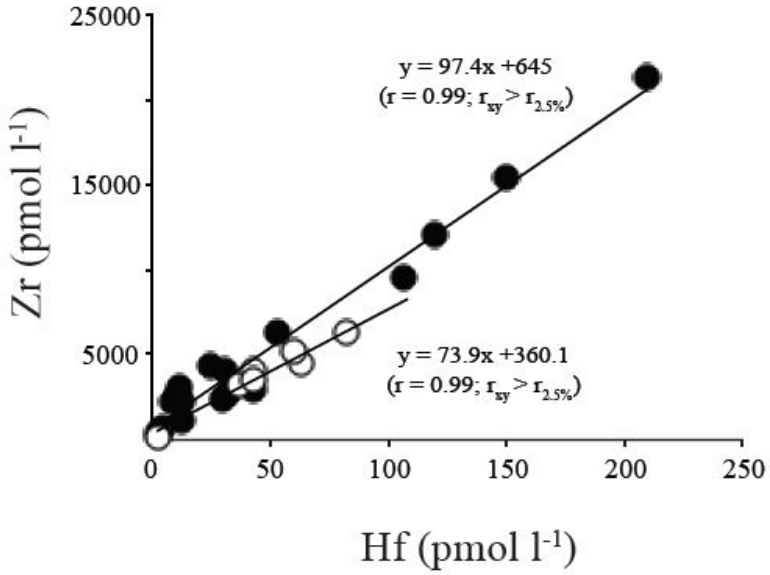

Fig. 4.6-Linear relationship between Zr and Hf concentrations in the alkaline condensates samples. The angular coefficient forthe high-temperature fumaroles (full circles) is higher than samples from the low-temperature fumaroles (open circles).

As observed for the REE, Zr and Hf are also enriched in sublimates, while still leaving in the remaining gaseous fraction a concentration greater than that left by REE. Therefore, these results suggest that the sublimation process is less efficient in distilling a depleted fraction in Zr and Hf than REE. Moreover, the fractionation degree is higher for Hf which is enriched in sublimates more than Zr. As a result, the concentrations of Zr span between about 1.3 10^5 to more than 4 10^6 pmol kg^{-1}, between 1.7 10^5 and 1.1 10^6 pmol kg^{-1}, between 1 10^7 and 1.7 10^8 pmol kg^{-1}, at Vulcano island, Phlegrean Fields and in other studied areas, respectively (Tab. 4.2).

Against this background, as was to be expected from the data for the condensates, the Zr/Hf ratios are mainly sub-chondritic. This confirms the greater capacity of the volcanic fluids to transport Zr rather than Hf in the gas phase. This point of view represents a new contribution to this field of research because, to the author's knowledge, there are not informations about the degree of the Zr and Hf mobilization in high-temperature volcanic fluids in natural systems, for which it has so far been considered that the hydrolysis processes and transport of elements "refractory" as Zr and Hf

have taken place both in the gas phase and in the aqueous medium in a similar way (Pokrovski et al., 2013 and references therein).

DISCUSSION

These findings suggest that the REE transport in fumarolic fluids is determined by the formation of Cl-complexes in the volcanic areas studied regardless of their geological setting in subduction (Santorini, Vulcano) and distensive (Phlegrean Fields) tectonic domains or hot spots (Canary and Cape Verde islands). This suggestion is corroborated by the linear relationship observed between the amplitude of Gd anomaly and HCl/HF (Fig. 4.3) and by the influence of the latter ratio on the shape of shale-normalised REE patterns (Fig. 4.5). Both these findings are consistent with the results of Haas et al. (1995) showing that the amplitude of Gd anomaly is characteristic of the stability constants of several chloride-REE complexes and the largest stability constants for Gd-chloride species is more noticeable for $[REECl_3]^0$ complex. Although the findings reported by Haas et al. (1995) have been recently considered with some caution for temperature exceeding 250 °C being values extrapolated from ambient temperature data (Migdisov and William-Jones, 2014 and references therein), is accepted that Haas's data underestimate the experimentally determined stability constants (Migdisov and William-Jones, 2007; Migdisov et al., 2009). On the other hand, also results reported by Migdisov et al. (2009) are not obtained during field researches by resulting from experimental determinations under lab conditions.

$[GdCl_3]^0$ is the Gd-complex, where the number of the chloride ions directly bound to the coordinating atom corresponds to that experimentally found during X-ray synchrotron analyses carried out between 300° and 500 °C, representing the temperature range where $[REECl_3]^0$ complex is more stable (Mayanovic et al., 2007). Therefore, the lack of correlation reported in Fig. 4.3 for Gd anomaly and HCl/HF data in samples from fumaroles with temperatures lower than 250° is explained by the reduced stability of $[REECl_3]^0$ complex in lower temperature fluids. Haas et al. (1995) report that $[CeCl_3]^0$ and $[GdCl_3]^0$ are the chloride-REE complexes with the highest

stability constant. Moreover, the key role played by the temperature on the stability of chloride-REE complexes is also enhanced in Fig. 4.2 by the absence of Ce and Gd anomaly in condensates from the Erta Ale fumaroles (Zelenski et al., 2013) formed at about 1000 °C, then far from the stability field of Cl-complexes (Sheng and Liu, 2000). This high emission temperature involves a more limited fractionation along the REE series and leads to a more "refractory" behaviour of these elements than are associated with the silicate aerosol (Zelenski et al., 2013).

If the Ce/Ce* vs. Gd/Gd* relationship in condensates suggests that these elements are partitioned in gaseous phase, observed Eu/Eu* values both in condensates and in sublimates can represent evidences on interactions of volcanic fluids with outcropping rocks in studied areas. In Vulcano and Santorini negative Eu anomalies characterise the normalised REE patterns of volcanic rocks (Fulignati et al., 1999; Bailey et al., 2009) and similar features are also found in REE patterns of alkaline condensates and sublimates. Similarly, positive Eu anomalies are reported in REE patterns of condensates and sublimates coupled with analogous Eu/Eu* values in rocks of Isla de Fogo (Escring et al., 2005). On the contrary, although Phlegrean volcanic rocks show negative Eu anomalies (Pappalardo et al., 1999), less reducing conditions in volcanic fluids from Phlegrean Fields fumaroles and large Fe and As contents in these fluids allowed a preferential Eu scavenging onto sublimate surfaces producing slight positive Eu anomalies in these materials, in agreement with observed REE distributions evidenced in hydrothermal sulphates (Humphries and Bach, 2005; Ogawa et al., 2007).

The results obtained demonstrate that the sublimate concentrates REE transported in high temperature volcanic fluids one thousand times more than the residual gaseous phase. Moreover, different features observed in shale-normalised patterns of sublimates and condensates indicate that REE are fractionated during volcanic sublimation. Comparing REE patterns of sublimates with those calculated from the Erta Ale volcano (Zelenski et al., 2013), similar features are observed in terms of middle REE (MREE) enrichments relative to light and heavy REE (LREE and HREE, respectively). As a consequence, sublimates from Erta Ale fall close to those collected at Isla de

Fogo (Cape Verde Islands) and Phlegrean Fields in Fig. 4.7. Considering that the temperatures of these fumaroles are different (145 °C, between 200 and 266 °C, 1084 °C, at Phlegrean Fields, Isla de Fogo and Erta Ale, respectively) REE behaviour observed in these sublimates should not be influenced by the emission temperature. A possible explanation of the MREE enrichment shown in sublimates could be provided by recognising similar evidence in plume particles from Etna (Aiuppa et al., 2003) and in anhydrite samples from several submarine hydrothermal fields (Bach et al., 2003). The non-silicate fraction of volcanic plumes is mainly formed by sulphur-bearing compounds (Oppenheimer et al., 2013 and references therin), which, like sublimates, consist of a wide spectrum of oxides, sulphates and halides (Bau and Moller, 1992; Cheynet et al., 2000; Mather et al., 2003; Aiuppa et al., 2003). Very often these solids are Na- or Ca-rich phases where REE can be scavenged through an electrostatic mechanism, complexed onto surfaces according to an inner-sphere mechanism, or co-precipitated according to a crystal-chemical control. The REE occurrence as $[REECl_3]^0$ complexes in the volcanic fluids studied avoids the fractionation of these elements onto the same sublimate surface, because of the gaseous REE-complexes have the same charge. The surface complexation according to an inner-sphere mechanism is questionable since it is usually coupled to M-type tetrad effects in REE patterns (Kawabe, 1992) of sublimates that were not recognised. Therefore, the possibility that a crystal-chemical control can drive the features observed in REE patterns of sublimates is postulated. The same suggestion was made by Bach et al. (2003) to explain MREE enrichment characterising the shale normalised patterns of hydrothermal anhydrite samples from Manus Basin (Pacific Ocean) as a consequence of the crystal-chemical control on the REE substitution for Ca^{2+} in anhydrite crystal lattice. This indication is corroborated by similar REE behaviour during carbonate (Terakado and Masuda, 1988; Zhong and Mucci, 1995), sulphate (Kagi et al., 1993) and phosphate (Reynard et al., 1999) crystallization and might be expected also for Na^+-REE substitution, Na and Ca having similar ionic radii in six and eight-folder coordination (Shannon, 1976). Since Eu and other MREE are those having the closest ionic radii relative to Ca and Na, a characteristic “bulge” shaped REE

patterns centred on Eu would be expected as a consequence of REE partitioning during sublimation driven by the crystal-chemical control.

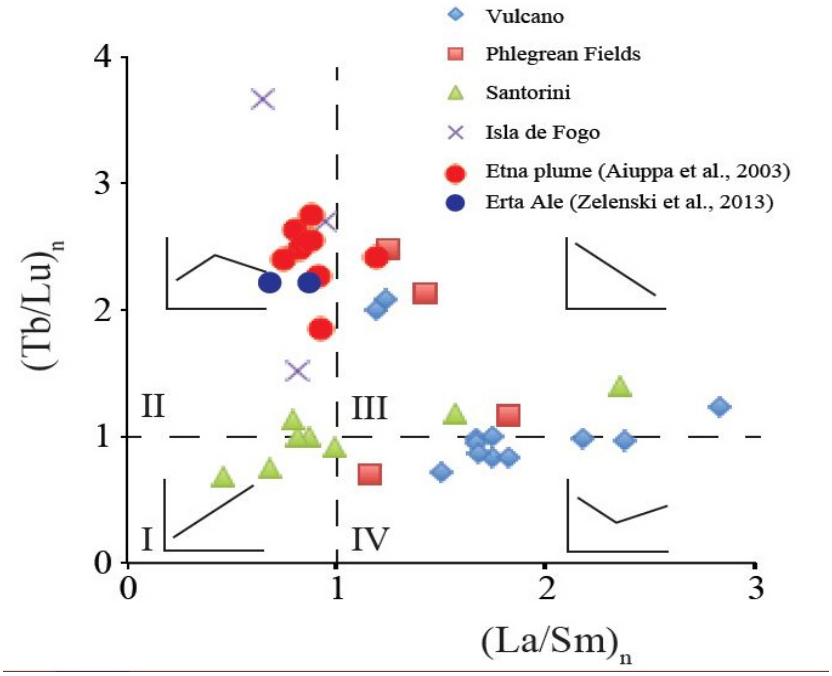

Fig. 4.7- Features of shale-normalised REE patterns in sublimates from studied areas in terms of La/Sm and Tb/Lu normalised ratios. Reference samples (Aiuppa et al., 2003; Zelenski et al., 2013) are reported for comparison.

Therefore, the REE behaviour in sublimates falling in quarter II of Fig. 4.7 is consistent with the deposition of solids incorporating elements close to Ca^{2+} and Na^{+} dimensions. On the contrary, if crystallising solids incorporate ions larger that Ca^{2+}, as Sr^{2+}, Ba^{2+}, Pb^{2+} and NH_4^{+}, the preferential LREE partitioning in sublimates should be observed according to the lanthanide contraction rule and sublimates will fall in quarter III of Fig. 4.7.

Confirmation of the crystallographic control of the REE fractionation in sublimates is provided by the geochemical behaviour of several sublimates from Vulcano fumaroles. These materials contain both several large ions bearing halides (NH_4^{+}, Bi^{3+}, Cd^{2+}, Pb^{2+}) and sulphosalts associated to Zn and Fe sulphides (Vurro et al., 1999; Cheynet et al., 2000; Garavelli et al., 2013). As a consequence, the preferential LREE and HREE relative to MREE incorporation should be expected substituting larger and smaller ions that Ca^{2+}, respectively, as showed in sublimates falling in quarter IV. Therefore, the hypothesis that the REE behaviour observed in sublimates can

be induced by a mineralogical control cannot be ruled out. The preferential MREE partitioning in sublimates and aerosol particles is also consistent with effects induced by dissolution of these materials in the environment. Recently, Tepe and Bau (2014) justified with the dissolution of freshly-erupted plume particles the unusual MREE enrichment observed in river waters from southern Iceland immediately after explosive eruptions of the Eyafjallajökull Volcano. Therefore, the REE contents of sublimates and the volcanic gas phase can also be quickly involved in the global geochemical circulation of the surrounding environment, as previously indicated by several research studies on other elements (Nriagu, 1989; Hinkley, 1991; Hinkley et al., 1999; Mather et al., 2003; Calabrese et al., 2011).

Considering the lack of data on Zr and Hf transport in volcanic fluids, some studies were carried out to determine the stability constants for halogen and sulfate complexes of Zr and Hf according to a quantum mechanic approach (Pershina et al., 2002; 2006; 2014). Although far from the complexity of the natural system, this approach is still the only one that enables us to predict the speciation of Zr and Hf in natural systems. Alternatively, a recent study by Louvel et al. (2013), also based on ab-initio calculation associated with laboratory experiments, suggests that the speciation of Zr and Hf is dominated by $[Me(H_2O)_8]^{4+}$ (with Me = Zr, Hf) in fluids at pressures and temperatures compatible with the subduction environment, without finding evidence of halogen complexes up to temperatures close to 420 ° C. In the absence of data in aqueous systems, indications about the relative stability of the halogen-complexes of Zr and Hf, a qualitative scenario of the behaviour of these elements can be suggested by the mutual behaviour during extraction processes of these metals in systems in which they are present as $[MeCl_4]$ complexes (Czerwinski et al., 1994; Kacher et al., 1996). These studies have shown that the Zr extraction in the volatile phase is more efficient than the Hf showing a higher sensitivity toward surfaces. A larger tendency to form stable halogen complexes of Zr and Hf is also reported by Peshina et al. (2002) confirming a larger stability of halogen-complexes of Zr rather than Hf.

Writing a generic complexation reaction in a medium in which both Zr and Hf aquo-ion are stable:

$$M[(H_2O)_8]^{4+} + 6HX \rightleftharpoons M[(H_2O)_7]^{3+} + HX + ... \rightleftharpoons [MX_6]^{2-} + 8H_2O + 6H^+$$

where M is Zr or Hf and X is F^- or Cl^-, complex formation occurs more easily for Zr than for Hf. However, F-complexes will formas F content attains 0.02 M whereasa chloride concentration spanning between 8 and 12 M is needed for Cl-complexes (Pershina et al., 2002). Therefore, [(Zr, Hf)$F_2(H_2O)_6]^{2+}$complexes could occureasier in high temperature volcanic fluids that Hf species although to a limited extent. Our findings agree with this suggestion and are consistent with the sub-chondritic values reported by Bau (1996) in highly evolved magmatic rocks and the sub-chondritic terms of Zr/Hf in sublimates, compared to super-chondritic values in fumarolic condensates.

The larger particle reactivity of Hf relative to Zr onto sublimates is hard to explain in terms of electrostatic interactions since it is difficult to model the Z potential of a surface immersed in a fluid stream at such high temperatures. On the other hand, the greater surface reactivity of Hf, compared to Zr, is known in the aqueous medium where it was often justified according to the formation of Coulomb- interactions type (Bau and Koschinsky, 2009).

Environmental consequences

However, the results obtained indicate that sublimates are the main source of REE from the volcanic gas phase, the observed distribution of these elements demonstrates that passive degassing volcanic systems as fumaroles with temperatures ranging between 100° and 400 °C can represent a suitable Gd atmospheric source if REE are transported via Cl-REE complexes. The positive Gd anomaly measured in volcanic gas residue from different fumarolic areas reflects an excess of Gd with respect to its neighbours along the REE series. The amplitude of this 'Gd_{excess}' can be calculated with the following expression:

$$Gd_{excess} = [Gd]\left(1 - \frac{Gd^*}{Gd}\right) \qquad (3)$$

(Moller et al., 2007) where [Gd] is the Gd concentration expressed in molar or weight units and Gd*/Gd is the inverse of Gd anomaly (see eq. 1). We found that Gd excess can reach values up to 161 ng l^{-1} in Vulcano fumaroles and about 12.2 ng l^{-1} in lower temperature emissions in Phlegrean Fields, Cape Verde and Canary Islands. Considering that these areas produce about 42, 556, 68 and 39 tons (*103) y^{-1} of CO_2 (Inguaggiato et al., 2012; Burton et al., 2013; Dionis et al., 2013) and assuming the constant CO_2/Gd concentration ratio in these emissions, we estimate that the Gd flux released from the fumaroles studied is 0.92, 0.08, 0.04 and 0.01 kg y^{-1} for Vulcano, Phlegrean Fields, Cape Verde and Canary Islands, respectively.

The partitioning of some rare earths relative to other elements along the REE series is a difficult process to perform especially under lab conditions. Only the enhanced stability of the Gd^{3+} aquo-ion relative to other REE was postulated to explain the anomalous Gd enrichment reported for REE measurements in ocean waters (Mayanovic et al., 2007) and other natural Gd sources were not known until now. On the other hand, the anthropogenic Gd exploitation in medical practices started from the late '80s when the Gd magnetic properties induced the exploitation of some Gd organic complexes as contrast agents in magnetic resonance imaging (MRI). As a consequence of the discharge of these chemicals in continental waters, the presence of a high level of dissolved Gd compounds in German rivers was progressively found from the mid-1990s (Bau and Dulski, 1996). In 2000, the whole flux of anthropogenic Gd from German hospital wastewaters ranging from 2.1 and 4.2 kg y^{-1} was estimated (Kummeres and Helmers, 2000). These values are of the order of magnitude of the volcanic Gd flux assessed from the fumaroles studied, especially at Vulcano, with the significant difference that chloride-Gd volcanic complexes are highly water-soluble and aqueous Gd^{3+} is highly toxic (Darrah et al., 2009 and references therein). On the contrary, Gd-based MRI contrast agents are considered not dangerous for human health because of their large aqueous stability. This indication suggests that the delivery of highly mobile

Gd-chlorides from volcanic sources can have effects on the Gd distribution in the environment close to volcanic areas. Therefore, further studies are needed to establish if the Gd excess observed in the volcanic systems studied also occurs in other areas where chloride-REE complexes represent the main gaseous species responsible for the gaseous transport of these elements during passive volcanic degassing and establish the temperature of volcanic emission of these sources.

CONCLUSION

Our indications demonstrate that phase equilibria related to the sublimation of the volcanic gas phase cause REE fractionations whose amplitude is related to the emission temperature and REE speciation in the gas phase. REE are mainly concentrated in sublimates and only 1:1000 of their concentration remains in gas residue after sublimation. In alkaline condensates, the formation of REE-chloride complexes at temperatures ranging from 250° to 400 °C led to the growth of Ce and Gd anomalies that progressively decrease with decreasing temperature. As a consequence, gadolinium is preferentially partitioned relative to Eu and Tb in the residual gas phase until producing an out-and-out Gd excess in this phase. The amplitude of this excess, calculated for a year in the fumaroles studied, is of the same order of magnitude as the anthropogenic Gd flux delivered yearly from hospital wastewaters in Germany. Therefore, the passive degassing from fumaroles under the above mentioned conditions can contribute to an environmental Gd supply to the surrounding environment in higher soluble form relative to the anthropogenic sources. The REE signature in sublimates often shows MREE fractionation that closely resembles the REE behaviour both in subaerial plume particles and in authigenic anhydrite formed during the mixing between submarine hydrothermal vents and seawater. This evidence indicates that MREE are enriched in authigenic solids related to the emission of volcanic fluids according to a crystallographic control induced by the larger capability of MREE to substitute for Ca and Na in newly-formed phases.

The results obtained in the study of the behaviour of Zr and Hf during the sublimation of high-temperature volcanic fluids (100 ° - 420 °C) has allowed us to establish that the sublimation process involves a limited fractionation of the Zr in the fluid residual phase with respect to the Hf, which prefers to remain in the sublimates. The mechanism by which this process takes place cannot be hypothesized, but it is worth noting that the fractions of residual fluid, after the sublimation, are characterized by a correlation of the concentrations of Zr and Hf, having a slope near to 100.

CHAPTER 5

HYDROTHERMAL WATERS

RESULTS

Rare Earths

REE concentrations have been measured in the submarine hydrothermal vents of the Volcano and Santorini islands and wells, which are located at different depths in the Vulcano Porto area and the Thera island (Santorini) (see Tab.5.1). Moreover, it was decided to also analyse the natural boiling pools at Vulcano island, which present a good opportunity to study the influence of the atmospheric contribution to these systems.

The ***submarine hydrothermal springs*** span a wide range of concentrations, between 807.7 and 8.6 10^3 pmol l^{-1} and between 2.3 10^4 and 4.9 10^4 pmol l^{-1}, for the thermal springs of Vulcano and Santorini islands, respectively. The Y/Ho ratios (molar ratios) were calculated between 13.3 and 116.1 (Vulcano Island) and from 62.2 to 129.6 (Kameni Islands, Santorini). Most of the samples exhibit super-chondritic ratios, with the exception of some waters from Vulcano island that are characterized by significantly sub-chondritic ratios ($13.3 \leq Y/Ho \leq 34.2$). The latter values suggest that the dissolution of Ho-enriched phases occurs in these waters. In the ***hydrothermal wells and pools***, REE concentrations span between 121.6 and 1.9 10^5 pmol l^{-1} at Vulcano and between 876.5 and 5.6 10^3 pmol l^{-1}at Santorini. The highest concentrations have been measured in the natural boiling pools, acid-sulfate waters located in the isthmus at Vulcano. These waters show the lowest pH values of those found in the investigated waters, up to 2.0 and have Y/Hovalues predominantly sub-chondritic. Super-chondritic terms were found in a few wells at the Vulcano island under acidic pH conditions. Here, Y/Ho values next to the chondritic signature ($Y/Ho \approx 52$, Taylor and McLennan, 1995) are recorded only in one case, suggesting that the REE distribution is probably the result of solid-liquid interactions, to which waters are subject, with the aquiferrocks

and the mineral phases and particulate authigenic. The natural pools are characterized by Y/Ho values from weakly sub-chondritic to chondritic (up to 50.7).

Shale-normalised patterns of REE (Taylor and McLennan, 1995) are different depending on whether the waters have negative or positive Eh values (Fig. 5.1). In the first case, the patterns are poorly fractionated with weak enrichments (HREE) and values of the Y/Ho ratio around the chondritic signature are found. In the waters with positive Eh values, normalised patterns show a greater enrichment in HREE than the light REE (LREE). This is coupled with different behaviour for Y and Ho, which in these waters show molar ratios both super- and sub-chondritic (Fig.5.1). The REE behaviour in the water of two springs on Vulcano island is marked by patterns that show a flat trend, with a slight decrease in normalized concentrations from Gd to Lu. This evidence suggests that the REE are the product of the leaching of solids having a "chondritic" composition of these elements. The atmospheric particulate could represent this type of material, having an almost flat pattern of the normalised REE (Greaves et al., 1999; Censi et al., 2004). I valori di anomalia di Eu nelle acque indagate variano fra 0.27 e 2.49. However, only 4 for samples coming from the island of Vulcano show Eu/Eu* >1. The speciation of REE, computed in the waters investigated, shows that the waters with negative Eh values are those in which the dominant species sulfate- and halogen complexes. Moreover, for these waters it is possible to model an equilibrium or super-saturation with respect to carbonate minerals, mainly dolomite and Mg-calcite. The waters having these characteristics will be henceforth defined as group 1. Instead, clustered in group 2 are the waters with positive Eh values, for which the most abundant species of REE are the carbonate-complexes. In group 2, the waters are mostly saturated or super-saturated with respect to Fe-oxyhydroxides.

Zirconium and hafnium

The concentrations of Zr and Hf measured in the investigated submarine springs, are distributed as follows: Zr=1.2 10^4 - 23.9 pmol $l^{-1}$and Hf= 147.7 - 0.68 pmol l^{-1} for Vulcano island, Zr= 4.1 10^3 - 63.0 pmol l^{-1} and Hf=49.6 - 0.03 pmol l^{-1} for Santorini island (Tab. 5.1).

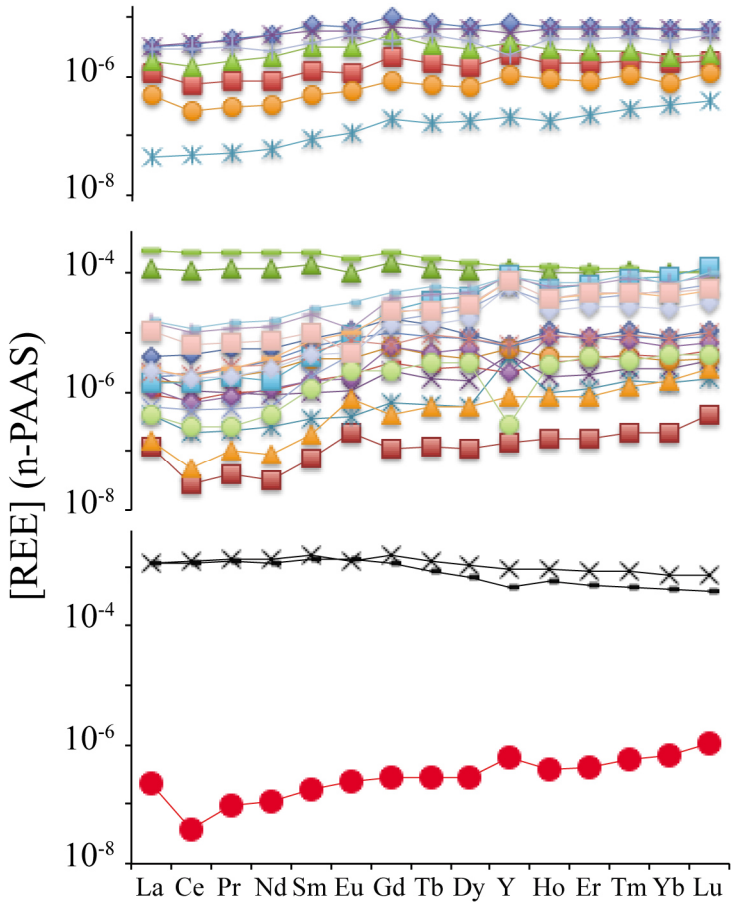

Fig. 5.1- Shale-normalised patterns of REE in hydrothermal waters from Vulcano and Santorini islands. Sea-water (red circles) and , in the lower transept; samples with positive Eh value, in the middle transept; samples with negative Eh value, in the higher transept.

These two elements are significantly linearly related to each other. Fig. 5.2 shows that the waters of group 1 have concentrations of Zr and Hf that display a trend with a slope close to 100, while the samples of group 2 are aligned along a trend with a slope close to 250. The fact that the two groups of waters differ in terms of being saturated or supersaturated with respect to different mineralogical phases, as evidenced by the first speciation calculations, suggests that the mutual

behaviour of Zr and Hf is influenced by the reactivity that the dissolved species of these elements can have in respect to the areas with which they may come into contact.

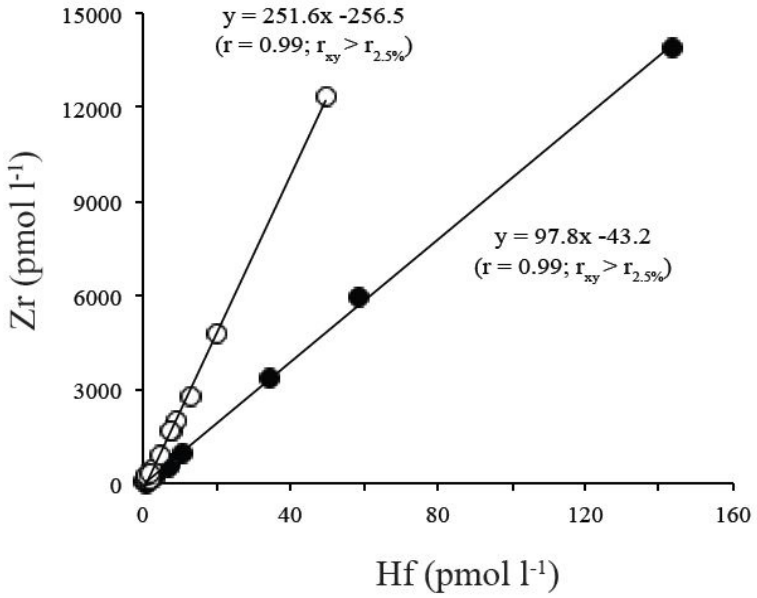

Fig. 5.2- Zirconium and Hafnium relationship in hydrothermal springs from Vulcano and Santorini islands. Open circles represent waters with positive Eh values (group 2), whereas full circles indicate waters with negative Eh values (group 1).

In order to assess this aspect, speciation calculations have been extended to Zr and Hf. They show that the dominant species occurring in the investigated waters are $[Zr(OH)_4]^0$and $[Hf(OH)_5]^-$, respectively. Only in the water of "Vasca" at Vulcano isthmus the dominat Hf specie is $[Hf(OH)_3]^+$ with pH close to 2. This is in agreement with the few items of data for Zr and Hf speciation in natural waters mainly limited to hydroxo-complexes (Byrne, 2002) whereas sulphate- and fluorine-complexes can occur under defined laboratory conditions (Monroy-Guzman et al., 2010; Kalaji et al., 2014). According to the speciation calculations, a different reactivity of Zr and Hf towards solid surfaces is expected in the presence of Coulomb-dominated interactions and this difference can involve Zr-Hf. This aspect deserves further discussion.

SEM investigations of the suspended fraction (ø ≥ 0.45 μm) in studied waters shows that microorganisms occur in waters at Santorini island(group 2) where environmental conditions not so different from those recently found in the Venus Lake at Pantelleria Island occur (Censi et al., 2013). These colonies, together with the high concentration of Fe-oxyhydroxide, could be responsible for the increase in the concentration of Zr and Hf and higher values of the relative ratio observed in the waters of Santorini island.

DISCUSSION

In hydrothermal systems, features of normalised REE patterns are often considered useful indications of the rocks' aquifers and sources of deep fluids (Moller et al., 2003; 2007; 2012). On the other hand, it cannot be excluded that the form assumed by the normalized patterns in hydrothermal water aquifers is rather influenced by solid-liquid separation processes due to the formation of solid authigenic (Censi et al., 2013) and not just as a result of rock-water interactions. In order to evaluate which of the above mentioned processes can be responsible for the geochemical behaviour of REE in the water investigated, the study of the pattern's shape in Fig. 5.1 has been rationalised based on the normalised La/Sm and Tb/Lu ratios. Since REE are subdivided into LREE, MREE and HREE, the normalised ratios La/Sm and Tb/Lu are representative of the splitting LREE-MREE and MREE-HREE, respectively. The use of the aforementioned normalised ratios follows the approach of Leybourne and Johannesson (2008), allowing a quick evaluation of the fractionations between the aforesaid groups of REE, without such representation it would be affected by the presence of geochemical anomalies of REE, which usually occur for Ce, Eu and Gd in natural waters. In this regard, Fig. 5.3 shows that there are no samples whose values of La/Sm and Tb/Lu fall in field III, that is, the field in which there is a clear split of the LREE compared to the other elements in the series.

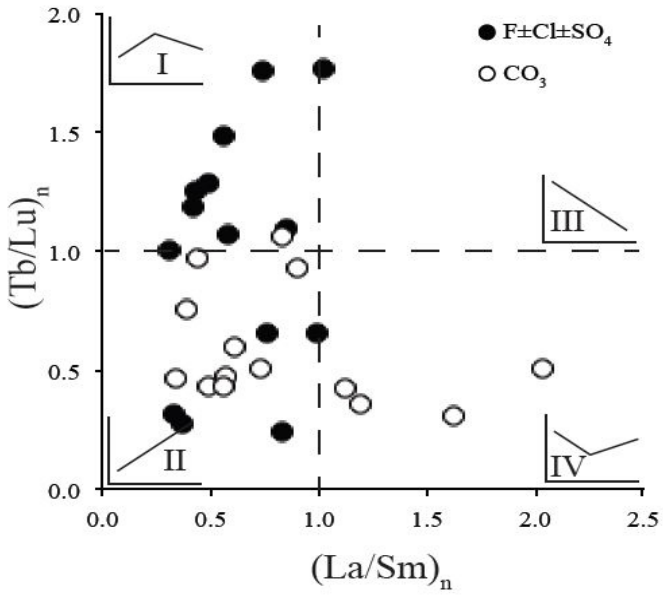

Fig. 5.3- Shale- normalised REE patterns rationalised based on the calculation of the normalised La/Sm and Tb/Lu ratios.

Since the distribution of the REE, characteristic of the rocks making up the aquifers of Santorini and Vulcano, and from which come the investigated waters, is characterised by LREE enrichment (De Astis et al., 1997; Gioncada et al., 1998, 2003; Fulignati et al., 1999; Vespa et al., 2006; Bailey et al., 2009; Gertisser et al., 2009), the absence of the latter evidence in the waters suggests that the distribution observed of REE in the dissolved phase is only partially influenced by water-rock interactions. Instead, the samples of group 1 fall in fields I and II corresponding to monotonic increasing trends of normalised patterns (range I) or characterized by MREE enrichment (range II). Instead, the samples of group 2 fall in the fields II and IV in the graph, which differ from each other only in the degree of LREE enrichment. Furthermore, model calculations indicate that the two groups of water also differ in order to be balanced with carbonates (group 1) and Fe-oxyhydroxides (group 2), as confirmed by the finding of phases in authigenic suspended particulate in the water. On the other hand, though the effect of the water-rock interactions would seem to be less important in determining the geochemical behaviour of REE in the waters, the explanation of the latter is to be found in the speciation of these elements, or

fractionations associated with the formation authigenic phases, as suggested in the case of low-temperature hydrothermal fluids (Bau and Moller, 1992). The effect of the formation of authifenic carbonates and Fe-oxyhydroxides suggested by model calculations in Group 1 and 2 waters could influence the dissolved REE behaviour in studied samples in terms of Y/Ho vs. Eu/Eu* values that are inversely correlated (Fig. 5.4). This evidence is consistent with preferential Eu and Ho partitioning during the crystallization of these solids evidenced by lab experiments (Tanaka et al., 2004; 2008; Qu et al., 2009). The large similarity between the observed linear trends suggests the similar effect played by carbonate and Fe-oxyhydroxide crystallization of REE behaviour in dissolved phase.

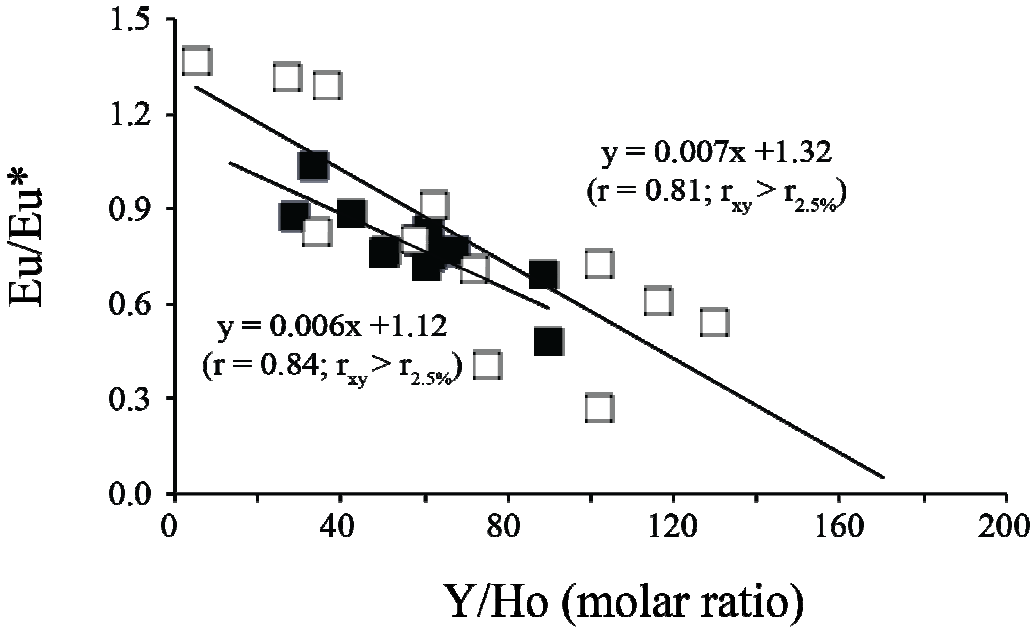

Fig. 5.4 – Relationship between Y/Ho and Eu anomaly values in studied Group 1 (full squares) and Group 2 waters (open squares).

Group 1 waters

In these waters, the REE are present as $[REE]SO_4^+$ (19%-82%), fluoride and chloride complexes (1%-71% e 1% -19%, respectively). The distribution of REE as sulfate complexes does not result in particular fractionations along the series (Haas et al., 1995), whereas the stability of the carbonate complex progressively increases from La to Lu with limited fluctuations (Liu and Byrne, 1998; Ohta and Kawabe, 2000; Luo and Byrne, 2004). The halogen-based complexing,

although with highly dependent temperature patterns (Haas et al., 1995; Migdisov et al., 2009), seems to involve a trend of increasing HREE concentrations in solution (Wood, 1990; Haas et al., 1995; Luo and Byrne 2000) unlike the Cl-complexes whose stability decreases along the series of REE (Wood, 1990; Haas et al., 1995; Migdisov et al., 2009). Due to limited impact of Cl-complex shown by the calculations of the model, as the depletion in LREE (fields I and II of Fig. 5.3) as that in HREE (range I of Fig. 5.3) does not appear to be due to speciation of REE. In order to justify their presence, it can therefore only be suggested that there is a fractionation of REE induced by the formation of authigenic carbonates predicted by the model calculation. Hence, there exists a mineralogical control on the behaviour of REE in the waters of group 1. This is in agreement with the results of Bau and Moller (1992), which show that both the LREE as the HREE are depleted during the crystallization of carbonate from hydrothermal solutions in natural hydrothermal systems of low and medium temperature. Moreover, a mineralogical control on the fate of the REE during the carbonate crystallization is also observed by Terakado and Masuda (1988) during laboratory experiments, when an enrichment in MREE carbonate precipitate is reported in some laboratory conditions. It therefore seems reasonable to suggest that a mineralogical control on the distribution of the REE in the waters of group 1 is consistent with the data collected, at least for most of the samples that fall in field I of Fig. 5.3.

Group 2 waters

These waters, falling in fields II and IV of Fig. 5.3, are enriched with HREE with respect to MREE (fields II and IV of Fig. 5.3), whereas a slight LREE enrichment is sometimes observed in some samples (field IV of Fig. 5.3). In agreement with previous observations, an effect of carbonate complexation can be suggested by the shapes of the REE pattern falling in field II. However, the possibility that the latter features can be caused by the leaching of authigenic solids formed during the between hydrothermal fluids and seawater (Bach and Irber, 1998) cannot be ruled out. Given the hypothesis formed, the latter suggestion can also explain the features observed in REE patterns clustered in field II, Fig. 5.3, whereas those falling in field IV agree with deeper

dissolution of authigenic solids. According to Bach and Irber (1998), waters falling in field II represent those samples where REE leached from authigenic solid was lesser than those falling in field IV. The suggestion that authigenic solids are formed during the mixing between hydrothermal fluids and shallow aquifers in wells or with seawater is consistent with W-type tetrad effects observed that occur especially in submarine spring waters (Fig. 5.4).

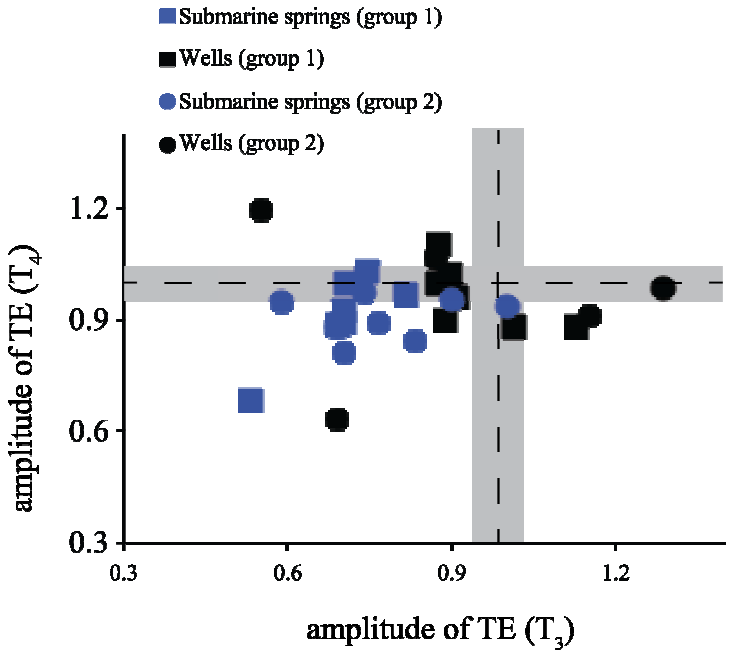

Fig. 5.5 – W-type tetrad effects mainly occur in submarine springs rather than in samples from wells.

These findings confirm that dissolved REE distribution is a consequence of the dissolution by solid interaction (Masuda et al., 1987). Submarine hydrothermal waters show from chondritic to superchondritic Y/Ho values consistently with the preferential Ho removed during the deposition of Fe-oxyhydroxides (Bau, 1999). This scenario is consistent with the relationship observed between Y/Ho values and the amplitude of tetrad effects in a submarine spring from group 2 waters (Fig. 5.6).

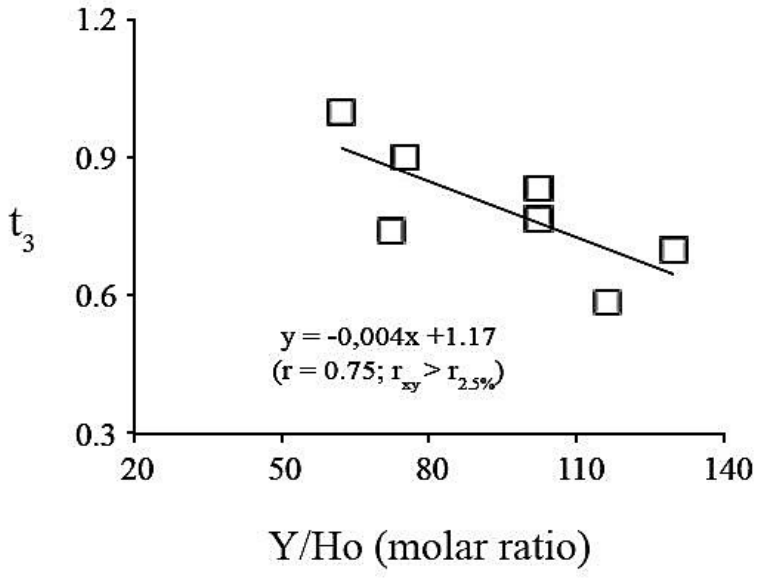

Fig. 5.6- Relationship between amplitude of the W-type tetrad effect and Y/Ho ratio insubmarine spring from group 2 waters.

Y-Ho decoupling can also occur during the authigenic carbonates deposition, as recognised during lab experiments (Tanaka et al., 2008; Qu et al., 2009), and in natural systems (Censi et al., 2014). Therefore, the discovery of a superchondritic marker also in group 1 waters is justified.

Surfaces of Fe-oxyhydroxides are weakly positively charged (Kozin et al., 2013) as carbonate surfaces at pH <8 (Pokrovsky et al.,1999; Pokrovsky and Schott, 1999). Since the dominant species Zr and Hf species in the water studied are $[Zr(OH)_4]^0$ and $[Hf(OH)_5]^-$ respectively, the preferential Hf scavenging relative to Zr is expected and the chondritic to superchondriticZr/Hf signature observed in group 1 and 2 waters is consistent with processes invoked for the waters studied.

However, findings in the larger slope of the group 2 trend in Fig. 5.2 suggest that these interactions are larger between dissolved Hf and in Fe-oxyhydroxide surfaces. This effect could be related to the characteristics of surface roughness of Fe-oxyhydroxides (see Kozin, 2014). But the possibility that interactions between $[Hf(OH)_5]^-$ and Fe-oxyhydroxides can achieve the inner-sphere surface complexation for hafnium cannot be ruled out.

Comparing the Y/Ho and Zr/Hf signature of the waters studied with those collected close to submarine springs at Panarea Island (Aeolian Archipelago) and with Mediterranean seawater not subjected to interactions with deep fluid waters from Vulcano mainly fall in an elliptical field characterised by progressively increasing Y/Ho and Zr/Hf ratios from chondritic values towards superchondritic terms (Fig. 5.7).

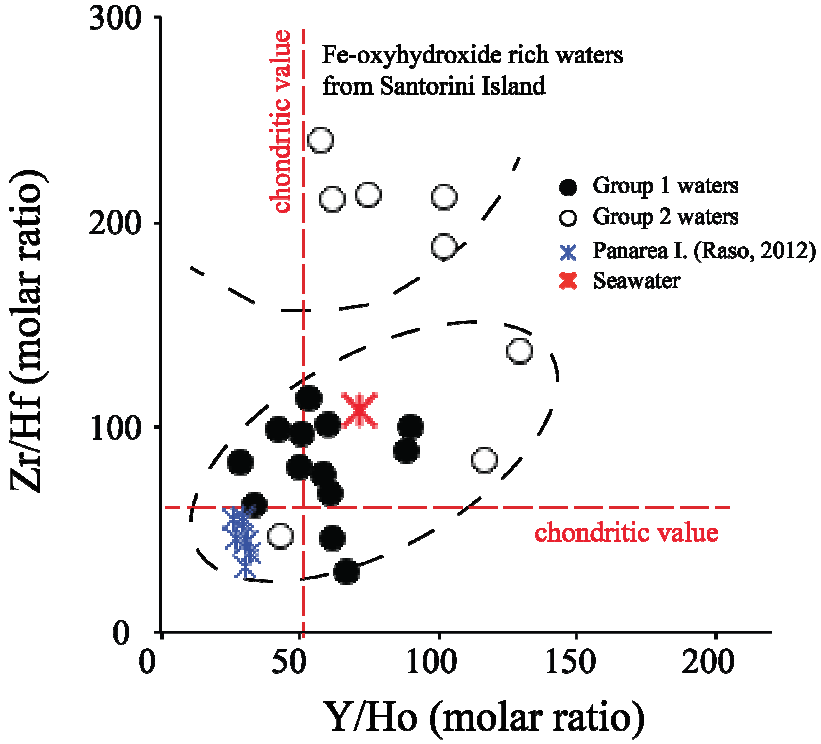

Fig. 5.7 – Distribution of Zr/Hf vs. Y/Ho values in studied waters from Vulcano and Santorini islands. Seawater composition measured far from hydrothermal vents and the composition of hydrothermal vents from Panarea island (Aeolian archipelago) are also reported.

This behaviour suggests that the formation of authigenic carbonates equilibrated with group 1 waters contributes only to limited Y-Ho and Zr-Hf fractionations in opposition to the formation of Fe-oxyhydroxides that we consider primarily responsible for the behaviour of Zr and Hf in the waters of Santorini. Only submarine spring waters from Santorini island fall far from this field, showing higher Zr/Hf ratio values. The recognition of large diatom deposits (Fig. 5.8) and other microbial colonies (Fig. 5.9) in these waters can be explained by the large affinity of Hf relative to Zr towards silica-rich materials (Firdaus et al., 2011; Censi et al., 2013).

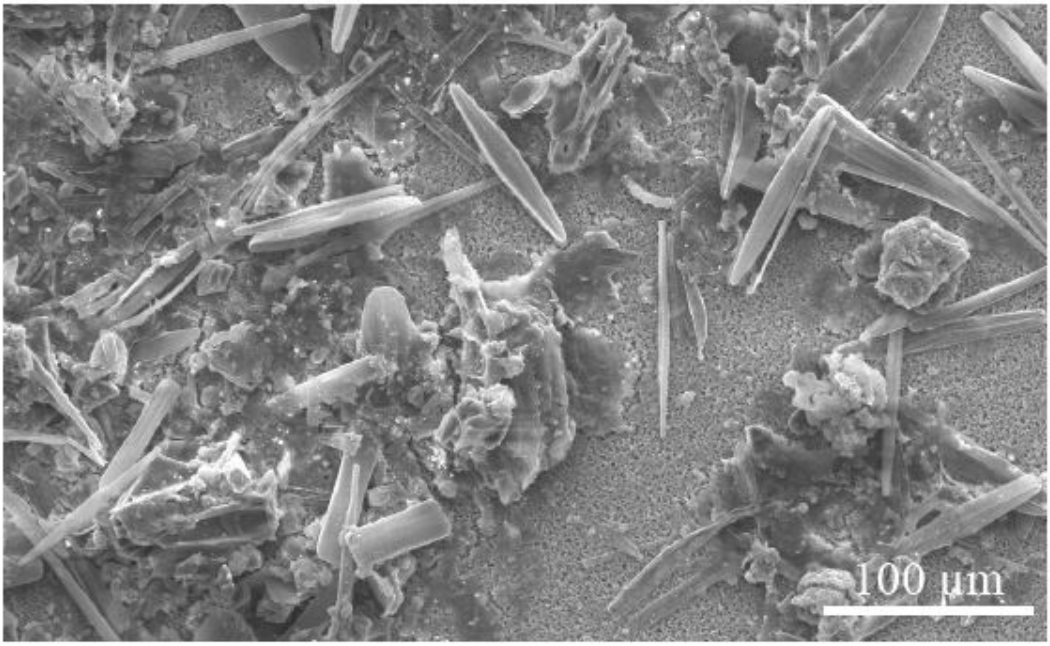

Fig. 5.8 –SEM image of suspended particulate from PKA submarine hydrothermal water (Santorini Island) showing diatoms and other silica rich organism.

In particular, Censi et al. (2013) indicate that the hydroxo-complexes of Zr and Hf have a high reactivity toward carboxylic sites of attack on biological surfaces in agreement with experimental studies (Monji et al., 2008) and electrostatic considerations (Bau and Koschinsky 2006). During these interactions, $[Hf(OH)_5]^-$ should be fractionated in preference to $[Zr(OH)_4]^0$ onto biological surfaces.

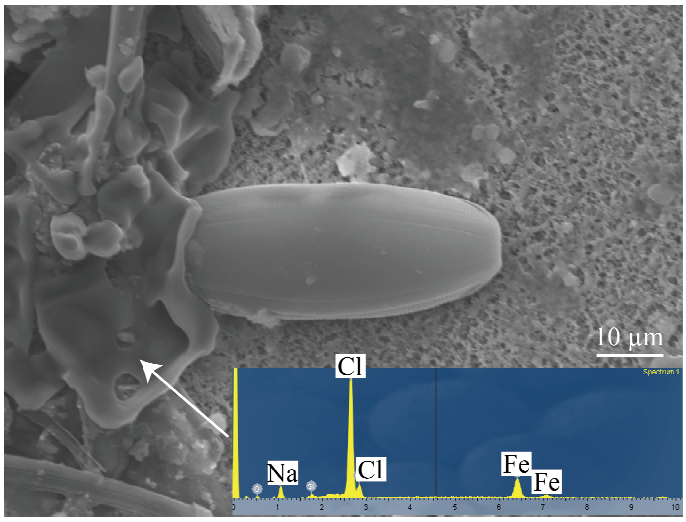

Figure 5.9 – Microbial material associated to Fe-oxyhydroxides in suspended particulates from submarine hydrothermal springs at Santorini island.

CONCLUSION

In the hydrothermal vents studied, the geochemical behaviour in the dissolved phase of Zr, Hf and REE is largely determined by the presence of solid interfaces of an inorganic and biological nature and by dissolved speciation. On the other hand, at least for REE, the evidence suggests that the interaction that takes place between these surfaces and the REE is related to a competition between their dissolved speciation and the inclusion of ligand species from the authigenic surfaces in the inner REE coordination sphere to form surface complexes. This phenomenon involves the growth of W-type Tetrad Effects in normalized patterns from waters. During this competition between dissolved and surface complexation, the REE behaviour is subjected to a mineralogical control that apparently affects Zr and Hf distributions also mainly in the presence of Fe-oxyhydroxides. According to the wide natural occurrence of Fe-oxyhydroxides and their well-known ability to retain electrolytes from the dissolved phase, the mechanism of interaction between Zr, Hf and Fe-oxyhydroxides deserves to be the subject of a subsequent research. At the same time, the progress of this research has to be focused on the effects of microbial colonies on the Zr and Hf distributions in hydrothermal fluids.

CONCLUSIVE REMARKS

The results of this study allow us to draw both geochemical and environmental conclusions about the behaviour of Zr, Hf and REE in volcanic systems where the knowledge of the transport mechanisms for these elements is limited and only scarce previous data about the Zr and Hf behaviour in volcanic fluids are known. Interest in these elements comes from their increasing exploitation in the hi-tech sector a confident requirement for allowing their next accumulation from anthropogenic sources in the environment, as it occurs for gadolinium.

This study indicates that Cl-complexes can represent a suitable transport mechanism for REE in volcanic fluids under several geodynamic settings. The efficiency of this transport depends on the temperature that is a prerequisite affecting Chloride complexation in volcanic gases. When these fluids reach the surface or near the surface, solid sublimates are deposed or formed by the less volatile gas components. During the sublimation almost all of the REE and large Zr and Hf contents originally present in the volcanic fluids are fractionated in these solids.

Only about 1 ‰ of the original contents of REE in the fluid remains in the gaseous residual fraction, where they cause positive Ce and Gdanomalies. For gadolinium, positive anomalies observed from passive volcanic degassing in the areas studied correspond to an elemental flux into the atmosphere reaching a significant amplitude. Approximate but reasonable model calculations based on the Gd/CO_2 ratio in volcanic fluids show that the Gd delivery to the atmosphere is of the same order of magnitude on annual basis as that released from hospital wastewater in river waters of Germany in 2000. But, volcanic fluids release highly water soluble and then bioavailable Gd species, whereas Gd-based contrast agents for Magnetic Resonance Imaging (MRI) applications are poorly hydrolysable and bioavailable in aqueous medium. Evidence of this scenario is reported in the REE behaviour in submarine spring waters where positive Gd anomalies attain 1.6 reporting evidence of delivery of deep hydrothermal fluids to seawater.

The occurrence of positive Gd anomalies in the fluids studied suggests that Gd Cl-complexes in the gas phase are more stable than those of its neighbours, similar to that observed

for complexes of Gd dissolved in some natural waters. Although this hypothesis needs further tests, it suggests that Gd-bearing complexes are more stable in lower structural order grade media where the larger stability of the spherical distribution in the electronic density of *4f* orbital can make a difference during coordination bonds. To evaluate this hypothesis a quantum mechanical approach is needed and would represent a suitable progression of this study.

The distribution of Zr and Hf concentrations in condensates, sublimates and waters from the investigated volcanic areas, shows that a limited Zr-Hf decoupling relative to chondritic signature is consistent with the transport of these elements in volcanic fluids. This decoupling leads to Zr/Hf molar values clustered around 100 and this value is shown as an indicator of direct contribution of hydrothermal fluids to the deep waters, differentiating the latter from those in which it is mainly the effect of scavenging on the surfaces of authigenic minerals as an explanation of the Zr/Hf observed values. Therefore, the simultaneous presence of Zr/Hf ratios next to 100, W-type tetrad effects and positive anomalies of Gd in the waters where the REE speciation is dominated by halo-complex and less oxidizing conditions are needed, indicates that the geochemical behaviour observed for investigated elements is justified by significant contributions of volcanic fluids. Still unclear, as already done for the REE, is the mechanism of interaction of the Zr and Hf dissolved complexes with the surfaces of authigenic minerals with which these elements are in contact in volcanic-hydrothermal systems.

ACKNOWLEDGEMENTS

I would like to express my special appreciation and thanks to my supervisors Professor Paolo Censi and Dr. Francesco Sortino, you have been special mentors for me. I would like to thank you for encouraging my research and for allowing me to grow as a research scientist. I would also like to thank my riviewers, Professor Michael Bau (Jacobs University, Germany) and Professor Orlando Vaselli (University of Firenze, Italy) for your brilliant comments and suggestions, thanks to you. I would especially like to thank Dr. Filippo Saiano (University of Palermo, Itlay) for strong ales, large smiles and all the valuable suggestions on the handling of my samples, of which I could not do without. I would affectionately like to thank the members of ICP-MS lab (I.N.G.V. National Institute of Geophysics and Volcanology of Palermo), Dr. Lorenzo Brusca and Dr. Segio Bellomo, for the analisis of that they performed of Zr, Hf and REE in condensates, sublimates and hydrothermal waters and IC lab (I.N.G.V. National Institute of Geophysics and Volcanology of Palermo), Salvatore Francofonte, for his availability at any time. You have given me unforgettable memories.

A special thanks to my family. Words cannot express how grateful I am to my extraordinary mother, my dearest father and my precious sister for all of the sacrifices that you've made on my behalf, for the tireless support in particularly difficult times which I have crossed. I dedicate to you this thesis.

I would also like to thank my friends ever, Andrea Di Piazza, Sonia La Felice and Francesco Romengo, for the joy, encouraging words and friendship that always demonstrate to me.

A special thanks to my friend Nancy Romengo, example of strength and courage, who passed away during my PhD, but I feel at my side at all times.

Thanks to my new friends, Antonella Cusimano, Elisa Tamburo, Daniela Varrica and Enrico Vitanza, met during this difficult but truly amazing path, for their honesty, their affection and for

incented me to strive towards my goal. At the end I would like to thank my wonderful "Jean De Phantal" for many things, the most important for making better my time simply for being as he is (and also for making memorable the bibliography correction of this thesis).

REFERENCES

Africano F., Van Rompaeyi G.,Bernard A. and Le Guern F. (2002). Deposition of trace elements from high temperature gasesof Satsuma-Iwojima volcano. Earth Planets Space, 54, 275-286.

Ahrland S., Chatt J., and Davies N.R. (1958). Quart. Rev. Chem. Soc., 12, 265-276.

Aiuppa A., Dongarrà G., Capasso G. and Allard P. (2000). Trace elements in the thermal groundwaters of Vulcano Island (Sicily). Jour. Volcanol. Geoth. Res., 98, 189–207.

Aiuppa A., Dongarrà G., Valenza M., Federico C. and Pecoraino G. (2003). Degassing of trace metals during the 2001 eruption of Etna. In: Robock A. and Oppenheimer C. Eds. Volcanism and the Earth's Atmosphere, Geophysical Monograph 139, 41-54.

Aiuppa A., Federico C., Giugice G., Gurrieri S. and Valenza M. (2006). Hydrothermal buffering of the SO_2/H_2S ratio in volcanic gases:Evidence from La Fossa Crater fumarolic field, Vulcano Island. Geoph. Research Lett., 33, L21315, doi:10.1029/2006GL027730.

Alibo D.S. and Nozaki Y. (1999). Rare earth elements in seawater: Particle association, shale-normalization, and Ce oxidation. Geochim. Cosmochim. Ac 63, 363-372.

AllardP., Maiorani A., Tedesco D., Cortecci G. and Turi B. (1991). Isotopic study of the origin of sulfur and carbon in Solfatara fumaroles, Campi Flegrei caldera, J. Volcanol. Geotherm. Res., 48, 139–159.

Araña V. (1995). Notes on Canarian Volcanism, in J. Martí and J. Mitjavila (eds), A Field Guide to the Central Volcanic Complex of Tenerife (Canary Islands), Serie Casa de Los Volcanes, 4. Cabildo de Lanzarote, 3–17.

Bach W. and Irber W. (1998). Rare earth element mobility in the oceanic lower sheeted dyke complex: evidence from geochemical data and leaching experiments. Chem. Geol. 151, 309–326.

Bach W., Roberts S., Vanko D.A., Binns R.A., Yeats C.J., Craddock P.R., Humphris S.E. (2003). Controls of fluid chemistry and complexation on rare-earth element contents of anhydrite from the Pacmanus subseafloor hydrothermal system, Manus Basin, Papua New Guinea. Miner Deposita, 38, 916-935.

Baes C.F. and Mesmer R.E. (1976). The hydrolisys of cation. John Wiley and Sons, New York, 489 pp.

Bailey B., Templeton A., Staudigel H., Tebo B. M. (2009). Utilization of substrate components during basaltic glass colonization by Pseudomonas and Shewanella isolates. Geomicrobiol. J., 26, 648–656.

Baldi P., Ferrara G. and Panichi C. (1975) -Geothermal research in western Campania (southern Italy): chemical and isotopic studies of thermal fluids in the Campi Flegrei. In: 2nd U.N. Symp. Development and Use of Geothermal Resources, San Francisco, 1, 687-697.

Barberi F., Innocenti F., Lirer L., Munno R., Pescatore T. and Santacroce R. (1978). The campanian ignimbrite: a major prehistoric eruption in the Neapolitan area (Italy). Bulletin Volcanologique 41, 10-31.

Barberi F., et al.(1994). Plio-Pleistocene geological evolution of the geothermal area of Tuscany and Latium. Mem. Descr. Carta. Geol. Ital. 49, 77–134.

Bau M. (1991). Rare-earth element mobility during hydrothermal and metamorphic fluid–rock interaction and the significance of the oxidation state of europium. Chem. Geol. 93, 219–230.

Bau M. and Moller P. (1992). Rare earth Element fractionation in metamorphic hydrothermal calcite, magnesite and siderite. Mineral. Petrol., 45, 231-246.

Bau M. (1996). Controls on the fractionation of isovalent trace elements in magmatic and aqueous system: evidence from Y/Ho, Zr/Hf, and lanthanide tetrad effect. Contrib. Mineral. Petrol., 123, 323-333.

Bau M. (1999). scavenging of dissolved yttrium and rare earth earth by precipitating iron oxyhydroxide: Experimental evidence for Ce oxidation, Y-Ho fractionation, and lanthanide tetrad effect. Geochimica e Cosmochimica Acta, 63(1), 67-69.

Bau M. and Dulski P. (1995). Comparative study of yttrium and rare-earth element behaviours in fluorine-rich hydrothermal fluids. Contribution to Mineralogy and Petrology, 2-3(119), 213-223.

Bau M. and Koschinsky A. (2006). Hafnium and neodymium isotopes in seawater and in ferromanganese crusts: The "element perspective". Earth and Planetary Science Letters, 3-4(241), 952-961.

Bau M. and Koschinsky, A. (2009). Oxidative scavenging of cerium on hydrous Fe oxide: Evidence from the distribution of rare earth elements and yttrium between Fe oxides and Mn oxides in hydrogenetic ferromanganese crusts. Geochemical Journal, 1(43), 37-47.

Beccaluva L., Gabbianelli G., Lucchini P. Rossi L. and Savelli C. (1985). Petrology and K/Ar ages of volcanics dredged from the Aeolian seamounts: Implications for geodynamic evolution of the southern Tyrrhenian basin, Earth Planet. Sci. Lett. 74, 187–208.

Bernard A. (1985). Les mécanismes de condensation des gaz volcaniques (chimie, minéralogie et équilibres des phases condensées majeures et mineures). These de doctorat, Université Libre de Bruxelles.

Bolognesi L. and D'Amore F. (1993). Isotopic variation of the hydrothermal system on Vulcano Island Italy. Geochim. Cosmochim. Acta, 9, 2069–2082.

Bonatti E., Honnorez J., Joensuu O. and Rydell H.S. (1972a). Submarine iron deposits from the Mediterranean Sea. In: D.J. Stanley (Editor), Symposium on the Sedimentation in the Mediterranean Sea, 8th Int. Sediment. Congr., Heidelberg, pp. 701--710.

Bonatti E, Fisher D.E., Joensuu O., Rydell H.S. and Beyth M. (1972b). Iron--manganese--barium deposit from the northern Afar Rift. Econ. Geol., 67 : 717--730.

Böstrom K. and Widenfalk L. (1984). The origin of iron-rich muds at the Kameni Islands, Santorini, Greece' Chemical Geology, 42 (1-4) 203-218.

Brondi M. and Dall'Aglio M. (1991). Evolution of mercury, arsenic, antimony radon and helium contents in ground waters and fumaroles since through at Vulcano Island (Southern Italy). Acta Vulcanol. 1, 233–241.

Bruno P.P.G. (2004). Structure and evolution of the Bay of Pozzuoli (Italy) using marine seismic reflection data: implications for collapse of the Campi Flegrei caldera, Bull. Volcanol., 66(4), 342–355.

Bruno P.P.G., Rapolla A. and Di Fiore V. (2003). Structural settings of the Bay of Naples (Italy) by seismic reflection data: Implications for the Campanian volcanism, Tectonophysics, 372, 192– 213.

Burton M.R., Sawyer G.M., Granieri D. (2013). Deep carbon emissions from volcanoes. In: Rev. in Mineralogy and Geochemistry 75, 323-354.

Butuzova G.Yu. (1966). Iron ore deposits at the fumarole fields at the Santorin volcano; composition and genesis. Dokl. Akad. Nauk, S.S.S.R., 168(6): 1400--1402 (in Russian).

Butuzova G.Yu. (1969). Recent volcano-sedimentary iron ore process in Santorin Volcano Caldera and its effect on the geochemistry of the sediments. Akad. Nauk, S.S.S.R., Geol. Inst., Tr. 194, Izd. Nauka, Moscow, 114 pp, (in Russian).

Byrne R.H. and Li B. (1995). Comparative complexation behavior of the rare earths. Geochim Cosmochim Ac 59, 4575-4589.

Byrne R., and Sholkovitz E. (1996). Marine chemistry on geochemistry of the lanthanides. In handbook of the physics and chemistry of rare earth. 23, 497-593.

Byrne R.H., Liu X., Schijf J. (1996). The influence of phosphate coprecipitation on rare earth element distributions in natural waters. Geochimica et Cosmochimica Acta, 60, 3341-3346.

Byrne R.H. (2002). Inorganic speciation of dissolved elements in seawater: The influence of pH on concentration ratios. Geochemical Transactions 3, 11–16.

Cabaniss S. E. (1987). Titrator: An interactive program for aquatic equilibrium calculations, Environ. Sci. Technol., 21, 209–210.

Calabrese S., Aiuppa A., Allard P., Bagnato E., Bellomo S., Brusca L., D'Alessandro W. and Parello F. (2011). Atmospheric sources and sinks of volcanogenic elements in a basaltic volcano (Etna, Italy). Geochim Cosmochim Ac 75, 7401-7425.

Caliro S., Chiodini G., Moretti R., Avino R.,Granieri D., Russo M.and Fiebig J. (2007). The origin of the fumaroles of La Solfatara (Phlegrean Fields, South Italy), Geochim. Cosmochim. Acta, 71, 3040-3055.

Cantrell K.J. and Byrne R.H. (1987). Rare earth complexation by carbonate and oxalate ions. Geochimicaet Cosmochimica Acta, 51(3), 597–605.

Capasso G., Dongarrà G., Favara R., Hauser S. and Valenza M. (1991). Chemical changes in waters from Vulcano Island: an update. Acta Vulcanol. 1, 199–209.

Capasso G., Dongarrà G., Favara R., Hauser S. and Valenza M. (1992), Isotope composition of rain water, well water and fumarole steam on the island of Vulcano, and their implications for volcanic surveillance, J. Volcanol. Geotherm. Res.,49, 147–155.

Capasso G., Favara R., Francofonte S. and Inguaggiato S. (1999.)Chemical and isotopic variations in fumarolic discharge and thermal waters at Vulcano Island (Aeolian Island Italy) during 1996: evidence of resumed volcanic activity. J. Volcanol. Geotherm. Res. 88, 167–175.

Caprarelli G. (1991). Geochemistry and isotope geochemistry of rock samples coming from geothermal wells of Mofete and San Vito—Phlegrean Fields Naples, Southern Italy. PhD Thesis, University of Rome.

Caprarelli G., Tsutsumi M. and Turi B. (1997). Chemical and isotopic signatures of the basement rocks from the Campi Flegrei geothermal field, Naples, southern Italy: inferences about the origin and evolution of its hydrothermal fluids. J. Volcanol. Geotherm. Res., 76, 63–82.

Caradossi N. (1980). Rendiconti Società Italiana di Mineralogia e Petrologia, 36 (2), 573-514.

Carapezza M., Nuccio P.M. and Valenza M. (1981). Genesis and evolution of the fumaroles of Vulcano (Aeolian Island Italy). Bull Volcanol 44: 547-563.

Carapezza M., Dongarra G., Hauser S. and Longinelli A. (1983). Preliminary isotopic investigations on thermal waters from Vulcano Island Italy. Mineral. Petrogr. Acta 27, 221–232.

Carapezza M., Nuccio P.M. and Valenza M. (1984). Geochemical surveillance of the Solfatara of Pozzuoli (Phlegrean Fields) during 1983. Bulletin of Volcanology, 47, 303–311.

Celico P., Dall'Aglio M., Ghiara M.R., Stanzione D., Brondi M. and Prosperi M. (1992a). Geochemical monitoring of the thermal fluids in the Phlegraean Fields from 1970 to 1990. Boll. Soc. Geol. Ital. 111, 409– 422.

Cellini Legittimo P., Martini M. and Piccardi G. (1980). Il contenuto di metalli pesanti nelle acque freatiche di Vulcano e l'influenza di fluidi idrotermali. Rend. Soc. Mineral. Petrol. 36, 253–260.

Censi P., Mazzola S., Sprovieri M., Bonanno A., Patti B., Punturo R., Spoto S.E., Saiano F. and Alonzo G. (2004). Rare Earth Elements distribution in seawater and suspended particulate of the Central Mediterranean Sea. Chem. Ecol., 20, 323–343.

Censi P., Saiano F., Zuddas P., Nicosia A., Mazzola S. and Raso M. (2013). Authigenic phase formation and microbial activity control Zr, Hf, and rare earth element distributions in deep-sea brine sediments. Biogeosciences, 11, 1125–1136.

Censi P., Saiano F., Zuddas P.,Nicosia A., Mazzola S. and Raso M. (2014). Authigenic phase formation and microbial activity control Zr, Hf,and rare earth element distributions in deep-sea brine sediments. Biogeosciences, 11, 1125–1136.

Chao E.C.T., Back J.M., Minkin J.A. and Ren Y.C.(1992). Host-rock controlled epigenetic, hydrothermal metasomatic origin of the Bayan Obo REE-Fe-Nb ore deposit, Inner Mongolia, P.R.C. Applied Geochemistry, 7, 443–458.

Cheynet B., Dall'Aglio M., Garavelli A., Grasso M.F. and Vurro F. (2000). Trace elements from fumaroles at Vulcano Island (Italy): rates of transport and thermochemical model. Jour. Volcan. Geoth. Res., 95, 273-283.

Chiodini G., Cioni R., Guidi M., Marini L., Raco B.and Taddeucci G. (1992). Gas geobarometry in boiling hydrothermal systems: a possible tool to evaluate the hazard of hydrothermal explosions, Acta Vulcanol., 2, 99-107.

Chiodini G., Cioni R., Marini L. and Panichi C. (1995) Origin of the fumarolic fluids of Vulcano island, Italy, and implication for volcanic surveillance. Bull Volcanol 57, 99-110

Chiodini G., Frondini F. and Raco B. (1996).Diffuse emission of CO2 from the Fossa crater, Vulcano Island (Italy), Bulletin of Volcanology, 58 (1), 41-50.

Chiodini, G. and Marini, L. (1998). Hydrothermal gas equilibria: The $H_2O–H_2–CO_2–CO–CH_4$ system, Geochim. Cosmochim. Acta, 62, 2673-2687.

Chiodini G., Cioni R., Guidi M., Magro G., Marini L., Panichi C., Raco B. and Russo M. (2000). Vesuvius and Phlegrean Fields; gas geochemistry; geochemical monitoring of the Phlegrean Fields and Vesuvius (Italy) in 1996, Acta Vulcanol., 12, 117-119.

Chiodini G., Frondini F., Cardellini C., Granieri D., Marini L. and Ventura G. (2001a) CO2 degassing and energy release at Solfatara volcano, Campi Flegrei, Italy. J. Geophys. Res. 106, 16213–16221.

Chiodini G., Marini L. and Russo M. (2001b) Geochemical evidence for the existence of high-temperature hydrothermal brines at Vesuvio volcano, Italy. Geochim. Cosmochim. Acta 65, 2129–2147.

Chiodini G., Todesco M., Caliro S., Del Gaudio C., Macedonio G. and Russo M. (2003) Magma degassing as a trigger of bradyseismic events; the case of Phlegrean Fields (Italy). Geophys. Res. Lett. 30, 1434. http://dx.doi.org/10.1029/ 2002GL016790.

Chiodini G., Caliro A., Cardellini C., Frondini F., Inguaggiato S., Matteucci F.(2011). Geochemical evidence for and characterization of CO_2-rich gas sources in the epicentral area of the Abruzzo 2009 earthquakes: Earth and Planetary Science Letters, v. 304, p. 389–398, doi:10.1016/j.epsl.2011.02.016

Cioni R. and D'Amore F. (1984). A genetic model for the crater fumaroles of Vulcano Island (Sicily, Italy). Geothermics 13 (4), 375-384.

Cioni R., Corazza E. and Marini L. (1984). The gas/steam ratio as indicator of heat transfer at the Solfatara fumaroles, Phlegraean Fields (Italy), Bull. Volcanol., 47, 295-302.

Cioni R., Corazza E., Fratta M., Duidi M., Magro G. and Marini L. (1989). Geochemical precursors at Solfatara Volcano, Pozzuoli (Italy), Springer-Verlag, Berlin.

Cortecci G., Noto P. and Panichi C. (1978). Environmental isotopic study of the Campi Flegrei (Naples, Italy) geothermal field. J. Hydrol., 36, 143–159.

Coryell C.D. , Chase J.W. and Winchester J.W.A. (1963).Procedure for geochemical interpretation of terrestrial rare earth abundance patterns. Geophys. Res., 68, 559-566.

Courtillot V., Davaille A., Besse J. and Stock J. (2003). Three distinct types of hotspots in the Earth's mantle. Earth and Planetary Sci. Letters 205, 295-308.

Cronan D.S., Varnavas S.P. and Hodkinson R. (2000). Hydrothermal mineralizing processes and associated sedimentation in the Santorini hydrothermal embayments. Mar. Georesour.Geotechnol., 18, 77- 118.

Cronan D.S., Varnavas S.,and Perissoratis C. (1995). Hydrothermal sedimentation in the caldera of Santorini, Hellenic Volcanic Arc. Terra Research, 7, 289–293.

Czerwinski K.R., Buckau G., Scherbaum F. and Kim J.I., (1994). Complexation of theuranyl–ion with aquatic humic-acid. Radiochim. Acta, 65, 111–119.

Dando P.R., Aliani S., Arab H., Bianchi C.N., Brehmer M., Cocito S., Fowler S.W., Gundersen J.,Hooper L.E., Kolbi R., Kuever J., Linke P., Makropoulus K.C., Meloni R., Miquel J.C., Morri C.,Muller S.,

Robinson C., Schlesner H., Sievert S., Stohr R., Stuben D., TommM., Varnavas S.P. and Ziebis W. (2000). Hydrothermal Studies in the Aegean Sea. Phys. Chem. Earth, 25, 1, 1–8.

D'Antonio M., Civetta L. and Di Girolamo V. (1999), Mantle source heterogeneity in the Campanian Region (South Italy) as inferred from geochemical and isotopic features of mafic volcanic rocks with shoshonitic affinity, Mineral. Petrol., 67, 163– 192.

Darrah T.H., Prutsman-Pfeiffer J.J., Poreda R.J., Ellen Campbell M., Hauschka P.V. and Hannigan R.E. (2009). Incorporation of excess gadolinium into human bone from medical contrast agents. Metallomics 1, 479-488.

De Astis G., La Volpe L., Peccerillo A. and Civetta L. (1997).Volcanological and petrologicalevolution of the Vulcano Island (Aeolian Arc,Southern Tyrrhenian Sea): Journal of Geophysical Research, 102, 8021–8050.

De Astis G., Pappalardo L. and Piochi M. (2004). Procida Volcanic History: New insights in the evolution of the Phlegraean Volcanic District (Campania region, Italy), Bull. Volcanol., 66, 622– 641, doi:10.1007/s00445-004-0345.

Dall'Aglio M., Martini M. and Tonani F. (1972). Rilevamento geochimico delle emanazioni vulcaniche dei Campi Flegrei. Quad. Ric. Sci. CNR 83, 152–181.

De Vivo B., Rolandi G., Gans P.B.,. Calvert A, Bohrson W.A., Spera F.J. and Belkin H.E. (2001). New constraints on the pyroclastic eruptive history of the Campanian volcanic Plain (Italy), Mineral. Petrol., 73, 47– 65.

Di Girolamo, P.(1970). Differenziazione gravitativa e curve isochimiche nella «Ignimbrite Campana» («Tufo Grigio Campano» Auct.). Rend. Soc. Min. Petr., 26 (2), 547–588.

Di Girolamo P., Ghiara M.R., Lirer L., Munno R., Rolandi G. and Stanzione D. (1984). Vulcanologia e petrologia dei Phlegrean Fields. Boll. Soc. Geol. It., 103, 349-413.

Dionis S., Melian G., Padron E., Bandomo Z., Fernandes P., Silva S., Barrancos J., Rodriguez,F., Padilla G., Nolasco D., Calvo D., Hernandez P., Péres N., Semedo H and Gonzalves A. (2013). Diffuse CO2 and H2S degassing from summit crater of Pico do Fogo. Geophys. Res. Abs. 15, EGU2013-940.

Dongarrà G., Hauser S., Capasso G. and Favara R. (1988). Characteristics of variations in water chemistry of some wells from Vulcano Island. Rend. Soc. Ital. Mineral. Petrol. 43, 1123–1131.

Dongarra`G. and Varrica D. (1998). The presence of heavy metals in air particulate at Vulcano island (Italy). Sci. Tot. Environ. 212, 1–9.

Dotsika E., Poutoukis D., Michelot J.L., Raco B. (2009). Natural tracers for identifying the origin of the thermal fluids emerging along the Aegean volcanic arc (Greece): evidence of arc-type magmatic water (ATMW) participation. J. Volcanol. Geoth. Res., 179, 19–32.

Egoroff B. (1965). L'éruption du volcan Mihaga en 1954. Inst. Para Nat. du Congo (Exploration du Parc Nat.Albert Mission d'Etudes Volc.), IV.

Erel Y. and Stolper E.M. (1993). Modeling of Rare-Earth Element Partitioning between Particles and Solution in Aquatic Environments. Geochim Cosmochim Ac, 57, 513-518.

Erlank A. J., Smith H. S., Marchant J. W., Cardoso M.P. and Ahrens L.H. (1978) Hafnium. Handbook of Geochemistry (Wedepohl, K. H., ed.), 72C1–72O1, Springer-Verlag, Berlin, Heidelberg, New York.

Escrig S., Doucelance R., Moreira M. and Allègre C.J. (2005). Os isotope systematics in Fogo Island: Evidence for lower continental crust fragments under the Cape Verde Southern Islands. Chem. Geol., 219, 93–113.

Ferrara G., Garavelli A., Pinarelli L. and Vurro F. (1995). Lead isotope composition of the sublimates from the fumaroles of Vulcano (Aeolian Islands Italy): inferences on the deep fluid circulation. Bull. Volcanol. 56, 621–625.

Ferrucci F., Gaudiosi G., Hirn A. and Nicolich R. (1991).Ionian Basin andCalabrian Arc: some new elements from DSS data, Tectonophysics, 195, 411-419.

Firdaus M., Minami T., Norisuye K., and Sohrin Y. (2011). Strong elemental fractionation of Zr-Hf and Nb-Ta across the Pacific Ocean. nature geoscience, 4, 227-230.

Flynn R.T. and Burnham C.W. (1978). Anexperimental determination of rare earth partition coefficients between a chloride containing vapor phase and silicate melts, Geochim. Cosmochim. Acta.,42, 685-701.

Fulignati P., Marianelli P. and Sbrana A. (1998): Newinsights on the thermometamorphic-metasomatic magma chamber shell of the 1944 eruption of Vesuvius,Acta Vulcanol.,10(1), 47-54.

Fulignati P., Gioncada A. and Sbrana A. (1999). Rare-earthelement (REE) behaviour in the alteration facies of the active magmatic–hydrothermal system of Vulcano(Aeolian Islands, Italy). J. Volc. Geotherm. Res., 88, 325–342.

Garavelli A. (1994). Mineralogia e geochimica di fasi vulcaniche condensate. I sublimati dell'isola di Vulcano tra il 1990 ed il 1993. PhD thesis, Univ. Bari.

Garavelli A., Laviano, R. and Vurro, F. (1997). Sublimate deposition from hydrothermal fluids at the Fossa Crater—Vulcano Italy. Eur. J. Mineral. 9, 423–432.

Garavelli A., Mitolo D., Pinto D., Vurro F. and Lucabindiite F. (2013). $(K,NH_4)As_4O_6(Cl,Br)$, a new fumarole mineral from the "La Fossa" crater at Vulcano, Aeolian Islands, Italy. Am. Mineral., 98, 470-477.

Caravetta G., Tecce F., Serracino M., De Vivo B. (1988).Fluid inclusion, sulphur and strontium isotopes in hydrothermal anhydrite from the Isola di Vulcano-1 deep well, Aeolian Islands, Italy, Rend. Soc. Ital. Mineral. Petrol. 43975–985.

Gertisser R., Preece K. and Keller J. (2009). The Plinian Lower Pumice 2 eruption, Santorini, Greece: Magma evolution and volatile behaviour. Journal of Volcanology and Geothermal Research, 186,387-406.

Gemmell B.J. (1987). Geochemistry of metallic trace elements in fumarolic condensates from Nicaraguan and Costa Rican volcanoes. J. Volcanol. Geotherm. Res. 33, 161–18.

Ghiara M.R. and Stanzione D. (1988). Studio geochimico sul sistema idrotermale dei Campi Flegrei (Campania Italia). Rend. Accad. Sci. Fis. Mat. Napoli LV (IV), 61– 83.

Gilbert C.D., Williams-Jones A.E. (2008). Vapour transport of rare earth elements (REE) in volcanic gas: Evidence from encrustations at Oldoinyo Lengai. J Volcanol Geoth Res, 176, 519-528.

Gill J.B., Hiscott R.N. and Vidal. P. (1994).Turbidite geochemistry and evolution of the Izu-Bonin Arc and continents, in Tectonics, Metamorphism and Magmatism in Island Arcs, edited by R. J. Arculus et al., Lithos,33, 135–168.

Gioncada A., Clocchiatti R., Sbrana A., Bottazzi P., Massare D. and Ottolini L. (1998). A study of melt inclusions at Vulcano (Aeolian islands, Italy): insight on the primitive magmas and on the volcanic feeding system. Bull. Volcanol., 60, 286-306.

Gioncada A., Mazzuoli R., Bisson M. and Pareschi M.T. (2003), Petrology of volcanic products younger than 42 ka on the Lipari Vulcano complex (Aeolian Islands, Italy): An example of volcanism controlled by tectonics, J. Volcanol. Geotherm. Res., 122, 191–220.

Goldschmidt V.M. (1937). The principles of distribution of chemical elements in minerals and rocks. J Chem. Soc., 655–673.

Greaves M. J., Elderfield H. and Sholkovitz E.R. (1999). Aeolian sources of rare earth elements to the Western Pacific Ocean.Marine Chemistry, 68, 31–38.

Guglielminetti M. (1996). Mofete geothermal field. Geothermics 15, 781–790.

Gültekin A.H., Örgun K. and Suner F. (2003). Geology, mineralogy and fluid inclusion data of the Kizilcaörenfluorite–barite–REE deposit, Eskisenhir, Turkey. Journal of Asian Earth Sciences 21, 365–376.

Haas J.R., Shock E.L., Sassani D.C. (1995). Rare-Earth Elements in Hydrothermal Systems - Estimates of Standard Partial Molal Thermodynamic Properties of Aqueous Complexes of the Rare-Earth Elements at High-Pressures and Temperatures. Geochim Cosmochim Ac, 59, 4329-4350.

Hawley S. A. (1971). Reversible pressure-temperature denaturation of chymotrypsinogen. Biochemistry. 10:2436–2442.

Heinrich C.A., Günther D., Audétat A., Ulrich T. and Frischknecht R. (1999). Metal fractionation between magmatic brine and vapor, determined by micro-analysis of fluid inclusions. Geology, 27, 755-758.

Hinkley T.K. (1991). Distribution of metals between particulate and gaseous forms in a volcanic plume. Bulletin of Volcanology, 53, 395-400.

Hinkley T.K., Lamothe P.J., Wilson S.A., Finnegan D.L. and Gerlach T.M. (1999). Metal emissions from Kilauea, and a suggested revision of the estimated worldwide metal output by quiescent degassing of volcanoes. Earth and Planetary Science Letters, 170, 315-325.

Hodkinson R.A., Stoffers P., Scholten J., Cronan D.S., Jeschke G. and Rogers T.D.S. (1994). Geochemistry of hydrothermal manganese deposits from the Pitcairn Island hotspot, southeastern Pacific. Geochim. Cosmochim. Acta 58, 5011 – 5029.

Hogness T.R., Jonhson W.C. and Armstrong A.R. (1972). Qualitative Analysis and Chemical Equilibrium. 5a. ed., Holt, Rinehart and Winston, Inc., N.Y.

Hoskin P.W.O. and Schaltegger U. (2003) The composition of zircon and igneous and metamorphic petrogenesis. Rev. Mineral. Geochem., 53, 27–62.

Humphris S.E. and Bach,W. (2005). On the Sr isotope and REE compositions of anhydrites from the TAG seafloor hydrothermal system. Geochim. et Cosmochim. acta, 69, 1511-1525.

Inguaggiato S., Mazot A., Diliberto I.S., Inguaggiato C., Madonia P., Rouwet D. and Vita F. (2012). Total CO2 output from Vulcano island (Aeolian Islands, Italy). Geochem Geophy Geosy 13.

Irber W. (1999). The lanthanide tetrad effect and its correlation with K/Rb, Eu/Eu*, Sr/Eu, Y/Ho, and Zr/Hf of evolving peraluminous granite suites. Geochim. et Cosmochim. acta, 3-4(63), 489-508.

Jochum K.P., Seufert H.M., Spettel B. and Palme H. (1986). The solar-system abundances of Nb, Ta, and Y, and the relative abundances of refractory lithophile elements in differentiated planetary bodies. Geochim Cosmochim Ac, 50, 1173-1183.

Jørgensen C.K. (1970). The“Tetrad effect”of Peppard is a variation of the nephelauxetic ratio in the third decimal. J. inorg. nucl. Chem .32, 3127–3128.

Jørgensen C.K. (1979). Theoretical chemistry of rare earths, in Handbook on the Physics and Chemistry of Rare Earth, Vol. 3. Amsterdam: North-Holland, pp. 111–69.

Kacher C.D., Gregorich K.E., Lee D.M., Watanabe Y., Kadkhodayan B., Wierczinski B., Lane M.R., Sylwester E.R., Keeney D.A., Hendricks M., Stoyer N.J., Yang J., Hsu M., Hoffman D.C. and Bilewicz A., (1996). Chemical Studies of Rutherfordium (Element 104): Part III. Solvent Extraction into Triisooctylamine from HF Solutions. Radiochim. Acta, 75, 135–139.

Kagi H., Dohomoto Y., Takano S. and Masuda A. (1993). Tetrad effect in lanthanide partitioning between calcium sulphate crystal and its saturated solution. Chem. Geol., 107, 71-82.

Kalaji A., Skanthakumar S., Kanatzidis M. G., Mitchell J. F. and Soderholm L. (2014). Changing Hafnium Speciation in Aqueous Sulfate Solutions: A High-Energy X-ray Scattering Study. Inorg. Chem., 53, 6321−6328.

Kawabe I. (1992). Lanthanide tetrad effect in the Ln3+ ionic radii and refined spin-pairing energy theory. Geochem. Journ., 26, 309-335.

Keller J. (1980). The island of Vulcano. Rendiconti della Societa Italiana di Mineralogia e Petrologia, 36, 369-414.

Kilias S.P., Nomikou P., Papanikolaou D., Polymenakou P.N., Godelitsas,A., Argyraki A., Carey S., Gamaletsos P., Mertzimekis T. J., Stathopoulou E., Goettlicher J., Steininger R., Betzelou K., Livanos I., Christakis C., Croff Bell C. and Scoullos M. (2013). New insights into hydrothermal vent processes in the unique shallow-submarine arc-volcano, Kolumbo (Santorini), Greece. Scientific Report, 3 : 2421, 1-13.

Koschinsky A. and Hein J.R. (2003). Uptake of elements from seawater by ferromanganese crusts: solid-phase associations and seawater speciation. Mar. Geol. 198, 331-351.

Kozin P.A., Shchukarev A. and Boily J.F. (2013). Electrolyte Ion Binding at Iron Oxyhydroxide Mineral Surfaces. Langmuir, 29, 12129−12137.

Kozin P.A. (2014). H Charge Development at Iron Oxyhydroxide Surfaces: The Interplay between Surface Structure, Particle Morphology and Counterion Identity. PhD Thesys, 02-20, KBC-huset, KB3B1, Umeå universitet, Umeå.

Kummerer K. and Helmers E. (2000). Hospital effluents as a source of gadolinium in the aquatic environment. Environ Sci Technol, 34, 573-577.

Lee J.H. and Byrne R.H. (1992). Examination of comparative rare earth element complexation behavior using linear free-energy relationships. Geochimica et Cosmochimica Acta, 56, 1127–1137.

Le Guern F. and Bernard A. (1982). A new method for sampling and analyzing volcanic sublimates - application to Merapi volcano, Java. J Volcanol Geoth Res, 12, 133-146.

Leybourne M. I. and Johannesson K.H. (2008). T Rare earth elements (REE) and yttrium in stream waters, stream sediments, and Fe–Mn oxyhydroxides: Fractionation, speciation, and controls over REE + Y patterns in the surface environment. Geochim. et Cosmochim. Acta, 72, 5962–5983.

Lewis A.J., Komninou A., Yardley B.W.D. and Palmer M.R.(1998). Rare earth element speciation in geothermal fluids from Yellowstone National Park, Wyoming, USA. Geochimica et Cosmochimica Acta, 62, 657–663.

Linnen R.L. and Keppler H. (2002). Melt composition control of Zr/Hf fractionation in magmatic processes. Geochimica et Cosmochimica Acta, 66, 3293–3301.

Linnen R.L., Samson I. M., Williams-Jones A.E. and Chakhmouradian A.R. (2014). Geochemistry of the Rare-Earth Element, Nb, Ta, Hf, and Zr Deposits. Elsevier Ltd., 13 (21), 543-564.

Lirer L., Mastrolorenzo G. and Rolandi G. (1987). Un evento pliniano nell'attività recente dei Phlegrean Fields. Boll Soc Geol It, 106, 461-473.

Liu X. and Byrne R.H. (1998). Comprehensive investigation of yttrium and rare earth element complexation by carbonate ions using ICP-mass spectrometry. J. Sol. Chem., 27, 803–815.

Louvel M., Sanchez-Valle C., Malfait W.J., Testemale D. and Hazemann J. L. (2013). Zr complexation in high pressure aqueous fluids and silicate melts and implications for HFSE mobilization in subduction zones. Geochim. Cosmochim. Acta, 104, 281–299.

Luo Y.R. and Byrne R.H. (2000) The ionic strength dependence of rare earth and yttrium fluoride complexation at 25 °C. J. Solut. Chem.,29 , 1089–1099.

Luo Y.R. and Byrne R.H. (2004). Carbonate complexation of yttrium and the rare earth elements in natural waters. Geochim. Cosmochim. Acta, 68, 691–699.

Martini M. (1980). Geochemical survey on the phreatic waters of Vulcano (Aeolian Island Italy). Bull. Volcanol. 43, 265–274.

Masuda A. (1962). Regularities in variation of relative abundances of lanthanide elements and an attempt to analyse separation index patterns of some minerals. J. Earth Sci. Nagoya Univ., 10, 173–187.

Masuda A., Kawakami O., Dohomoto Y. and Takenaka T. (1987) Lanthanide tetrad effects in nature: two mutually opposite types, W and M. Geochem. J , 21, 119–124.

Mather T.A., Allen A.G., Oppenheimer C., Pyle D.M. and McGonigle A.J.S. (2003). Size-resolved characterisation of soluble ions in the particles in the tropospheric plume in Masaya volcano, Nicaragua: Origins and plume processing. Journal of Atmospheric Chemistry, 46, 207-237.

Mayanovic R.A., Anderson A.J., Bassett W.A., Chou I.M. (2007). On the formation and structure of rare-earth element complexes in aqueous solutions under hydrothermal conditions with new data on gadolinium aqua and chloro complexes. Chem Geol, 239, 266-283.

Mendrinos D., Choropanitis I., Polyzou O. and Karytsas C. (2010). Exploring for Geothermal Resources in Greece. Geothermics, vol. 39, issue 1, pp. 124-137.

Michard A. (1989). Rare earth element systematics in hydrothermal fluid. Geochim Cosmochim Acta 53, 745-750.

Migdisov A.A, Williams-Jones A.E. (2007) An experimental study of the solubility and speciation of neodymium (III) fluoride in F-bearing aqueous solutions. Geochim Cosmochim Acta 71:3056–3069.

Migdisov A.A. and Williams-Jones A.E. (2008). Response to the comment by J. Schijf and R.H. Byrne on "An experimental study of the solubility and speciation of neodymium (III) fluoride in F-bearing aqueous solutions". Geochim. Cosmochim. Acta, 72, 5578-5579.

Migdisov Art. A., Williams-Jones A.E., and Wagner, T. (2009). An experimental study of the solubility and speciation of the Rare Earth Elements (III) in fluoride- and chloride-bearing aqueous solutions at temperatures up to 300 °C. Geochim. Cosmochim. Acta, 73, 7087-7109.

Migdisov Art. A.and Williams-Jones A.E. (2014). Hydrothermal transport and deposition of the rare earth elementsby fluorine-bearing aqueous liquids. Miner Deposita, 49.

Millero F.J., Sotolongo S. and Izaguirre M. (1987). The kinetics of oxidation of Fe(II) in seawater. Geochim. Cosmochim. Acta, 51, 793–801.

Minissale A., Duchi V., Kolios N., Nocenti M. and Verrucchi C. (1997). Chemical patterns of thermal aquifers in the volcanic islands of the Aegean Arc, Greece. Geothermics, 26, 4, 501–518.

Mizutani Y. (1970) .Copper and zinc in lumarolic gases 01 Showashinzan volcano, Hokkaido, Japan. Geochem. J., 4, 87·91.

Möller P., Dulski P. and Morteani G. (2003). Partitioning of rare earth elements, yttrium, and some major elements among source rocks, liquid and vapour of Larderello-Travale Geothermal Field, Tuscany (Central Italy). Geochim. Cosmochim. Acta, 67, 171-183.

Möller P., Rosenthal E., Geyer S., Guttman J., Dulski P., Rybakov M., Zilberbrand M., Jahnke C. and Flexer A. (2007). Hydrochemical processes in the lower Jordan valley and in the Dead Sea area. Chem. Geol., 239, 27-49.

Moller T., Schultz H., Hamann Y., Dellwig O. and Kucera M. (2012). Sedimentology and geochemistry of an exceptionally preserved last interglacial sapropel S5 in the Levantine Basin (Mediterranean Sea). Marine Geology, 291-294, 24-38.

Monecke T., Kempe U., Monecke J., Sala M. and Wolf D. (2002). Tetrad effect in rare earth element distribution patterns: a method of quantification with application to rock and mineral samples from granite-related rare metal deposits. Geochim. Cosmochim. Acta, 66, 1185–1196.

Monji A.B., Ahmadi S.J. and Zolfonoun E. (2008). Selective Biosorption of Zirconium and Hafnium from Acidic Aqueous Solutions by Rice Bran, Wheat Bran and Platanus Or ientalis Tree Leaves. Separation Science and Technology 43, 597-608.

Monroy-Guzman F., Trubert D., Brillard L., Hussonnois M., Constantinescu O. and Le Naour C. (2010). E Anion Exchange Behaviour of Zr, Hf, Nb, Ta and Pa as Homologues of Rf and Db in Fluoride Medium. J. Mex. Chem. Soc., 54(1), 24-33.

Morgan W.J. (1971). Convection plumes in the lower mantle. Nature, 230, 42-43.

Morton-Bermea O., Armienta M. Aurora and Ramos S. (2010). Rare-earth element distribution in water from El Chichón Volcano Crater Lake, Chiapas Mexico. Geof. Intern., 49, 43–54.

Naughton J.J., Greenberg V.A. and Gouguel R. (1976). Incrustations and fumarolic condensates at Kilauea Volcano, Hawaii: field, drill-hole and laboratory observalions. J. Volc. Geotherm.Res., l, 149-165.

Norén B. (1967). The fluoride complexes of Zirconium(IV). Acta Chemical Scandinavica,(21), 2457-2462.

Nriagu J.O. (1989). A global assessment of natural sources of atmospheric trace metals. Nature, 338, 47-49.

Nuccio P.M., Paonita A. and Sortino F. (1999). Geochemical modeling of mixing between magmatic and hydrothermal gases: The case of Vulcano Island (Italy), Earth Planet. Sci. Lett., 167, 321–333.

Nugent L.J. (1970). Theory of the tetrad effect in the lanthanide(III) and actinide(III) series. Journal of Inorganic Nuclear Chemistry, 32, 3485– 3491.

Ogawa Y., Shikazono N., Ishiyama D., Sato H., Mizuta T. and Nakano T. (2007). Mechanisms for anhydrite and gypsum formation in the Kuroko massive sulfide–sulfate deposits, north Japan. Miner Deposita, 42, 219-233.

Oppenheimer C., Fischer T.P., Scaillet B. (2013). Volcanic degassing: processes and impact. In.: Treatise of Geochemistry vol., 3, 110-179.

Ohta A. and Kawabe I. (2000). Rare earth element partitioning between Fe oxyhydroxide precipitates and aqueous NaCl solutions doped with NaHCO3: Determinations of rare earth element complexation constants with carbonate ions. Geochem. Jour., 34, 439 –454.

Panichi C. and Noto P. (1992). Isotopic and chemical composition of water, steam and gas samples of the natural manifestation of the Island of Vulcano (Aeolian Arc, Italy). Acta Vulcanol. 2, 297–312.

Panichi C. and Volpi G. (1999), Hydrogen, oxygen and carbon isotope ratios of Solfatara fumaroles (Phlegraean Fields, Italy): Further insight into source processes, J. Volcanol. Geotherm. Res., 91, 21–328.

Panichi C., La Ruffa G., Kavouridis T., Leontiadis J., Leonis C, Liberopoulou V. and Dotsika E. (2000). Geochemical Assesement of Hydrothermal Fluids Emerging along the Aegean Volcanic Arc. Proceedings World Geothermal Congress, Japan.

Paonita A., Favara R., Nuccio P.M. and Sortino F. (2001). Genesis of fumarolic emissions as inferred by isotope mass balances: CO2 and water at Vulcano Island, Italy. Geochim. Cosmochim. Acta, 66, 759-772.

Pappalardo L., Civetta L., D'Antonio M., Deino A. L., Di Vito M.A., Orsi G., Carandente A., De Vita S., Isaia R. and Piochi M. (1999). Chemical and isotopical evolution of the Phlegraean magmatic system before the Campanian Ignimbrite (37 ka) and the Neapolitan Yellow Tuff (12 ka) eruptions. J Volcanol Geoth Res 91:141–166

Patriat, M. and Labails, C. (2006). Linking the Canary and Cape-Verde Hot-Spots, Northwest Africa. Marine Geophys. Res., 27(3), 201-215.

Pearson, R.G. (1963). Hard and soft acids and bases. Journal of the American Chemical Society 85, 3533-3539.

Peppard D.F., Mason G.W. and Lewey S.A. (1969).Tetradeffectintheliquid-liquidextractionorderingof lanthanides(III). J. InorgNucl Chem,31,2271-2.

Pershina V., Trubert D., Le Naour C. and Kratz J.V. (2002).Theoretical predictions of hydrolysis and complex formation of group-4 elements Zr, Hf and Rf in HF and HCl solutions. Radiochim. Acta, 90, 869–877.

Pershina V. and Polakova D. (2006). Theoretical Predictions of Complex Formation of Group-4 Elements Zr, Hf, and Rf in H_2SO_4 Solutions. NUSTAR-SHE-CHEM-03.

Pershina V., Borschevsky A. and Iliaš M. (2014). Theoretical predictions of properties and volatility of chlorides andoxychlorides of group-4 elements. I. Electronic structures and properties of MCl_4 and $MOCl_2$ (M = Ti, Zr, Hf, and Rf). The Journal Of Chemical Physics, 141.

Piccardi G., Martini M. and Legittimo Cellini P. (1979). On the presence of Cu, Zn, Cd, Sb, Bi and Pb in the fumarolic gases of Vulcano (Aeolian Island). Soc. Ital. di Min. e Petr. 35, 627–632.

Pichler T. and Veizer J. (1999). Precipitation of Fe(III) oxyhydroxide deposits from shallow-water hydrothermal fluids in Tutum Bay, Ambitle Island, Papua New Guinea. Chemical Geology, 162, 15-31.

Pokrovsky O.S., Schott J. and Thomas F. (1999). Dolomite surface speciation and reactivity in aquatic systems. Geochim. Cosmochim. Acta, 63, 3133–3143.

Pokrovsky O.S. and Schott J. (1999). Processes at the magnesium- bearing carbonate/solution interface. II Kinetics and mechanism of magnesitedissolution.Geochim. Cosmochim. Acta, 63, 881–897.

Pokrovski G.S., Borisova A.Y. and Bychkov A.Y. (2013). Speciation and transport of metals and metalloids in geological vapours. Rev. in Mineral. Geochem. 76, 165-218.

Pol A., Heijmans K., Harhangi H.R.,Tedesco D., Jetten M.S.M., Op den Camp H.J.M. (2008). Methanotrophy below pH 1 by a new Verrucomicrobia species. Nature, Letter, 460, doi:10.1038/nature06222.

Puchelt H., Schock H.H., Schroll E., and Hanert E. (1973). Rezente marine Eisenerze auf Santorini, Griechland. Geologische Rundschau, 62, 786–812.

Quisefit J.P., Toutain J.P., Bergametti G., Javoy M., Cheynet B. and Person A. (1989). Evolution versus cooling of gaseous volcanic emissions from Momotombo Volcano, Nicaragua: Thermochemical model and observations, Geochim. Cosmochim. Acta, 53 , 2591 – 2608.

Qu X.M.,Wang R.J., Xin H.B., Zhao Y.Y. and Fan, X.T. (2009). Geochronology and geochemistry of igneous rocks related to the subduction of the Tethys oceanic plate along the Bangong Lake arc zone, the western Tibetan Plateau. Geochimica 38 (6), 523–535. (in Chinese with English abstract).

Raso M., Censi P. and Saiano F. (2013). Simultaneous determinations of zirconium, hafnium, yttrium and lanthanides in seawater according to a co-precipitation technique onto iron-hydroxide. Talanta 116, 1085-1090.

Reynard B., Lécuyer C. and Grandjean P. (1999). Crystal-chemical controls on rare-earth element concentrations in fossil biogenic apatites and implications for paleoenvironmental reconstructions. Chem. Geol., 155, 233-241.

Richards J.P.(2011): Magmatic to hydrothermal metal fluxes in convergent and collided margins. Ore Geology Reviews, 40, 1-26.

Rolandi G. and Stanzione D. (1993). Aspetti idrogeologici e idrogeochimici nei Campi Flegrei settentrionali nell'area compresa tra i vulcani Astroni e Pisani. Rend. Accad. Sci. Fis. Mat., Napoli, Ser. IV 60, 215–251.

Rosi M. and Sbrana A. (1987). Quaderni della ricerca scientifica, Phlegrean Field 114, 9, 60-79.

Sakellariou D., Sigurdsson H., Alexandri M., Carey S, Rousakis, G., Nomikou P, Georgiou P. and Ballas D. (2010) Active tectonics in the Hellenic Volcanic Arc: the Coloumbo submarine volcanic zone. Bull GeolSoc Greece XLIII/2, 1056–1063.

Salvi S., and Williams-Jones A.E. (2006). Alteration, HFSE mineralisation and hydrocarbon formation in peralkaline igneous systems: Insights from the Strange Lake Pluton, Canada. Lithos, 91, 19-34.

Scandone P. (1982). Structure and Evolution of the Calabrian Arc. Earth Evolution Science, 3, 172-180.

Scandone R., Bellucci F., Lirer L. and Rolandi G. (1991). The structure of the Campanian Plain and the activity of the Neapolitan volcanoes (Italy), J. Volcanol. Geotherm. Res., 4 , 1-31.

Smith P.A. and Cronan D.S. (1983). The geochemistry of metalliferous sediments and waters associated with shallow hydrothermal activity (Santorini, Greece). Marine Geology, 39, 241–262.

Shannon R.D. (1976). Revised effective ionic radii and systematic studies of interatomic distances in halides and chalcogenides. ActaCrystallographica, B25, 925-946.

Shaw T.J., Duncan T. and Schnetger B. (2003). A Preconcentration/Matrix Reduction Method for the Analysis of Rare Earth Elements in Seawater and Groundwaters by Isotope Dilution ICPMSAnal.Chem., 75,3396–3403.

Sheng D. and Liu J.C. (2000). Cast Irons Containing Rare Earths. Tsinghua University Press, Beijing.

Shimizu A., Sumino H., Nagao K., Notsu K. and Mitropoulos P. (2005). Variation in noble gas isotopic composition of gas samples from the Aegean arc, Greece. Journal of Volcanology and Geothermal Research, 140, 321–339.

Sohrin Y., Urushihara S., Nakatsuka S., Kono T., Higo E., Minami T., Norisuye K. and Umetani S. (2008). Multielemental determination of GEOTRACES key trace metals in seawater by ICP-MS after Preconcentration Using an Ethylenediaminetriacetic Acid Chelating Resin. Analytical Chemistry, 80, 6267-6273.

Sortino F., Inguaggiato S. and Francofonte S. (1991). Determination of HF, HCl, and total sulphur in fumarolic fluids by ion chromatography. ActaVulcanol., 1, 89–91.

Sortino F. and Bichler M. (1997). Elementi in traccia: genesi e trasporto nei gas fumarolici. In: La Volpe L., Dellino P., Nuccio M., Privitera E. and Sbrana, A. (Eds.), Progetto Vulcano. CNR-GNV, Felici Editore, pp. 147–152.

Sortino F., Nonell A., Toutain J.P., Munoz M., Valladon M. and Volpicelli G. (2006). A new method for sampling fumarolic gases: Analysis of major, minor and metallic trace elements with ammonia solutions. J VolcanolGeoth Res, 158, 244-256.

Stoiber, R.E., Rose, W.I., 1970. The geochemistry of Central American volcanic gas condensates. Geol. Soc. Am. Bull. 81, 2891–2912.

Stoiber R.E. and Rose W.I.(1974). Fumarole incrustations at active central America volcanoes. Geochim. Cosmochim. Acta, 38, 495–516.

Symonds R.B., Rose W.I., Reed M.K., Lichte F.E. and Finnegan D.L. (1987). Volatilization, transport and sublimation of metallic and non-metallic elements in high temperature gases at Merapi Volcano, Indonesia. Geochim. Cosmochim. Acta 51, 2083–2101.

Symonds R.B. and Reed M.K. (1993). Calculation of multicomponent chemical equilibria in gas–solid–liquid system. Part II. Thermochemical data and application to studies of high temperature volcanic gases with examples from St. Helens. Am. J. Sci. 293, 758–864.

Tanaka K., Ohta A. and Kawabe I. (2004) Experimental REE partitioning between calcite and aqueous solution at 25°C and 1 atm: Constraints on the incorporation of seawater REE into seamount-type limestones. Geochem. J. 38, 16–32..

Tanaka R., Makishim, A. and Nakamura E. (2008). Hawaiian double volcanic chain triggered by an episodic involvement of recycled material: constraints from temporal Sr–Nd–Hf–Pb isotopic trend of the Loa-type volcanoes. Earth Planet. Sci. Lett. 265, 450–465.

Tassi F., Vaselli O., Papazachos C. B., Giannini L., Chiodini G., Vougioukalakis G. E., Karagianni E., Vamvakaris D. and Panagiotopoulos D. (2013). Geochemical and isotopic changes in the fumarolic and submerged gas discharges during the 2011–2012 unrest at Santorini caldera (Greece). Bull. Volcanol., 75–711.

Taylor S.R. and McLennan S.M. (1995). The geochemical evolution of the continental crust. Reviews of Geophysics, 33, 241-265.

Tedesco D. and Scarsi P. (1999). Chemical (He, H2, CH4, Ne, Ar, Ne) and isotopic (He, Ne, Ar, C) variations at the Solfatara crater (southern Italy): mixing of different sources in relation to seismic activity. Earth Planet. Sci. Lett.; 171: 465–480.

Tepe N. and Bau M. (2014). Importance of nanoparticles and colloids from volcanic ash for riverine transport of trace elements to the ocean: Evidence from glacial-fed rivers after the 2010 eruption of Eyjafjallajökull Volcano, Iceland. Science of The Total Environment 488/489, 243-251.

Terakado Y. and Masuda A. (1988) Trace element variations in acidic rocks from the Inner Zone of South-west Japan. Chem. Geol., 67, 227–241.

Toutain J.P. (1987). Contribution a` l'étude des sublimésvolcaniques. Minéralogie, géochimie, thermodynamique. Exemple du Momotombo, du Piton de la Fournaise et du Poas. Thesis, Universite´ Pierre et Marie Curie, 190.

Toutain J. P., Aloupogiannis P., Delorme H., Person A., Blanc P.andRobaye G. (1990). Vapor deposition of trace elements from degassed basaltic lava, Piton de la Fournaise volcano, Reunion Island. J. Volcanol. Geotherm. Res. 40 , 257–268 J. Volcanol. Geotherm. Res., 40 , 257–268.

Turner D.R., Whitfield M. and Dickson, A. G., (1981). The equilibrium speciation of dissolved components in freshwater and seawater at 25°C and 1 atm pressure. Geochim. cosmochim. Acta, 45,855-881.

Valentino G.M., Cortecci G., Franco E. and Stanzione D. (1999) - Chemical and isotopic compositions of minerals and waters from the Campi Flegrei volcanic system, Naples, Italy. Journal of Volcanology and Geothermal Research, 91, 329- 344.

Valentino G.M. and Stanzione D. (2004) - Geochemical monitoring of the thermal waters of the Phlegraean Fields. Journal of Volcanology and Geothermal Research, 133, 261-289.

Varnavas S.P. and Cronan D.S. (2005). Submarine hydrothermal activity off Santorini and Milos in the Central Hellenic Volcanic Arc: A synthesis. ChemGeol, 224, 40-54.

Vaselli O., Tassi F., Tedesco D., Poreda J.R. And Caprai A. (2011). Submarine and inland gas discharges from the Phlegrean Fields (southern Italy) and the Pozzuoli Bay: geochemical clues for a common hydrothermal-magmatic source. Procedia Earth and Planet. Sci., 4, 57 – 73.

Vespa M., Keller J. and Gertisser R. (2006). Interplinian explosive activity of Santorini volcano (Greece) during the past 150,000 years . Jour. Volcanol. and Geotherm. Res., 153, 262–286.

Vougioukalakis G.E. and Fytikas M. (2005). Volcanic hazards in the Aegean area, relative risk evaluation, monitoring and present state of the active volcanic centers. In: Fytikas M, Vougioukalakis G (eds) The South Aegean active volcanic arc: present knowledge and future perspectives: developments in volcanology, 7. Elsevier, Amsterdam, 161–183.

Vurro F., Garavelli A., Garbarino C., Moëlo Y. and Borodaev Y.S. (1999). Rare sulfosalts from Vulcano, Aeolian Islands, Italy. II. Mozgovaite, $PbBi_4(S,Se)_7$, a new mineral species. Can. Mineral., 37, 1499-1506.

Washington H.S. (1906). The Roman Comagmatic Region. Carnegie Inst. Washington, 36, 1-220.

Wilke M., Schmidt C., Dubrail B., Appel K., Borchert M., Kvashnina K. and Manning C.E. (2012). Zircon solubility and zirconium complexation in $H_2O + Na_2O + SiO_2 + 7Al_2O_3$ fluids at high pressure and temperature. Earth and Planetary Science Letters 349–350, 15–25.

Wilke M., Jahn S., Schmidt C., Dubrail B., Appel K., Borchert M., Kvashnina K., Pascarelli S. and Manning C.E. (2013). Insights from X-ray absorption/fluorescence spectroscopy and ab-initio molecular dynamics on concentration and complexation of Zr and Hf in aqueous fluids at high pressure and temperature. Journal of Physics: Conference Series, 43.

Williams-Jones A.E. and Heinrich C.A. (2005). Vapor transport of metals and the formation of magmatic-hydrothermal ore deposits. Econ. Geol., 100, 1287–1312

Williams-Jones A.E. and Wood S.A. (1992). A preliminary petrogenetic grid for rare earth element fluorocarbonate and related minerals. Geochim. Cosmochim. Acta, 56, 725-738.

Williams-Jones A.E., Samson I.M., Olivo G.R. (2000). The genesis of hydrothermal fluorite-REE deposits in the Gallinas Mountains, New Mexico. Econ Geol, 95, 327–341.

Willie S.N. and Sturgeon R.E. (2001). Determination of transition and rare earth elements inseawater by flow injection inductively coupled plasmatime-of-flight mass spectrometry.SpectrochimicaActa PartB-Atomic Spectroscopy, 56,170 7- 1716.

Wood S.A. (1990a). The aqueous geochemistry of the rare-earth elements and yttrium: 1. Review of available low-temperature data for inorganic complexes and the inorganic REE speciation of natural waters. Chem. Geol., 82, 159–186.

Wood, S.A. (1990b).The aqueous geochemistry of the rare-earth elements and yttrium: 2. Theoretical predictions of speciation in hydrothermal solutions to 350 °C at saturation water vapor pressure. Chem. Geol., 88, 99–125.

Wood, S.A. and Samson, I.M. (2006) The aqueous geochemistry of gallium, germanium, indium and scandium. Ore Geol. Rev. 28, 57-102.

Zelenski M.E., Fischer T.P., de Moor J.M., Marty B., Zimmermann L., Ayalew D., Nekrasov A.N. and Karandashev V.K. (2013). Trace elements in the gas emissions from the Erta Ale volcano, Afar, Ethiopia. ChemGeol, 357, 95-116.

Zhong S.J. and Mucci A. (1995). Partitioning of Rare-Earth Elements (REEs) between Calcite and Seawater Solutions at 25-Degrees-C and 1 Atm, and High Dissolved REE Concentrations. GeochimCosmochimActa, 59, 443-453.

Zhu R.S., Wang J.H. and Lin M.C. (2007). Sublimation of Ammonium Salts: A Mechanism Revealed by a First-Principles Study of the NH_4Cl System. Chem. Geol., 88, 99–125.J. Phys. Chem. C 111, 13831-13838.

Zhu Y., Umemura T., Haraguchi H., Inagaki K. and Chiba K.(2009). Determination of REEs in seawater by ICP-MS after on-line preconcentration using a syringe-driven chelating column. Talanta78(2009) 891–895.

Appendix-1

Tab. 4.1–Zr, Hf and REE concentrations in studied fumarolic condensates

sampling area	sample name	date	T °C	HF	HCl	Y	La	Ce	Pr	Nd	Sm	Eu	Gd	Tb	Dy	Ho	Er	Tm	Yb	Lu	Zr	Hf	Y/Ho	Zr/Hf	Ce/Ce*	Eu/Eu*	Gd/Gd*	Gd excess
Vulcano	F0-1	03.01.2013	351	259,94	2409,39	1,027	0,961	1,803	0,153	0,471	0,083	0,009	0,134	0,011	0,071	0,018	0,064	0,013	0,117	0,023	27512,2	149,66	58,15	183,83	1,07	0,56	2,50	0,0801
	F0-2	09.06.2013	377	239,97	1591,23	0,097	0,110	0,923	0,019	0,062	0,013	0,002	0,044	0,002	0,008	0,002	0,006	0,002	0,008	0,003	2213,2	3,83	40,65	577,52	4,58	0,75	3,68	0,0321
	F0-3	10.24.2013	378	357,76	1883,64	0,042	0,068	0,243	0,012	0,039	0,006	0,001	0,008	0,001	0,004	0,001	0,002	0,000	0,003	0,000	2680,1	32,14	53,78	83,40	1,95	0,54	2,68	0,0052
	F2-1	03.01.2013	265	398,05	507,97	0,343	0,066	0,192	0,028	0,114	0,029	0,005	0,034	0,005	0,029	0,007	0,018	0,004	0,022	0,005	481,5	2,12	52,50	226,65	1,00	0,82	1,30	0,0078
	F2-2	08.05.2013	277	1442,89	6768,80	0,235	0,337	0,757	0,059	0,188	0,031	0,002	0,046	0,004	0,021	0,005	0,015	0,003	0,019	0,003	653,9	0,73	51,31	896,22	1,23	0,38	2,84	0,0301
	F2-3	10.24.2013	251	139,98	420,82	0,970	2,236	3,605	0,272	0,818	0,118	0,004	0,154	0,011	0,055	0,011	0,034	0,005	0,033	0,005	7012,9	108,05	84,64	64,90	1,02	0,21	3,62	0,1114
	FFR-1	03.01.2013	241,6	208,04	3533,68	0,586	0,379	7,288	0,084	0,291	0,056	0,014	0,315	0,010	0,052	0,012	0,036	0,006	0,038	0,007	23184,4	209,44	48,00	110,70	9,43	1,05	5,28	0,2557
	FFR-2	08.05.2013	254	215,73	2557,04	0,027	0,033	0,057	0,006	0,026	0,004	0,000	0,005	0,000	0,002	0,001	0,002	0,000	0,002	0,000	1087,6	12,14	52,04	89,62	0,93	0,63	2,07	0,0025
	FFR-3	10.24.2013	261	67,83	1301,12	0,034	0,080	0,097	0,008	0,027	0,005	0,001	0,005	0,001	0,003	0,001	0,002	0,000	0,002	0,000	2916,1	43,30	54,40	67,34	0,80	0,90	1,64	0,0020
	F5-1	03.01.2013	365	472,18	535,45	0,256	0,039	0,965	0,011	0,044	0,013	0,002	0,050	0,004	0,021	0,005	0,014	0,003	0,015	0,002	2299,6	5,01	52,53	458,62	10,78	0,51	3,17	0,0342
	F5-2	08.02.2013	416	622,83	3586,57	0,110	0,138	0,278	0,024	0,079	0,014	0,001	0,019	0,002	0,009	0,002	0,007	0,001	0,007	0,001	6290,0	52,87	55,45	118,96	1,10	0,57	2,33	0,0110
	F5-3	09.06.2013	421	144,24	2542,78	0,200	0,318	0,980	0,052	0,161	0,029	0,003	0,052	0,003	0,018	0,004	0,012	0,002	0,014	0,002	3153,1	2,10	52,71	1500,46	1,73	0,59	3,02	0,0346
	F5-4	10.24.2013	421	89,26	626,59	2,126	4,031	6,293	0,608	1,901	0,312	0,019	0,348	0,034	0,185	0,039	0,117	0,017	0,119	0,017	12043,9	193,97	54,23	62,09	0,91	0,35	2,45	0,2058
	GBC-1	03.01.2013	374	197,67	1609,78	0,133	0,199	1,735	0,032	0,104	0,018	0,004	0,083	0,003	0,011	0,003	0,009	0,002	0,010	0,002	4293,8	24,61	46,78	174,51	4,97	0,97	4,95	0,0665
	F11-1	08.03.2013	321	798,45	3621,07	0,064	0,060	1,689	0,012	0,048	0,009	0,001	0,060	0,001	0,006	0,001	0,004	0,001	0,004	0,001	4122,7	30,62	51,17	134,65	14,32	0,73	8,91	0,0529
	F11-2	09.06.2013	331	412,45	3815,33	0,180	0,184	0,539	0,035	0,169	0,020	0,003	0,034	0,003	0,014	0,003	0,010	0,002	0,011	0,002	2671,5	5,98	57,19	446,62	1,54	0,64	2,44	0,0202
	F11-3	10.24.2013	345	160,15	2054,59	0,053	0,082	0,664	0,013	0,044	0,008	0,001	0,018	0,001	0,005	0,001	0,003	0,000	0,003	0,001	2430,7	29,72	51,82	81,78	4,59	0,69	4,07	0,0138
Phlegrean Fields	Bocca Nuova 1	06.14.2013	145	9,40	173,08	0,097	0,050	0,650	0,011	0,037	0,008	0,001	0,030	0,001	0,006	0,001	0,005	0,001	0,015	0,003	3317,8	34,45	70,65	96,31	1,09	0,30	2,66	0,0185
	Bocca Grande 1	10.06.2012	164	14,50	182,75	0,004	0,003	0,007	0,001	0,003	0,001	0,000	0,001	0,000	0,000	0,000	0,000	0,000	0,000	0,000	218,7	2,22	52,52	98,65	1,21	1,01	1,70	0,0003
	Bocca Grande 2	06.14.2013	164	20,20	248,86	0,060	0,038	0,093	0,008	0,033	0,006	0,001	0,008	0,001	0,004	0,001	0,003	0,000	0,003	0,000	3211,0	36,43	67,62	88,13	1,35	0,60	2,02	0,0038
Tenerife	Teide	03.22.2014	82,3	bdl	129,71	0,074	0,046	0,126	0,010	0,042	0,008	0,001	0,010	0,001	0,006	0,001	0,005	0,001	0,004	0,001	4018,5	42,77	52,24	93,96	0,41	1,41	1,52	0,0035
Capo Verde	Fogo FF	03.22.2014	199	bdl	170,32	0,095	0,168	0,130	0,032	0,050	0,008	0,002	0,012	0,001	0,007	0,002	0,005	0,001	0,006	0,001	3512,8	42,90	54,49	81,88	1,30	1,80	1,28	0,0027
	Fogo F2	03.22.2015	266	bdl	186,68	0,115	0,098	0,292	0,027	0,100	0,021	0,007	0,031	0,003	0,013	0,002	0,007	0,001	0,006	0,001	6263,4	82,44	50,44	75,98	2,13	1,88	1,87	0,0143
	Fogo F3	03.22.2016	285	bdl	67,83	0,050	0,043	0,210	0,012	0,046	0,008	0,003	0,017	0,001	0,005	0,001	0,003	0,000	0,003	0,000	4483,9	62,64	51,80	71,58	1,78	1,43	2,46	0,0098

HCl and HF concentrations are given in µmol l^{-1}; REE in nmol l^{-1}; Zirconium and hafnium in pmol l^{-1} and Zr/Hf and Y/Ho as molar ratio. "bdl" stands for Below Detection Limits.

Appendix-2

Tab. 4.2– Zr, Hf and REE concentrations in studied fumarolic sublimates

Sampling area	sample name	date	T °C	Y	La	Ce	Pr	Nd	Sm	Eu	Gd	Tb	Dy	Ho	Er	Tm	Yb	Lu	Zr	Hf	Y/Ho	Zr/Hf	Ce/Ce*	Eu/Eu*	Gd/Gd*	Gd excess
Vulcano	GBC-1	09.05.2012	111	0.238	0.408	0.677	0.067	0.202	0.033	0.003	0.023	0.004	0.021	0.004	0.014	0.003	0.014	0.003	2058012.0	61293.6	58.95	33.58	0,93	0,51	1.21	0,0039
	GBC-2	09.14.2012	111	0.289	0.495	0.804	0.079	0.245	0.040	0.003	0.031	0.004	0.025	0.005	0.015	0.003	0.017	0.003	2528078.4	78260.5	55.48	32.30	0,93	0,34	1.71	0,0126
	GBC-3	09.24.2012	111	0.196	0.331	0.538	0.052	0.161	0.026	0.002	0.023	0.003	0.017	0.004	0.011	0.001	0.008	0.002	1965747.1	24740.9	53.40	79.45	0,93	0,40	1.75	0,0097
	GBC-1	03.08.2013	374	0.092	0.107	0.173	0.015	0.047	0.007	0.001	0.007	0.001	0.004	0.001	0.004	0.000	0.002	0.001	2361003.9	54376.1	80.50	43.42	0,97	0,94	1.12	0,0008
	GBC-2	09.19.2013	374	0.078	0.123	0.185	0.019	0.060	0.005	0.002	0.007	0.001	bdl	bdl	0.006	0.001	bdl	0.001	4195850.7	426599.3		9.84	0,87	1,61	1.00	0,0000
	GBC-3	09.29.2013	374	0.082	0.125	0.190	0.020	0.049	0.006	0.001	0.009	0.001	0.005	0.001	0.002	0.001	0.004	0.003	3320710.0	266979.3	75.76	12.44	0,87	0,82	1.27	0,0019
	F0	09.14.2012	377	0.411	0.736	1.177	0.120	0.377	0.065	0.006	0.057	0.008	0.037	0.008	0.022	0.004	0.025	0.004	4118377.9	61465.0	49.21	67.00	0,90	0,50	1.54	0,0198
	F2-1	09.05.2012	265	0.040	0.040	0.069	0.007	0.025	0.004	0.001	0.003	0.0004	0.002	0.0005	0.002	0.0003	0.003	0.001	133673.9	bdl	82.03		0,97	1,24	1.00	0,0000
	F2-2	09.14.2012	265	0.054	0.065	0.109	0.012	0.033	0.006	0.002	0.005	0.001	0.003	0.001	0.002	0.0003	0.002	0.001	260146.9	35397.0	77.14	7.35	0,90	1,48	0.92	-0,0005
	F2-3	09.24.2012	265	0.032	0.041	0.066	0.008	0.023	0.003	0.001	0.003	0.0004	0.002	0.001	0.001	0.0002	0.001	0.001	171270.8	32784.1	62.19	5.22	0,85	1,31	0.96	-0,0001
	F5-1	03.08.2013	365	0.247	0.507	0.793	0.078	0.246	0.042	0.008	0.032	0.004	0.022	0.005	0.015	0.003	0.014	0.003	2553285.2	70283.2	51.87	36.33	0,91	0,97	1.12	0,0034
	F5-2	09.19.2013	365	0.185	0.381	0.599	0.058	0.188	0.033	0.005	0.023	0.003	0.017	0.004	0.010	0.002	0.013	0.002	1875604.8	53692.8	49.85	34.93	0,92	0,85	1.10	0,0020
	F5-3	09.29.2013	365	0.174	0.384	0.596	0.059	0.194	0.029	0.005	0.021	0.004	0.019	0.004	0.011	0.003	0.009	0.002	1847577.1	42430.9	47.03	43.54	0,90	0,97	0.91	-0,0020
	F11-1	10.08.2013	235	0.057	0.113	0.171	0.017	0.051	0.007	0.001	0.006	0.001	0.005	0.001	0.004	0.001	0.003	0.001	643523.6	34718.1	65.68	18.54	0,88	0,98	1.13	0,0007
	F11-2	10.19.2013	235	0.072	0.127	0.193	0.018	0.055	0.007	0.002	0.007	0.001	0.006	0.001	0.004	0.001	0.004	0.001	771442.0	51467.5	73.22	14.99	0,91	0,98	1.16	0,0010
	F11-3	10.29.2013	235	0.060	0.105	0.156	0.015	0.048	0.008	0.003	0.007	0.001	0.004	0.001	0.004	0.001	0.002	0.001	556476.9	3413.8	51.91	163.0	0,89	1,96	0.70	-0,0030
	F12-1	03.08.2013	232	0.404	0.750	1.167	0.114	0.351	0.057	0.007	0.047	0.007	0.037	0.008	0.023	0.004	0.024	0.004	2556132.7	68818.0	52.47	37.14	0,90	0,61	1.30	0,0108
	F12-2	09.19.2013	232	0.413	0.893	1.338	0.131	0.401	0.065	0.009	0.048	0.007	0.035	0.007	0.023	0.004	0.029	0.004	3491215.6	101453.5	58.60	34.41	0,88	0,73	1.22	0,0087
	F12-3	09.29.2013	232	0.296	0.660	0.999	0.096	0.317	0.046	0.005	0.037	0.005	0.030	0.006	0.017	0.002	0.019	0.003	951670.1	2615.0	50.00	363.9	0,90	0,58	1.37	0,0100
Phlegrean Fields	Bocca Grande 1	10.06.2012	164	0.056	0.091	0.117	0.010	0.047	0.007	0.001	0.009	0.001	0.003	0.001	0.001	0.0002	0.001	0.0003	443754.1	10278.2	103.1	43.17	0,84	0,85	1.87	0,0043
	Bocca Grande 2	06.14.2013	164	0.035	0.064	0.087	0.011	0.039	0.007	0.002	0.008	0.001	0.004	0.001	0.002	0.0003	0.002	0.001	174806.0	5754.9	57.38	30.38	0,76	1,25	1.20	0,0013
	Bocca Nuova 1	10.06.2012	145	0.654	2.245	4.070	0.441	1.378	0.210	0.035	0.413	0.021	0.086	0.018	0.036	0.006	0.026	0.007	1091583.8	10107.6	36.31	108.0	0,94	0,51	3.00	0,2751
	Bocca Nuova 2	06.14.2013	145	0.738	2.497	4.820	0.484	1.610	0.245	0.037	0.417	0.025	0.105	0.022	0.043	0.008	0.034	0.010	262267.2	3035.7	34.11	86.39	1,01	0,50	2.73	0,2642
Santorini	FNK1-1	09.21.2012	87	1.323	4.225	6.421	0.474	1.359	0.240	0.058	0.467	0.031	0.157	0.030	0.085	0.013	0.078	0.011	165844763.5	2703820.6	43.97	61.34	0,99	0,74	2.17	0,2517
	FNK1-2	05.09.2013	87	3.022	5.290	9.514	0.845	2.563	0.450	0.083	0.763	0.063	0.325	0.071	0.204	0.029	0.193	0.027	311991492.3	3960907.9	42.45	78.77	1,02	0,62	2.09	0,3984
	FNK-3-1	09.21.2012	80	27.680	9.824	18.074	2.088	7.831	1.894	0.565	3.000	0.397	2.383	0.556	1.710	0.251	1.679	0.271	62050900.9	716095.5	49.75	86.65	0,92	1,04	1.26	0,6146
	FNK-3-2	05.09.2013	80	97.985	17.174	37.109	4.679	18.364	4.928	1.541	8.018	1.236	7.662	1.789	5.611	0.858	5.816	0.913	169653666.5	1620667.7	54.77	104.7	0,95	1,07	1.15	1,0451
	FNK3b-1	09.21.2012	81	2.714	2.064	5.264	0.420	1.438	0.278	0.040	0.462	0.043	0.233	0.052	0.158	0.023	0.159	0.024	51442940.2	750823.8	51.81	68.52	1,31	0,48	2.17	0,2486
	FNK3b-2	05.09.2013	81	2.785	2.048	5.118	0.454	1.562	0.312	0.037	0.490	0.047	0.257	0.055	0.164	0.024	0.157	0.024	48411775.5	679710.3	50.51	71.22	1,23	0,42	2.22	0,2690
	FNK10-1	09.21.2012	78	0.738	0.469	1.196	0.105	0.382	0.076	0.016	0.124	0.012	0.070	0.015	0.044	0.006	0.043	0.006	10306601.0	144836.1	47.94	71.16	1,25	0,73	1.73	0,0523
	FNK10-2	05.09.2013	78	0.656	0.571	1.424	0.133	0.482	0.096	0.016	0.142	0.014	0.070	0.015	0.044	0.006	0.042	0.006	11183971.7	150232.7	44.58	74.44	1,20	0,62	1.87	0,0661
Capo Verte	Fogo FF	03.22.2014	199	5.465	4.505	9.325	1.086	4.126	0.732	0.232	0.734	0.103	0.519	0.105	0.294	0.039	0.233	0.035	54164069.9	437730.6	52.15	123.7	0,98	1,46	0.92	-0,0636
	Fogo F2	03.22.2015	266	2.064	4.383	10.551	1.284	5.096	0.891	0.242	0.658	0.078	0.310	0.051	0.126	0.014	0.075	0.011	11689853.1	117841.3	40.32	99.20	1,02	1,47	0.89	-0,0820
	Fogo F3	03.22.2016	285	2.801	5.419	10.534	1.175	4.456	0.760	0.216	0.630	0.078	0.334	0.061	0.154	0.018	0.103	0.015	20969265.4	183460.1	45.84	114.3	0,97	1,45	0.92	-0,0574

REE concentration values are given in µmol kg^{-1}; Zirconium and hafnium in pmol kg^{-1} and Zr/Hf and Y/Ho as molar ratio. "bdl" stands for Below Detection Limits.

Appendix-3

Tab. 5.1 –Zr, Hf and REE concentrations in studied hydrothermal waters from Vulcano and Santorini islands

pmol l^{-1}	water group	Y	La	Ce	Pr	Nd	Sm	Eu	Gd	Tb	Dy	Ho	Er	Tm	Yb	Lu	Hf	Zr	Zr/Hf	Y/Ho	Eu/Eu*	∑REE
Istmo 10	GR-1	1083.2	492.3	841.7	117.0	508.3	118.2	21.4	143.2	17.0	82.6	17.6	45.3	6.4	35.3	5.8	1.3	59.3	45.6	61.5	0,75	3535
Istmo 7a	GR-1	1892.0	1096.0	2448.1	329.2	1235.0	302.9	79.1	507.9	67.2	276.0	65.3	146.0	25.5	140.6	26.6	7.8	642.8	82.4	29.0	0,88	8637
Istmo 9	GR-1	2376.7	875.5	1941.5	275.7	1205.1	270.9	49.3	298.2	37.4	191.1	40.5	114.2	16.7	99.0	15.2	2.7	207.2	76.7	58.7	0,80	7807
Istmo 8	GR-1	1705.8	483.7	1118.8	161.0	788.2	207.3	56.3	287.5	41.0	230.1	50.7	142.9	20.2	132.4	20.8	3.3	205.6	62.3	33.6	1,03	5447
Vasca	GR-1	38592.5	65281.2	124761.6	14154.5	50808.7	8540.5	1220.0	6610.7	855.4	4249.1	773.5	2112.7	284.1	1730.7	245.6	6.8	545.4	80.2	49.9	0,76	320221
Istmo 7b	GR-1	1632.2	412.3	800.0	114.2	523.7	130.6	25.5	173.6	21.5	109.1	24.3	66.3	9.3	54.2	9.2	0.8	23.9	29.9	67.2	0,76	4106
Istmo 6b	GR-1	322.9	134.4	145.2	19.5	79.0	18.2	3.9	24.4	3.6	19.7	5.3	13.9	2.5	12.8	2.8	0.7	47.4	67.7	60.9	0,83	808
Istmo 1	GR-1	662.1	325.5	369.4	52.9	272.1	57.8	12.4	166.7	22.2	157.4	49.7	148.3	17.5	92.2	17.1	0.9	41.5	46.1	13.3	0,49	2423
Laghetto b	GR-1	138581.0	321130.5	667286.0	75281.1	263247.5	50289.9	9196.1	33425.0	4022.1	19141.2	3260.1	8509.4	1098.1	6759.4	919.7	95.7	5329.4	55.7	42.5	1,04	1602147
Laghetto a	GR-1	269515.2	310210.1	685839.6	81760.0	301787.8	56530.4	8554.5	47618.1	6051.7	30126.6	5318.3	14569.6	1943.7	11672.9	1749.0	143.7	13915.4	96.8	50.7	0,77	1833248
Discarica a	GR-1	1580.4	894.4	2056.6	245.6	1200.0	208.6	40.0	208.6	30.2	178.3	37.3	105.9	15.1	103.5	14.4	34.4	3383.0	98.3	42.4	1,56	6919
Pozzo Istmo a	GR-1	36782.3	31902.6	64908.1	7748.5	28254.6	5024.3	733.9	4460.9	606.4	3111.6	609.8	1775.4	276.6	1673.3	280.8	58.5	5928.7	101.3	60.3	0,72	188149
Bambara a	GR-1	28767.7	393.0	806.3	109.9	379.8	144.3	66.8	694.6	171.3	1177.2	325.4	1083.1	196.5	1437.8	319.6	11.0	978.3	88.9	88.4	0,69	36073
Casamento	GR-1	259.8	43.4	28.9	6.7	21.1	7.0	5.5	12.8	2.8	15.8	4.9	14.8	2.9	25.6	6.0	1.1	125.1	113.7	53.0	2,47	458
Bambara b	GR-1	17406.7	159.9	286.5	31.8	138.7	64.6	29.6	461.5	98.7	728.1	194.0	652.5	104.0	816.9	159.1	2.5	249.2	99.7	89.7	0,48	21333
NK porto	GR-2	23694.6	695.4	1033.6	156.3	836.4	274.1	73.4	625.9	119.5	803.5	231.8	723.8	113.7	655.9	131.4	8.0	1695.2	211.9	102.2	0,72	30169
PK	GR-2	23388.4	3055.1	3668.5	415.8	1670.8	365.8	31.7	689.9	115.1	832.2	228.7	776.0	116.4	770.1	139.1	2.4	450.3	187.6	102.3	0,27	36264
Istmo 11	GR-2	1303.2	568.1	583.6	60.5	210.2	37.4	7.3	69.9	8.1	45.1	11.2	33.9	6.0	40.4	8.1	2.3	191.7	83.35	116.4	0,61	2993
Istmo 5	GR-2	699.4	303.4	418.8	51.3	201.5	45.4	8.3	60.9	8.2	42.4	9.7	28.7	4.3	27.1	4.5	1.1	171.6	156.0	72.10	0,71	1914
Istmo 6a	GR-2	632.7	244.1	412.3	63.0	246.0	57.7	13.7	91.8	11.7	79.3	18.5	63.9	10.0	65.6	12.6	4.6	872.9	189.8	34.20	0,83	2023
IRI	GR-2	18760.6	656.1	982.9	118.3	567.3	157.0	33.5	393.1	66.2	478.5	144.8	486.2	68.1	422.9	78.6	1.2	163.9	136.6	129.6	0,54	23414
PK A. Nikolaos	GR-2	27035.4	3941.1	5787.3	717.3	3016.8	725.0	84.4	1141.3	215.5	1363.9	360.6	1101.9	189.8	1110.4	216.6	9.3	1979.9	212.9	74.97	0,41	47007
NK A. Giorgios	GR-2	26084.9	4261.5	6733.0	890.7	3618.5	938.5	230.0	1361.0	293.9	1539.7	419.7	1149.5	227.0	1092.8	248.8	13.3	2800.0	210.5	62.15	0,91	49090
C. Sicilia b	GR-2	43.2	32.6	15.3	2.6	7.8	2.7	1.5	3.4	0.6	3.1	1.0	2.9	0.5	3.4	1.0	2.2	102.4	46.55	43.20	2,22	122
Pozzo Istmo b	GR-2	1173.2	115.9	117.6	13.9	59.4	13.0	2.7	19.9	3.0	16.6	5.7	19.4	3.8	24.4	4.3	0.9	226.3	251.4	205.8	0,73	1593
Discarica b	GR-2	63.2	12.0	26.6	3.2	13.7	3.3	0.8	5.5	0.8	5.1	1.1	3.9	0.7	5.3	1.0	20.0	4799.4	240.0	57.45	1,64	146
C. Sicilia a	GR-2	686.7	826.4	1606.6	195.3	632.2	133.0	35.9	121.0	24.8	114.2	25.6	70.4	10.9	65.2	11.9	7.6	1656.8	219.2	26.82	1,31	4560
Pozzo N5	GR-2	1962.9	577.7	1144.9	172.0	670.3	176.0	51.2	189.5	45.8	225.6	53.4	140.1	23.1	132.9	23.9	49.6	12319.5	248.4	36.76	1,29	5589
Pozzo N18	GR-2	87.0	118.3	149.8	16.2	95.2	41.2	16.8	69.7	15.5	93.5	17.2	67.4	8.3	70.1	10.4	2.1	321.9	153.3	5.06	1,37	877
Seawater		191.3	61.5	21.7	6.1	25.7	6.3	1.7	8.6	1.4	8.4	2.3	6.9	1.4	10.7	2.7	2.2	245.2	111.5	83.2	1,06	357